PHOTOSOLVOLYSIS OF 1-BENZOYL-5-BROMO-7-NITROINDOLINE

(A MECHANISTIC STUDY)

by

© STEFAN WEIGL, M.SC.

A Thesis

Submitted to the Faculty of Graduate Studies

in Partial Fulfilment of the Requirements

for the Degree

Doctor of Philosophy

McMaster University

June, 1988

PHOTOSOLVOLYSIS OF 1-BENZOYL-5-BROMO-7-NITROINDOLINE

DOCTOR OF PHILOSOPHY (1988)
(Chemistry)

McMASTER UNIVERSITY
Hamilton, Ontario

TITLE: Photosolvolysis of N-Benzoyl-5-bromo-7-nitroindoline (A Mechanistic Study).

AUTHOR: Stefan Weigl, B.Sc. (McMaster University)

M.Sc. (McMaster University)

SUPERVISOR: Professor R.F. Childs

NUMBER OF PAGES: xvi, 166

DEDICATION

To Irene, Kevin, and Andrew

ABSTRACT

This thesis describes a study of the photosolvolysis of N-benzoyl-5-bromo-7-nitroindoline. The investigation was instigated because N-acyl-5-bromo-7-nitroindolines have been considered as potential photoprotecting groups for the photolithographic formation of charge-mosaic membranes. However, no kinetic data, and only scant mechanistic information, has been reported for the photofragmentation process.

Both absorption and emission spectra of N-benzoyl-5-bromo-7-nitroindoline were obtained. Based on the electronic spectra, it would seem that the two lowest energy singlet excited states are nearly isoenergetic and their relative energies are a function of the solvent medium.

The distribution of photoproducts obtained from irradiation of N-benzoyl-5-bromo-7-nitroindoline in various solvent systems was investigated. It was shown that the photosolvolysis reaction is a function of the solvent properties. Thus 5-bromo-7-nitroindoline and benzoic acid were the only photoproducts formed in acetonitrile. In acetonitrile-water, 5-bromo-7-nitrosoindole as well as 5-bromo-7-nitroindoline and benzoic acid were identified. A correlation between solvent polarity, $E_T(30)$, and 5-bromo-7-nitrosoindole formation was observed.

The mechanism of the fragmentation mode was examined. The

presence of a free radical intermediate is suggested from the photoproduct distribution in tetrahydrofuran (THF). Observation of an electron spin resonance (e.s.r.) spectrum during irradiation of N-benzoyl-5-bromo-7-nitroindoline in an e.s.r. spectrometer cavity, ^{18}O incorporation into benzoic acid, and a linear free energy relationship with sigma dot ($\sigma\cdot$) corroborated the intermediacy of a free radical in the fragmentation process.

Quantum yields of N-benzoyl-5-bromo-7-nitroindoline disappearance in different solvents and quenchers were measured in order to establish the reactive excited state and the effect of the medium on the efficiency of the transformation process. A solvent dependency on both the excited state lifetime and photosolvolysis reaction efficiency was noted. The results were indicative of a change in mechanism with a variation in solvent polarity and/or hydrogen bonding ability.

A mechanism compatible with experimental results and applicable to previously reported N-acyl-2-nitroaniline photofragmentations is proposed.

"THERE SHOULD BE NO COMBINATION OF
EVENTS FOR WHICH THE WIT OF MAN
CANNOT CONCEIVE AN EXPLANATION."

'SHERLOCK HOLMES IN
ARTHUR CONAN DOYLE'S
"THE VALLEY OF FEAR"
(Part I, Chapter 6).

ACKNOWLEDGEMENTS

The author offers special thanks to his research director, Dr. R.F. Childs, for his guidance, 3M Canada for their support, and most of all my wife, Irene, for her constant encouragement and sacrifice.

Both, the Natural Sciences and Engineering Research Council and 3M Canada, are gratefully acknowledged for their financial support.

For the many discussions in photophysics the author is indebted to Dr. K.C. Wu. Thanks is also extended to Dr. M. Pankratz and Dr. M. Mahendran for their invaluable suggestions, Mr. K. Schoenfeld for his technical assistance, and, last but not least, Messrs. B. Sayer and I. Thompson for their assistance in NMR measurements.

Gratitude is extended to Gayle Storey for her help in preparing this thesis.

TABLE OF CONTENTS

		Page
CHAPTER I		
INTRODUCTION		
PART A:	Charge-Mosaic Membrane	2
PART B:	Nitroaromatic Photoprotecting Groups	
	(i) Introduction	4
	(ii) Differential Reactivity Based System - Nucleophilic Photosubstitution	4
	(iii) Intramolecular Redox Reactions	6
PART C:	Photochemistry of Nitroaromatics	
	(i) Introduction	13
	(ii) Excited States Involved in Photoreduction	15
	(iii) Photoreductions Under Neutral Conditions	17
	(iv) Photoreductions Under Basic Conditions	26
	(v) Photoreductions Under Acidic Conditions	27
PART D:	α-Cleavage Reactions of Amides	
	(i) Introduction	29
	(ii) Photo-Fries Rearrangement of N-Arylamides	29
	(iii) Further α-Cleavage Reactions Which Occur Without Rearrangement	32
PART E:	Statement of Problem and Objective	35
CHAPTER II		
RESULTS AND DISCUSSIONS		
PART A:	Introduction	37
PART B:	Synthesis	37
PART C:	Electronic Spectra of 1-Benzoyl-5-bromo-7-nitroindoline	
	(i) Introduction	39
	(ii) Results	
	(a) UV-Spectra	39
	(b) Fluorescence Spectra	39
	(c) Phosphorescence Spectra	41

TABLE OF CONTENTS

		Page
CHAPTER II (cont'd)		
PART C:	Electronic Spectra of 1-Benzoyl-5-bromo-7-nitroindoline (cont'd)	
	(iii) Discussion	43
PART D:	Photoproduct Analysis	
	(i) Introduction	46
	(ii) Results	
	(a) Isobestic Point	46
	(b) In Anhydrous Acetonitrile as Solvent	48
	(c) In Acetonitrile-Water as Solvent	48
	(d) In Anhydrous Tetrahydrofuran as Solvent	54
	(e) In Tetrahydrofuran-Water as Solvent	56
	(f) In Ethanol as Solvent	56
	(g) In Anhydrous Acetonitrile and 1,3-Cyclohexadiene	57
	(h) In Acetonitrile-Water and 1,3-Cyclohexadiene	57
	(i) Summary of Reaction Product Analysis	58
	(iii) Discussion	59
PART E:	Solvent Polarity and pH Effects	
	(i) Introduction	66
	(ii) Results	
	(a) Photoproduct Distribution as a Function of Solvent Polarity $E_T(30)$	66
	(b) Photoproduct Distribution as a Function of NaOH Concentration	68
	(iii) Discussion	71
PART F:	Fragmentation Study	
	(i) Introduction	75
	(ii) Results	
	(a) Electron Spin Resonance Measurements	75
	(b) Free Benzoyl Radical Interception	78
	(c) Hammett-Linear Free Energy Relationship	79
	(iii) Discussion	80
PART G:	Quantitative Measurements	
	(i) Introduction	86
	(ii) Results	
	(a) Quantum Yield Measurements in Anhydrous Acetonitrile and Acetonitrile-Water	86

TABLE OF CONTENTS

		Page
CHAPTER II (cont'd)		
PART G:	Quantitative Measurements (cont'd)	
(ii)	Results (cont'd)	
(b)	Quantum Yield Measurements in Tetrahydrofuran and Tetrahydrofuran-Water	87
(c)	Electron Transfer Quenching	88
(d)	Triplet State Quenching	89
(e)	Estimated Excited State Lifetimes	91
(iii)	Discussion	93
PART H:	Proposed Mechanism	
(i)	Introduction	99
(ii)	Primary Photochemical Process in Aprotic Solvents	102
(iii)	Secondary Processes in Aprotic Solvents	107
(iv)	Primary Photochemical Process in H-bonding Solvents	109
(v)	Secondary Processes in Polar H-bonding Solvents	112
PART I:	Unifying Concept	114
PART J:	Conclusion	117
CHAPTER III		
EXPERIMENTAL METHODS		
PART A:	General	
(i)	Materials	119
(ii)	Melting Points	120
(iii)	^{1}H NMR Spectra	120
(iv)	^{13}C NMR Spectra	120
(v)	Electronic Absorption Spectra	120
(vi)	Emission Spectra	121
(vii)	Infrared Spectra	121
(viii)	Gas Chromatography	121
(ix)	Mass Spectra	121
(x)	UV Reactors	122
PART B:	Synthesis	
(i)	1-Acetylindoline	122
(ii)	1-Acetyl-5-bromoindoline	122
(iii)	1-Acetyl-5-bromo-7-nitroindoline	123
(iv)	5-Bromo-7-nitroindoline	123

TABLE OF CONTENTS

		Page
CHAPTER III (cont'd)		
PART B:	Synthesis (cont'd)	
(v)	1-Benzoyl-5-bromo-7-nitroindoline	124
(vi)	1-(4'-Chlorobenzoyl)-5-bromo-7-nitroindoline	124
(vii)	1-(4'-Methylbenzoyl)-5-bromo-7-nitroindoline	125
(viii)	1-(4'-Methoxybenzoyl)-5-bromo-7-nitroindoline	125
(ix)	1-(4'-Cyanobenzoyl)-5-bromo-7-nitroindoline	126
PART C:	Emission Measurements	
(i)	Fluorescence	127
(ii)	Phosphorescence	127
PART D:	Photoproduct Distribution	
(i)	In Acetonitrile as Solvent	127
(ii)	In Acetonitrile-Water as Solvent	128
(iii)	In Tetrahydrofuran as Solvent	130
(iv)	In Tetrahydrofuran-Water as Solvent	131
(v)	In Ethanol as Solvent	131
(vi)	In Acetonitrile-1,3-Cyclohexadiene	132
(vii)	In Acetonitrile-Water-1,3-Cyclohexadiene	
(a)	One Stage Reaction (Without 1,3-Cyclohexadiene)	132
(b)	One Stage Reaction	133
(c)	One Stage Reaction (2 Hour Irradiation)	133
(d)	Two Stage Reaction (Without 1,3-Cyclohexadiene)	133
(e)	Two Stage Reaction	134
PART E:	Photoproduct Distribution	
(i)	As a Function of Mole Fraction of Water	134
(ii)	As a Function of NaOH Concentration	135
PART F:	Electron Spin Resonance (e.s.r.)	
(i)	Equipment	136
(ii)	Irradiation in e.s.r. Probe	136
PART G:	Free Benzoyl Radical Interception	138
PART H:	Disappearance Quantum Yield Measurements	
(i)	Optical Bench (PRA)	139
(ii)	Optical Bench (Kratos)	139
(iii)	Actinometry	140
(iv)	Isobestic Point Determination	141
(v)	In Acetonitrile-Water as Solvent (aerated)	141

TABLE OF CONTENTS

		Page
CHAPTER III (cont'd)		
PART H:	Disappearance Quantum Yield Measurements (cont'd)	
(vi)	In Acetonitrile-Water as Solvent (degassed)	143
(vii)	In Tetrahydrofuran-Water as Solvent (aerated)	144
(viii)	In Tetrahydrofuran-Water as Solvent (degassed)	144
(ix)	Electron Transfer Quenching	144
(x)	Triplet State Quenching	148
(xi)	As a Function of 4'-Substituent (Hammett-LFER)	151
PART I:	Cyclic Voltametry	
(i)	Equipment	154
(ii)	Measurements	154
CHAPTER IV		
APPENDIX		
PART A:	Calculation of Quantum Yield	156
REFERENCES		159

LIST OF TABLES

Table	Description	Page
1	Observed and Calculated ^{13}C NMR Chemical Shifts of 5-bromo-7-nitroindole, 25.	52
2	Medium Effects on the Formation of 25 in the Photofragmentation of 10a.	67
3	pH Effects on Photoproduct 25 in the Photofragmentation of 10a in CH_3CN-H_2O.	70
4	Quantum Yields for Disappearance of 4'-substituted 10a in Tetrahydrofuran-Water as a Function of Substituent.	80
5	Quantum Yields for Disappearance of 10a in CH_3CN and CH_3CN-H_2O.	86
6	Quantum Yields for Disappearance of 10a in Tetrahydrofurn and Tetrahydrofuran-Water.	87
7	Quantum Yields for Disappearance of 10a in CH_3CN as a Function of 1,4-Dimethoxybenzene.	88
8	Quantum Yields for Disappearance of 10a in CH_3CN-H_2O as a Function of 1,4-Dimethoxybenzene.	89
9	Quantum Yields for Disappearance of 10a in CH_3CN-H_2O as a Function of 1,3-Cyclohexadiene.	90
10	Cyclic Voltammetric Data for 10a in CH_3CN.	92
11	Raw Data for Photoproduct Distribution as a Function of [NaOH].	137
12	Raw Quantum Yield Data for Disappearance of 10a in Aerated Acetonitrile-Water.	142
13	Raw Quantum Yield Data for Disappearance of 10a in Degassed Acetonitrile-Water.	145

LIST OF TABLES

Table	Description	Page
14	Raw Quantum Yield Data for Disappearance of 10a in Aerated Tetrahydrofuran-Water.	146
15	Raw Quantum Yield Data for Disappearance of 10a in Degassed Tetrahydrofuran-Water.	147
16	Raw Quantum Yield Data for Disappearance of 10a in Aerated Acetonitrile-1,4-Dimethoxybenzene.	149
17	Raw Quantum Yield Data for Disappearance of 10a in Aerated Acetonitrile-Water and 1,4-Dimethoxybenzene.	150
18	Raw Quantum Yield Data for Disappearance of 10a in degassed Acetonitrile-Water-1,3-Cyclohexadiene.	152
19	Raw Quantum Yield Data for Disappearance of 4'-Substituted 10a in Aerated Tetrahydrofuran-Water.	153

LIST OF FIGURES

Figure	Description	Page
1	Schematics of a charge-mosaic membrane.	2
2	Triplet zwitterionic configuration, ^3Z.	17
3	A schematic potential energy diagram for Ph-NH...$COCH_3$ system.	33
4	Energy state diagram for acetanilide.	33
5	UV-absorption spectrum of 10a in (a) acetonitrile-cyclohexane (1:49) and (b) acetonitrile-water (2:3).	40
6	Fluorescence-emission spectrum of 10a in anhydrous acetonitrile.	40
7	Phosphorescence-emission spectrum of 10a in a 2-methyltetrahydrofuran glass matrix (77 K) with a 0.01 and 0.05 microsecond delay.	42
8	UV absorption spectrum of 10a in acetonitrile after 0, 30, 60, 90, 150, and 450 seconds irradiation in the Rayonet UV-reactor (RPR 3500 lamps).	47
9	UV absorption spectrum of 10a in acetonitrile-water after 0, 30, 60, 90, 150, and 450 seconds irradiation in the Rayonet UV-reactor (RPR 3500 lamps).	47
10	^1H NMR spectrum of 25.	51
11	^{13}C proton decoupled NMR spectrum of 25.	51
12	Variation of photoproduct 25, %(mole) 25, with the pH of water used for CH_3CN-H_2O solvent mixture.	69
13	Variation of photoproduct 25, log 25, with the solvent polarity value $E_T(30)$ in the photofragmentation of 10a.	73

LIST OF FIGURES

Figure	Description	Page
14	Solid matrix (120 K) e.s.r. spectrum from 10a irradiation in an e.s.r. cavity.	76
15	Ambient temperature e.s.r. spectrum after 10a irradiation at 120 K in an e.s.r. cavity and then warmed to ambient temperature.	76
16	Ambient temperature e.s.r. spectrum from 11a exposed only to visible light.	77
17	Solid matrix e.s.r. spectrum of 11a.	78
18	Log (Φ_X / Φ_H) versus $\sigma^{\bullet}$.	81
19	Stern-Volmer plot for disappearance of 10a as a function of 1,4-dimethoxybenzene concentration.	91
20	Quantum yield for disappearance of 10a as a function of mole fraction of water in tetrahydrofuran.	94
21	Quantum yield for disappearance of 10a as a function of mole fraction of water in acetonitrile.	94
22	Stern-Volmer plot for disappearance of 10a as a function of 1,3-cyclohexadiene concentration.	96
23	Model for nitroxide stabilization via hydrogen bonding.	113

CHAPTER I

INTRODUCTION

A. CHARGE-MOSAIC MEMBRANE

In 1983 a novel research project was initiated that combined the idea of controlled photochemical domain formation with membrane technology in order to develop a charge-mosaic membrane [1].

Essentially, a charge-mosaic membrane consists of discrete cation and anion permeable microdomains arranged in a two dimensional array across the membrane. Due to the presence of these exchange sites it is possible to initiate a forced transmembrane flow of ionic material. Thus, cations will be transported through the negative and anions through the positive segments resulting in a permeate enriched in salt compared to the feed. The flow is accompanied by a current circulating between the oppositely charged domains (Fig. 1). This type of membrane can be used for piezodialysis; a processes in which salt solutions are concentrated under pressure.

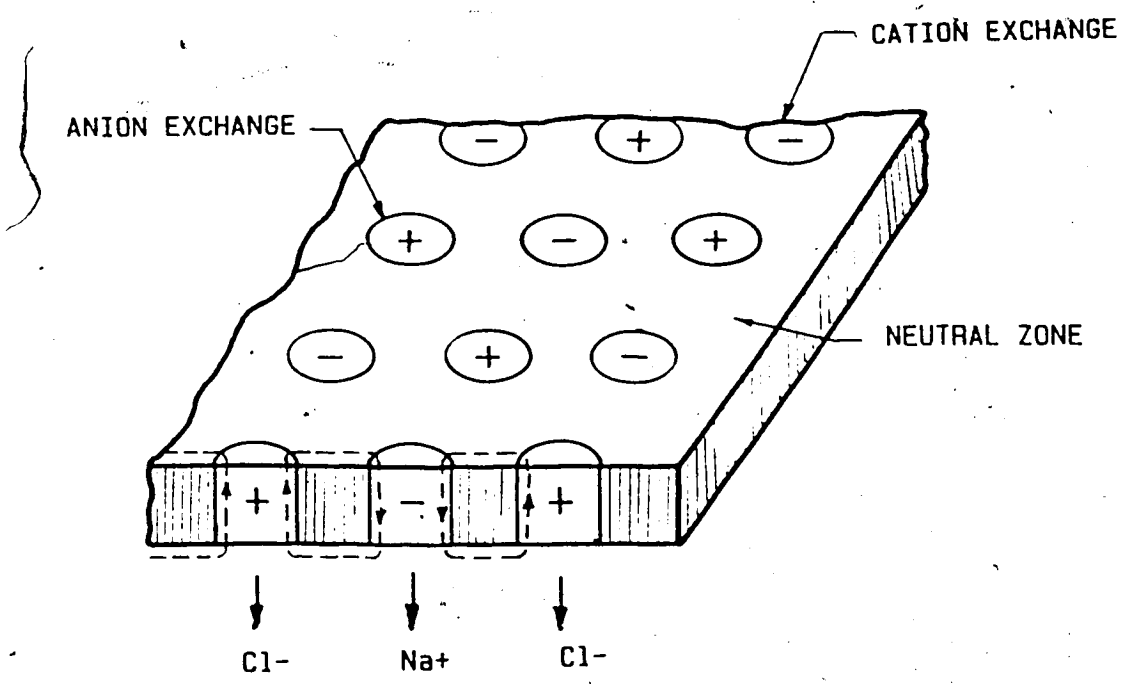

Figure 1: Schematics of a charge-mosaic membrane

The idea of interspersed domains of anion- and cation-selective materials for charged membranes was first advanced by Sollner in 1932 [2]. Several approaches to fabricating a charge-mosaic membrane have since been published [3,4]. This pioneering work has led to the formation of prototype membranes which have been used to confirm the potential of piezodialysis. However, they also clearly revealed the difficulty of manufacturing a usable charge-mosaic membrane, and to this date no commercially viable membrane exists.

The approach to the formation of a charge-mosaic membrane taken by the McMaster membrane group involved a photochemical method. This approach was modeled on the microlithography used in photoresist technology. What was needed was a neutral, photoactive polymer based membrane which would be converted on irradiation with long wavelength light to either a cation or an anion exchange membrane. By using suitable masks and a double irradiation technique, such a photoactive membrane could be converted to a charge-mosaic membrane.

The key to success in this project is finding a suitable photochemically active group which could be incorporated into a polymeric membrane. A variety of photoprotecting groups have been described, and many are used routinely in synthetic chemistry. A preliminary examination of the literature in this area showed that nitro substituted aromatic systems offered considerable promise, and the chemistry of these systems is reviewed in the following sections of this thesis.

B. NITROAROMATIC PHOTOPROTECTING GROUPS

(i) Introduction

A developing field in which the principles of organic photochemical reactions are being advantageously exploited is in the use of photochemically removable protecting groups. Ideally, a light sensitive protecting group is stable to a variety of chemical treatments, and should be removed quantitatively with unit efficiency. The wavelength of irradiating light should be such that it is absorbed only by the protecting group.

Aromatic nitro derivatives have been successfully utilized as photosensitive protecting groups in biochemical syntheses. For example, functional groups on peptides, glycosides, and nucleotides have been protected in this way in order to bring about specific transformations elsewhere in the molecule. Two classes of light sensitive nitroaromatic protecting groups appear in the literature. In the first, use is made of the different reactivity of the excited aromatic nitro compounds relative to their ground state. The second, and probably the largest class, utilizes an internal redox reaction of substituted ortho-nitroaromatics.

(ii) Differential Reactivity Based System - Nucleophilic Photosubstitution

Havinga et al [5] in 1956 were the first to report the photochemical solvolysis of a nitroaromatic (1). m-Nitrophenyl phosphate, 1, is stable in aqueous solutions over a wide pH range in the absence of light. However, upon irradiation with light that is absorbed by the

aromatic system, 1 undergoes smooth hydrolysis to the corresponding nitrophenol, 2, and phosphate, 3.

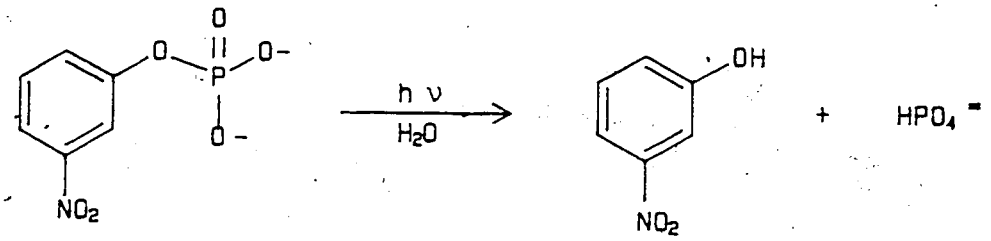

(1)

1 2 3

Of the three possible isomeric nitrophenyl esters, nucleophilic substitution occurs most efficiently with the m-nitrophenyl derivative. It was concluded that the meta-nitrophenolate anion is a better leaving group in the excited than ground state. In ground state chemistry on the other hand, the para-isomer is a better departing anion.

Amino functions in amino acids have been protected with the photolabile 3-nitrophenyloxycarbonyl group [6]. These derivatives regenerate the free amino acids upon irradiation in aqueous tetrahydrofuran (2).

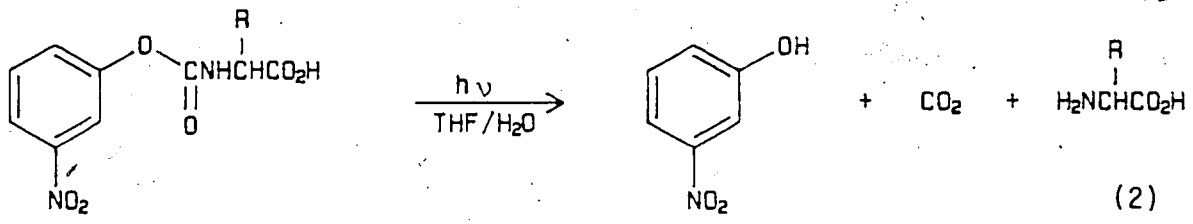

(2)

Photolysis of 2,4-dinitrobenzenesulfenyl derivatives of carboxylic acids in benzene solutions liberates carboxylic acids and simulataneously forms 2,4-dinitrodiphenylsulfide in near quantitative

yields [7]. From the evidence presented, the aromatic sulfide is formed by electrophilic attack on the solvent, benzene, by the excited state 2,4-dinitrobenzenesulfenium cation 4 (3).

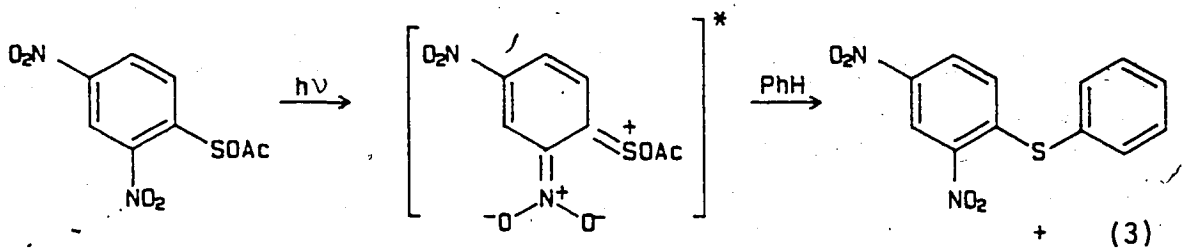

These nucleophilic photosubstitutions are useful reactions, but they are not easily applicable to the generation of both cationic and anionic sites in a polymer. As such they will not be considered further.

(iii) Intramolecular Redox Reactions

The use of esters of o-nitrobenzylalcohol as photoprotecting groups was first reported by Barltrop et al [8] in 1965. When they irradiated o-nitrobenzylbenzoate only 17% of benzoic acid was observed since the primary photoproduct, o-nitrosobenzaldehyde was further transformed into an azobenzene derivative which acted as an efficient internal light filter. However, carboxylic acids were recovered in 75-95% yield with α-substituted o-nitrobenzylesters [9]. Quantitative yields of the free acid were obtained when 2,2'-dinitrodiphenylmethanol was used as a blocking group for the carboxylic function [10] (4).

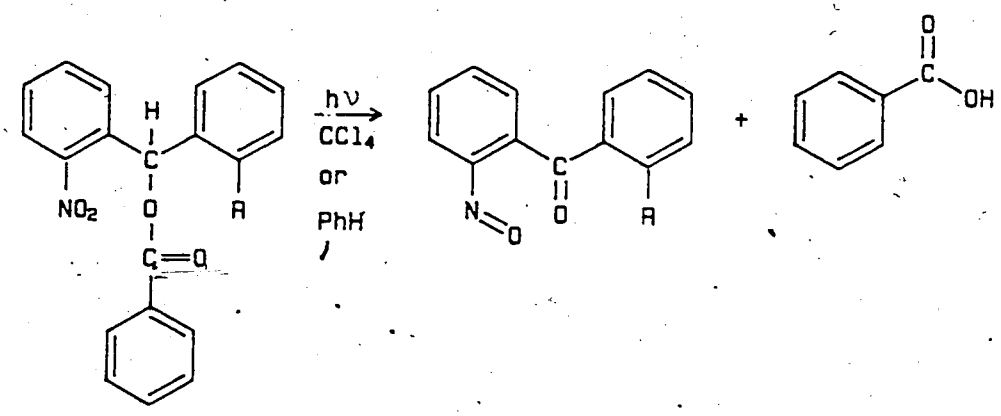

(4)

R = H or NO_2

Amines can be regenerated in good yields from 2-nitrodiphenylmethyloxycarbonyl derivatives [9]. Even the most light sensitive amino acid, tryptophan, could be successfully deblocked when protected as a urethane. Similarly, 6-nitroveratryls have been linked to amino acids as urethanes [10] (5).

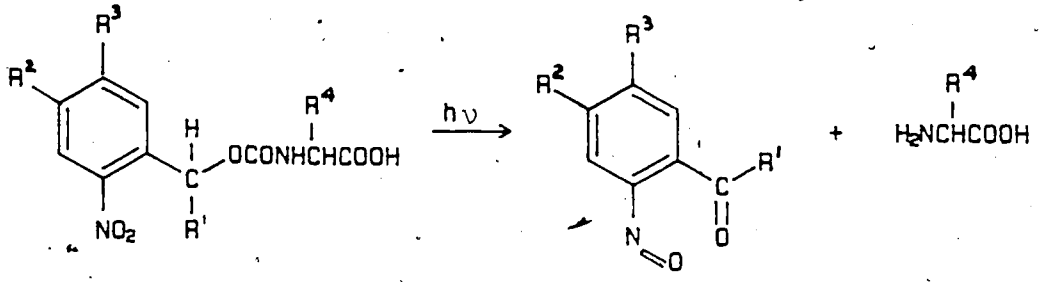

(5)

5	R^1	R^2	R^3
a	H	H	H
b	H	OCH_3	OCH_3
c	C_6H_5	H	H
d	$2\text{-}NO_2C_6H_4$	H	H

Removal of the urethane blocking group is virtually quantitative. However, the amino acid yield for reactant 5a and 5b (equation 5) is quantitative only if acid or aldehyde reagents are added to scavenge o-nitrosobenzaldehyde, and thus prevent further reactions of the aldehyde with the amino acids. In order to avoid this aldehyde reaction the secondary carbinols, (5c and 5d), were examined. With such alcohols a ketone is formed which is less reactive toward amines.

Amit et al [11] used the urethanes of o-nitrobenzyl and 6-nitroveratryl moieties as protecting groups for the amino functions in the synthesis of amino sugars. For the synthetic procedures in carbohydrate chemistry, the hydroxyl groups were protected as their o-nitrobenzyl, or 6-nitroveratryl ethers [12,13]. In mononucleotide synthesis [14] the o-nitrobenzyl moiety functions as a blocking group for 3'-o-acetylthymidine-5'phosphate 6 (6). Engels [15] proposed that the biologically active guanosine 3',5'-phosphate (aGMP) should be membrane-permeable as its stable o-nitrobenzylester, and generate aGMP in the cell upon irradiation with harmless near UV-light.

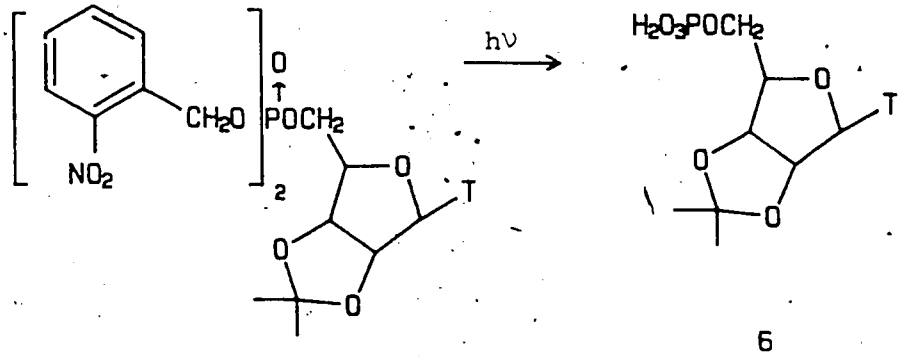

(6)

6

An o-nitrobenzyl-terminated styrene polymer has been prepared and

used for solid-phase synthesis of tert-butyloxycarbonyl-protected peptide acids [16]. The peptide, 7, is removed from the resin by photolysis. Similarly, a C-terminal peptide amide was synthesized, and again removed by photolysis [17] (Scheme 1).

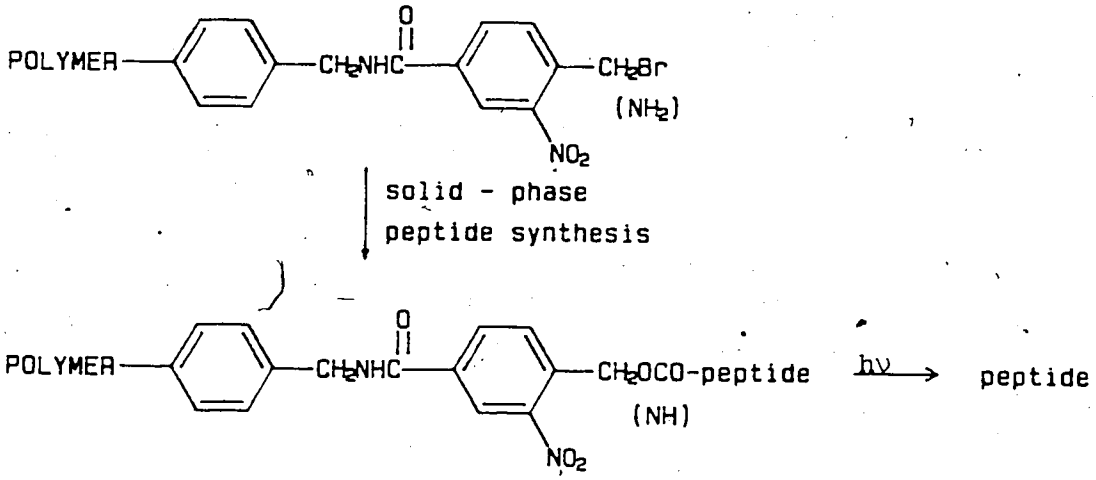

7

Scheme 1

The viability of this type of photoprotecting group has been elegantly demonstrated in the synthesis of biologically active Luteinizing hormone-releasing hormone. In liquid-phase peptide synthesis an o-nitrobenzyl moiety can be joined onto a polyethylene glycol support [18].

In summary, the o-nitrobenzyl and 6-nitroveratryl protecting groups can be linked to various functionalities. They withstand basic and acidic treatment, but cleave photolytically to regenerate the initial entity (7).

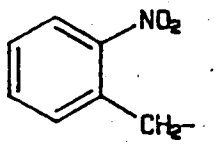

- OCONHR -----> RNH_2
- OR -----> ROH
- OCOR -----> RCO_2H
- NHCOR -----> $RCONH_2$
- $OP(OR)_2$ -----> $(RO)_2POH$ (O)

(7)

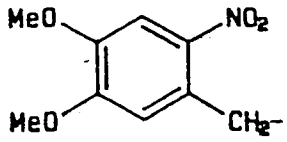

Aldehydes and ketones can be protected as acetals of o-nitrophenylethylene glycol [19]. These acetals are cleaved smoothly with light of wavelength longer than 320 nm. However, the stability of the acetal linkage in different reaction media has not been demonstrated (8).

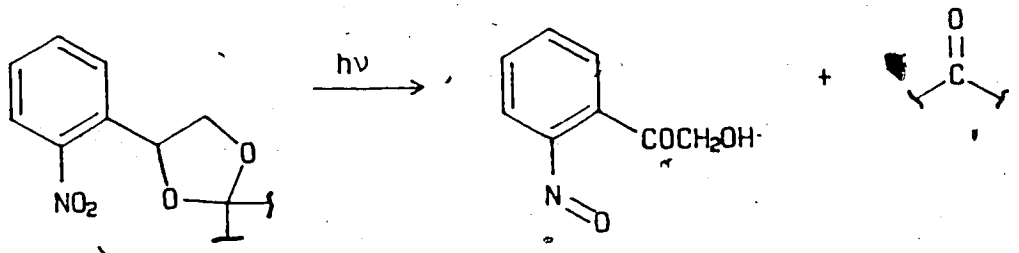

(8)

Amit and co-workers [20] first demonstrated the ability of N-acyl-2-nitroanilides, 8, to undergo photocleavage to furnish the corresponding free acids (9).

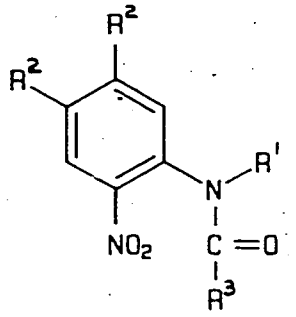

$\xrightarrow{h\nu}$ R^3COOH + Other Products (9)

8

R^1 = alkyl, benzoyl or phenyl

R^2 = H or OMe

R^3 = Me, Ph, or 2-$C_{10}H_7$

In the course of their study they quantitatively evaluated N-acyl-8-nitrotetrahydroquinolines [21], 9, and N-acyl-5-bromo-7-nitroindolines [22], 10, as potential photosensitive protecting groups for carboxylic acids. Excellent yields of the carboxylic acid were recorded in nearly all cases.

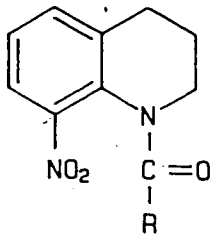

9

R = Ph or 3,4-$Cl_2C_6H_3$

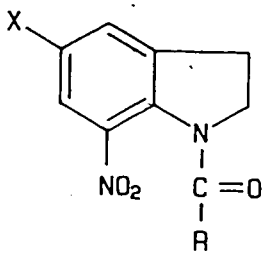

10

R = alkyl or aryl

X = Br or NO_2

Of all the N-acyl-2-nitroanilides investigated thus far only

N-acyl-5-substituted-7-nitroindolines, 10, are photosolvolyzed rather than photoreduced. In the presence of nucleophiles 5-substituted-7-nitroindolines, 11, and the corresponding carboxylic acid derivaties, 12, are formed in excellent yields (10). It is interesting to note that N-(3'-nitrobenzoyl)-5-nitroindoline, 10c, is photosolvolyzed in the presence of water, but photoreduced in alcohols.

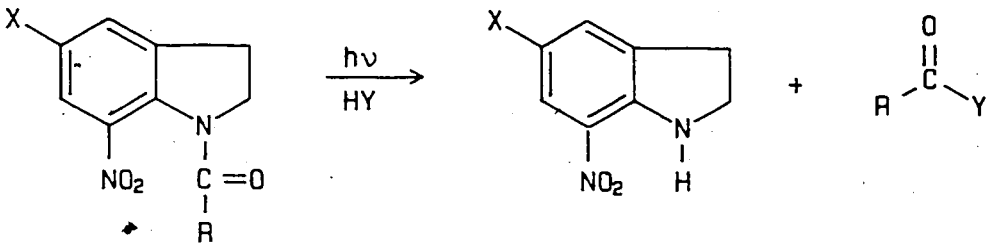

(10)

10 11 12

10 a, R = Ph ; X = Br

b, R = p-$MeOC_6H_4$; X = Br

c, R = m-$NO_2C_6H_4$; X = Br

d, R = 3,4-$Cl_2C_6H_3$; X = Br

e, R = 2-naphthyl ; X = Br

f, R = 2-furyl ; X = Br

g, R = n-C_7H_{15} ; X = Br

h, R = Ph ; X = NO_2

12 Y = OH

Y = OMe

Y = OEt

It would seem that the nitroindoline photoprotecting groups described by Amit have the potential for development in terms of the charge-mosaic uses described here.

It should be noted, however, that in all of Amit's studies attention has been directed only at the fate of the acyl unit, and little attempt has been made to identify the other reaction products.

In order to understand the detailed steps involved in the photochemistry of a molecule such as 10, it is helpful to review what is known about the photochemistry of nitroaromatics in general.

C. PHOTOCHEMISTRY OF NITROAROMATICS

(i) Introduction

The light induced reactions of aromatic nitro compounds attracted chemist's attention earlier than most other photoreactions [23]. However, despite these early results detailed synthetic and mechanistic studies have been only sporadic until fairly recently. The photochemistry of aromatic nitro compounds must still be regarded as a developing field, and in no way can our current understanding match the progress made in understanding carbonyl compound photochemistry.

In contrast to carbonyl photochemistry the transformations occurring after excitation of nitro compounds are intrinsically more complex in nature. The primary factors that contribute to the complexity of nitroaromatic photochemistry are weak excited state luminescence, the extremely short lifetimes of the excited state, and the plethora of secondary reactions both in excited and resulting ground states.

Although, electronically excited nitro compounds may undergo photoreduction [24,25,26], addition to π bonds [27,28], nucleophilic substitution at the aromatic nucleus [29,30], and rearrangements to

nitrites [31], only the aspect of photoreduction will be reviewed in detail here.

Depending on the reaction conditions, photochemical reduction of aromatic nitro compounds in hydrogen-donating solvents affords anilines and hydroxylamines with minor amounts of azo- and azoxybenzenes. Nitrobenzene, for example, was reported [32] to be photolytically reduced in isopropyl alcohol to give phenylhydroxylamine with a quantum yield of 1.14×10^{-2}. Subsequent secondary dark reactions accounted for the formation of azoxybenzene. While nitroso intermediates have been invoked to account for the azoxy-coupling reactions, their presence in the photolysis has not been proven.

Ortho and para monosubstituted nitrobenzenes with electron-withdrawing groups are photoreduced in 2-propanol to the corresponding anilines with quantum yields of disappearance of 0.12 - 0.45 (11). For systems with electron-donating substituents disappearance quantum yields of 0.02 - 0.03 were found, and phenylhydroxylamines were isolated (12). A linear correlation between the logarithms of the relative quantum yields of the substituted nitrobenzenes and nitrobenzene with the Hammett σ constant has been shown [33].

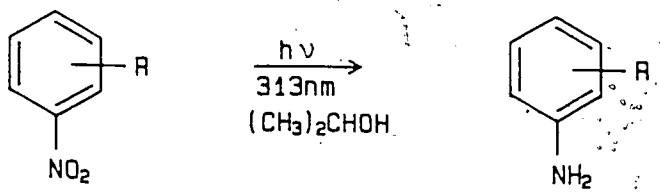

(11)

R = COOH, CN

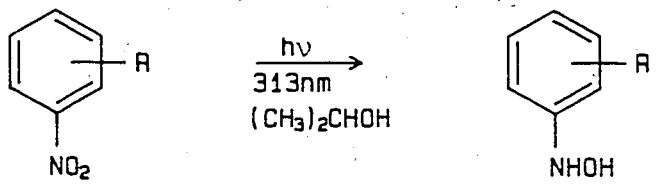

(12)

R = H, CH_3, OCH_3

(ii) Excited States Involved in Photoreduction

The triplet excited state is generally regarded as the reactive species in the photochemical reduction of aromatic nitrocompounds. Evidence for this conclusion is based on flash photolysis data [34], sensitization or quenching studies [35,36], and kinetic measurements [33,37]. For instance, the lack of photochemical reduction of nitrobenzene in the presence of perfluoronaphthalene (E_T =56 kcal/mole), a molecule with a relatively low triplet energy, has been interpreted as interception of triplet nitrobenzene before H atom transfer can occur [36]. Direct evidence for the involvement of a triplet reactive state in hydrogen abstraction was presented by Capellos [34] in the flash photolysis study of 2-nitronaphthalene.

Regardless of whether the lowest energy excited triplet state configuration is n,π^* or π,π^*, a relatively efficient singlet-triplet transition (Φ = 0.6 - 0.8) is common for nitroaromatics [37,38]. On the other hand, the quantum yields for photoreduction of nitroaromatics are generally very low. These facts, in conjunction with the low phosphorescence efficiencies, suggest fast radiationless decay as the prime energy dissipation mode. Energy transfer analysis corroborated a

short lifetime, ($\tau \simeq 10^{-9}$ s) for the lowest excited triplet of nitrobenzene. Even at high concentrations (2.4 moles/liter) of cis-piperylene not all nitrobenzene triplets can be quenched [37].

Frolov [39], by measuring the one-electron reduction potentials ($-E_{1/2}$) of various substituted nitroaromatics, and plotting these against their triplet energies, established the existence of three relationships. These, he claimed, correspond to various reactivities of the nitro compounds in the excited state. By analogy to carbonyl chemistry, compounds with lowest n, π^* (or π , π^* with considerable n, π^* contribution) triplet states possess well defined electrophilic character, and undergo predominantly hydrogen or electron abstraction. Those compounds with a lowest π , π^* state, such as 1-nitronaphthalene, have a diminished capacity to abstract hydrogen, and undergo photochemical substitution and reduction reactions. Finally, nitroaromatics with lowest charge-transfer triplet states do not correlate systematically, and are photochemically stable.

The relative energies and lifetimes of excited states in substituted nitroaromatics are strongly dependent on the solvent system. For example, the nanosecond flash photolysis of 2-nitronaphthalene in nonpolar and polar solvents showed a triplet excited state absorption. However, the absorption maximum and lifetime were dependent on solvent polarity [34]. The triplet excited state of 2-nitronaphthalene behaves like an n,π^* state in nonpolar solvents, while in polar media a intramolecular charge-transfer character is dominant [40]. Goerner and Schulte-Frohlinde [41] showed that temperature and solvent polarity have a marked effect on the triplet lifetime of 4-nitrostilbenes. A plot

of log τ as a function of the empirical solvent polarity parameter E_T [42] showed a linear relationship. Cowley [43] attributed the increased lifetime in polar solvents to a charge separation in the triplet state (Fig. 2). If the energy of the zwitterionic component, ^3Z, of the lowest triplet state, T_1, is increased by an increase in solvent polarity the T_1-S_0 energy gap becomes greater, and the radiationless passage from the T_1 to the S_0 surface is correspondingly slower.

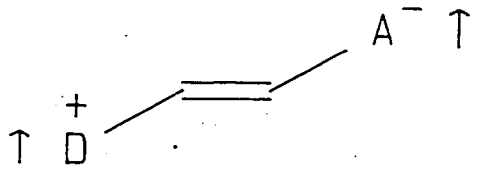

Figure 2: Triplet zwitterionic configuration, ^3Z.

Flash photolytic, phosphorescence and photochemical results [44] demonstrated that the lowest triplet state of p-nitroaniline is an intramolecular charge transfer state. In this state charge transfer from the amine to the aromatic ring is accentuated by the electron-withdrawing nitro moiety.

(iii) Photoreductions under Neutral Conditions

The primary step in the photochemical reduction mechanism of

nitrobenzene under neutral conditions is the abstraction of a hydrogen by the n,π^* triplet state. Several subsequent dark reactions involving the two initial products, $PhNO_2H\bullet$ and $R\bullet$, have been suggested to account for the formation of phenylhydroxylamine and acetone. Testa [32] proposed the following scheme for the photoreduction of nitrobenzene in 2-propanol:

$$ArNO_2 \xrightarrow{h\nu} {}^3(ArNO_2)^*$$

$${}^3(ArNO_2)^* + (CH_3)_2CHOH \longrightarrow ArNO_2H\bullet + (CH_3)_2COH\bullet$$

$$ArNO_2H\bullet + (CH_3)_2COH\bullet \longrightarrow ArN(OH)_2 + (CH_3)_2CO$$

$$ArN(OH)_2 + (CH_3)_2CHOH \longrightarrow ArNOH\bullet + (CH_3)_2COH\bullet + H_2O$$

$$ArNOH\bullet + (CH_3)_2COH\bullet \longrightarrow ArNHOH + (CH_3)_2CO$$

Scheme 2

Phenylhydroxylamine is believed to oxidize in air to nitrosobenzene. Coupling of phenylhydroxylamine with nitrosobenzene forms azoxybenzene (13), (14).

$$ArNHOH + 1/2\ O_2 \longrightarrow ArNO + H_2O \qquad (13)$$

$$ArNHOH + ArNO \longrightarrow ArN(O)NAr + H_2O \qquad (14)$$

For nitrobenzene, which has a lowest triplet state of n,π^* character, the rate constant for hydrogen abstraction, k_H, in 2-propanol is as high as $10^6\ M^{-1}s^{-1}$ [45]. Similarly, 4-nitro-N,N-dimethyl-naphthylamine, which also possesses a lowest n, π^* triplet state in

2-propanol, again displays a high rate of hydrogen abstraction ($k_H = 4x10^7\ M^{-1}s^{-1}$) [46]. A much slower hydrogen abstraction rate, however, was reported for 2-nitronaphthalene in 2-propanol ($k_H = 4.5x10^4\ M^{-1}s^{-1}$) [34]. This has been attributed to the high degree of intramolecular charge-transfer of 2-nitronaphthalene in 2-propanol.

Sutcliffe et al [47,48] and more recently Lunazzi [49] demonstrated that the photolysis of nitroaromatics in hydrogen-donor solvents also affords the corresponding alkoxy nitroxides $ArNO_2R\bullet$. These are formed by addition of the free radical, R•, to a ground state nitroaromatic molecule. It was suggested [48] that the decay mechanism of alkoxynitroxides derived from sterically hindered nitrobenzenes proceeds via homolytic N-OR bond fission leading to a nitrosoaromatic and an alkoxy radical (Scheme 3). It is interesting that the primary photochemical reduction product, $ArNO_2H\bullet$, has thus far eluded detection.

$$ArNO_2 \xrightarrow{h\nu} {}^3(ArNO_2)^*$$

$${}^3(ArNO_2)^* + R\text{-}H \longrightarrow ArNO_2H\bullet + R\bullet$$

$$ArNO_2H\bullet \longrightarrow \text{products} \quad \text{(Scheme 2)}$$

$$ArNO_2 + R\bullet \longrightarrow ArNO_2R\bullet$$

$$ArNO_2R\bullet \longrightarrow ArNO + RO\bullet$$

Scheme 3

Studies have shown that the mechanistic course followed in the photoreduction of the nitro moiety can take place intramolecularly if the molecule contains an appropriate ortho substituent.

Photoreduction of nitrobenzenes with ortho groups containing -CH=X bonds was observed as early as 1901. For example, Ciamician and Silber [23] reported the phototransformation of o-nitrobenzaldehyde to o-nitrosobenzoic acid (15).

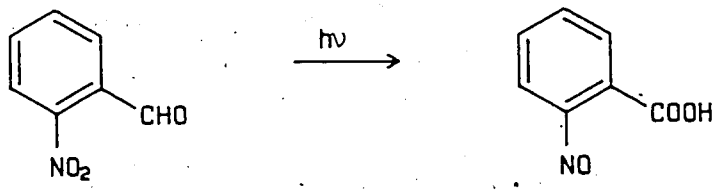

(15)

On the basis of a recent laser flash photolysis study, Scaiano [50] proposed that the photolysis of o-nitrobenzaldehyde in solution proceeds via a triplet state intermediate with a lifetime of 0.6 ns. Hydrogen abstraction from the aldehyde moiety forms a short lived biradical ($\tau < 10$ ns) which decays to the aci-nitro compound 13. This intermediate then decays both in the presence or absence of water to the product 14 (Scheme 4).

A year after Ciamician and Silber's reported transformation of o-nitrobenzaldehyde, Sachs [51] showed that 2-nitrobenzylideneaniline is converted, on irradiation in solution or the solid state, to 2-nitrosobenzanilide. Flash photolysis of 2-nitrobenzylideneaniline suggested a ketimine intermediate, 15, in the phototransformation [52] (16).

N-aryl-2-nitrobenzamides, 16, photoisomerize to 2-(2-hydroxyphenylazo)benzoic acid, 17 [53]. An amide H-abstraction has been suggested as the initial photochemical step (Scheme 5). When the anilide ring bears electron withdrawing groups, such that R^1, R^2 or R^3 is

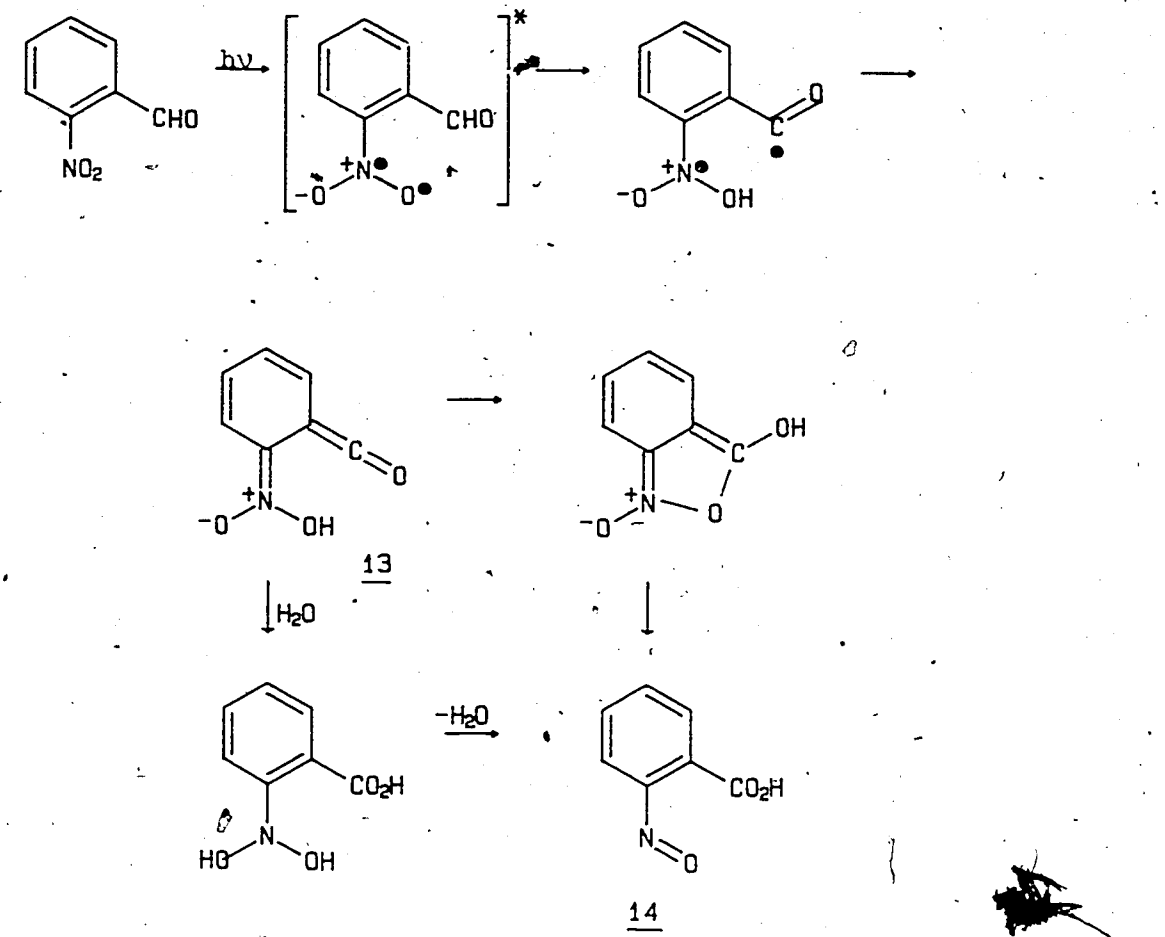

Scheme 4

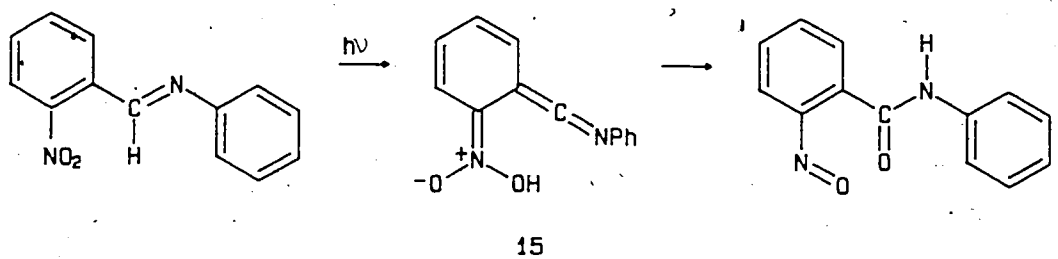

(16)

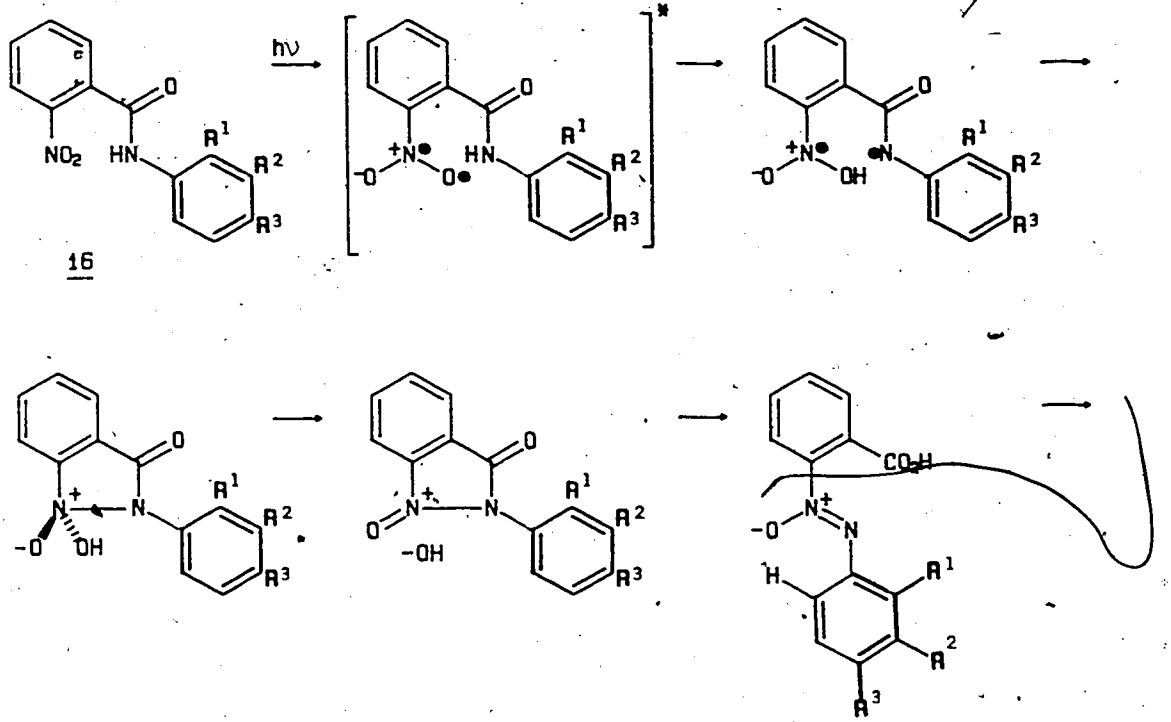

16

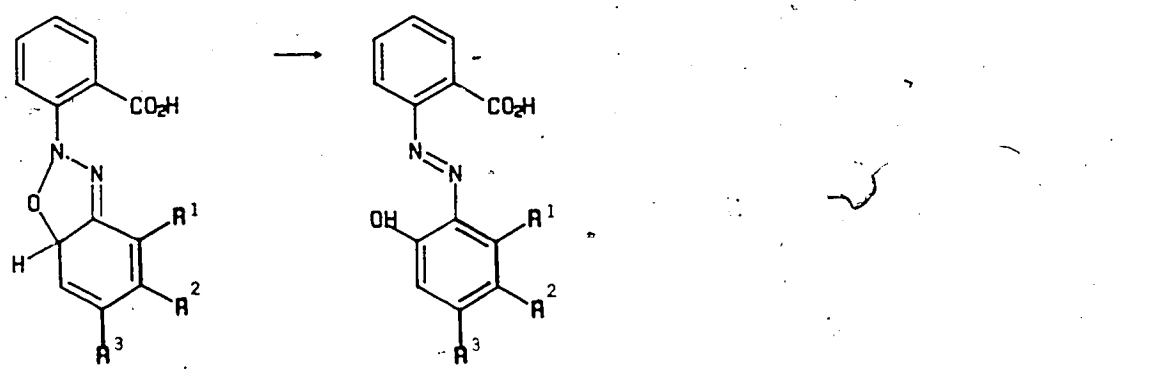

17

Scheme 5

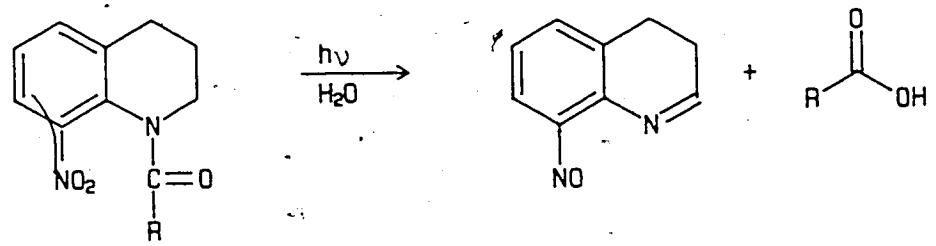

9

R = Ph or 3,4-$Cl_2C_6H_3$

(17)

NO_2 or CN, reactants are stable to irradiation. Similarly, N-alkyl substituted-2-nitrobenzamides or 4-nitrobenzamides are photostable.

When the ortho moiety of substituted nitrobenzenes is a heteroatom, fragmentation, as well as nitro reduction products are frequently observed. For example, a free carboxylic acid and a reduced nitro derivative are the photoproducts of N-acyl-2-nitroanilide 9 photolysis [21] (17).

Photolysis of N-acyl-2-nitrodiphenylamines 18, releases the acyl group as a carboxylic acid by oxygen transfer from the nitro to the benzoyl group [54]. When the photolysis of 18 is conducted in benzene some phenylbenzoate is formed. The conversion of 18 to 20 is most efficient when the acyl moiety is aromatic and the substituent R^1 is capable of stabilizing a radical intermediate. Maki [54] proposed a mechanism in which an excited nitro group (n, π^*) adds to an amide carbonyl C=O bond. The intermediate, 19, subsequently fragments to an acyloxy- and a nitroso radical (Scheme 6).

While the exact fragmentation mode of N-acyl-2-nitroanilides is still unknown, several important observations have been reported. Amit [20] in the photorearrangement of various N-acyl-2-nitroanilides established that only tertiary amides undergo a reaction to yield the appropriate free acids, and that the carboxylic acid hydrogen comes from the reactant or solvent, whichever is the better hydrogen-donating source. The most comprehensive observations were reported for the photocleavage of N-acyl-1,2,3,4-tetrahydro-8-nitroquinolines (17). From ^{18}O labelling experiments it was found that in the presence of $H_2{}^{18}O$ no ^{18}O was incorporated into the free carboxylic acid,

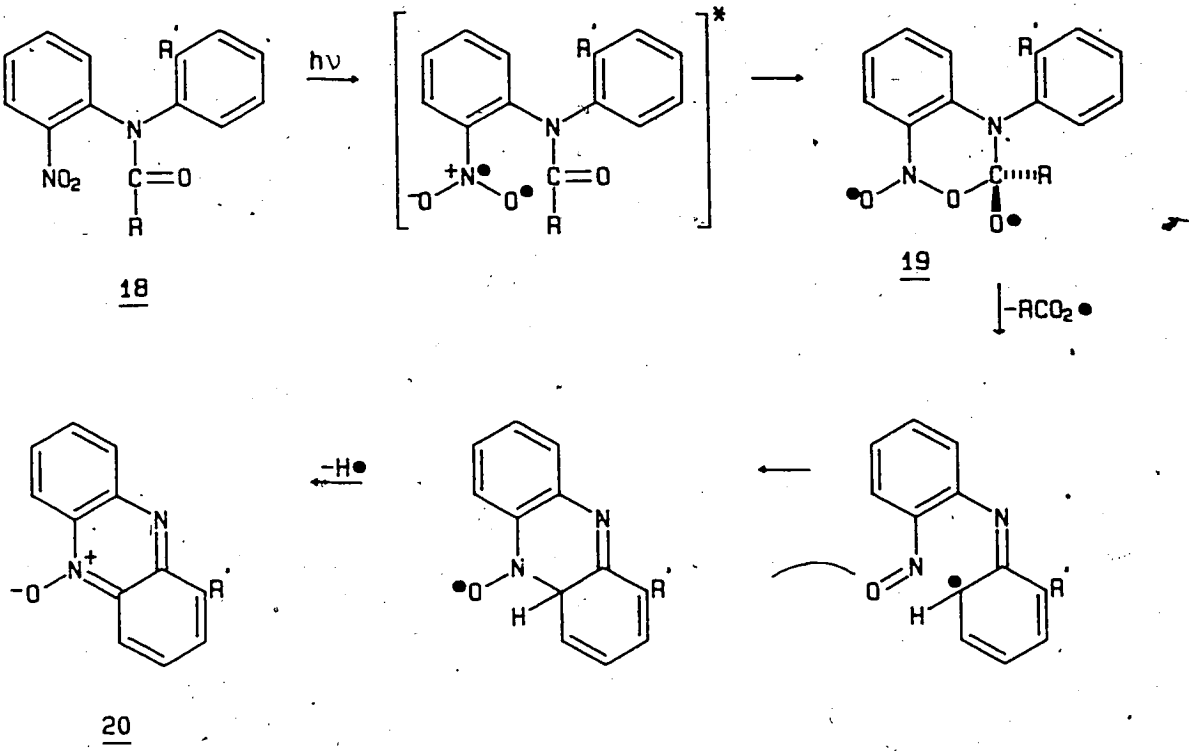

Scheme 6

rather, an ^{18}O atom was transferred from an ^{18}O-enriched nitro group to the acyl moiety. Since no dehydrogenation of H-donor solvent was observed, and the fragmentation process also takes place in poor H-donating solvents such as benzene, Amit concluded that oxygen transfer from the nitro group to the acyl unit precedes hydrogen abstraction.

Recently Binkley [55] proposed two mechanistic pathways for the photochemical cleavage of N-acyl-2-nitroanilides (Scheme 7): The pathway followed is primarily determined by the availability of the hydrogen

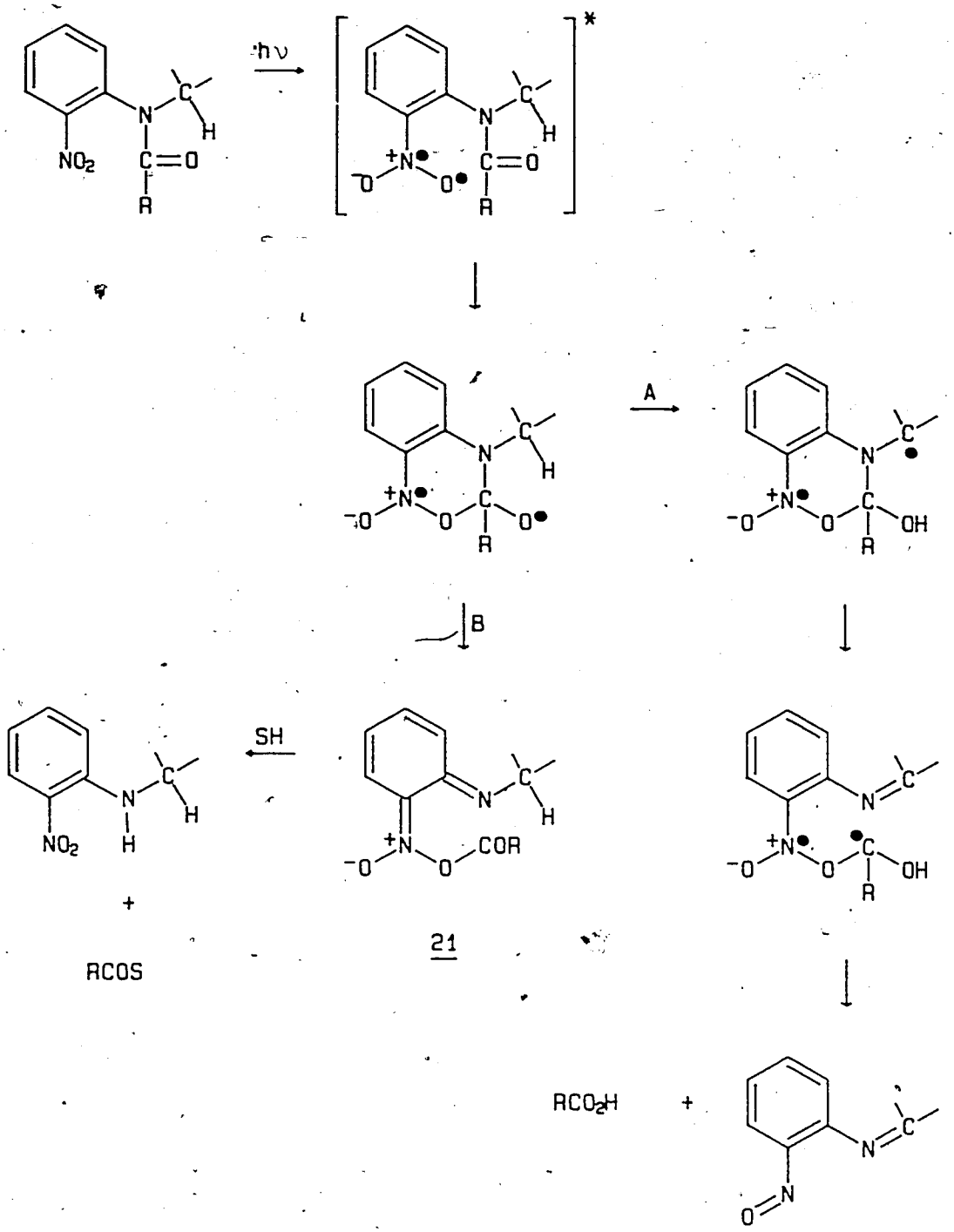

Scheme 7

attached to C-2. When a hydrogen is readily available, the reaction is thought to follow path A, and the nitro group loses an oxygen. For relatively rigid ring systems (e.g. five membered or smaller) H-2 is held too far from the carbonyl group for hydrogen abstraction, and a nitronic carboxylic acid anhydride intermediate 21 is thought to be formed (path B).

iv) Photoreductions Under Basic Conditions

Nitro compounds are smoothly reduced to hydroxylamines on irradiation under basic conditions. However, the principle products isolated are often azoxy- and azobenzenes which arise from the base catalyzed condensation of the hydroxylamine derivative with a nitroso intermediate. The fact that 1-nitronaphthalene resists hydrogen abstraction in ethanol [56], but is smoothly reduced in diethylamine [35], suggests a mechanism different from the hydrogen abstraction mechanism shown in Scheme 2. Irick and coworkers [57] in 1969 were the first to propose electron transfer, followed by proton transfer, as the initial stages of the reduction process (Scheme 8).

$$ArNO_2 \xrightarrow{h\nu} {}^3(ArNO_2)^*$$

$${}^3(ArNO_2)^* + R'_2NCH_2R \longrightarrow ArNO_2^{\bullet -} + R'_2NCH_2R^{\bullet +}$$

$$ArNO_2^{\bullet -} + R'_2NCH_2R^{\bullet +} \longrightarrow ArNO_2H^{\bullet} + R'_2NCHR^{\bullet}$$

$$ArNO_2 + R'_2NCHR^{\bullet} \longrightarrow ArNO_2^{\bullet -} + R'_2N{=}CHR^{+}$$

$$H_2O + R'_2N{=}CHR^{+} \longrightarrow R'_2NH + RCHO + H^{+}$$

$$ArNO_2H^{\bullet} \xrightarrow{red} ArNO$$

$$ArNO \xrightarrow{red} ArNHOH$$

Scheme 8

The quantum yield for disappearance of substituted nitrobenzenes in ethanol or methanol is greatly enhanced when the solvent contains sodium alkoxide or sodium hydroxides. Frovlov [58] demonstrated the participation of the alkoxides in the initial photoreduction step (Scheme 9). The relative reactivity of various alkoxides parallels their oxidation potentials i.e. $i\text{-PrO}^- > \text{EtO}^- > \text{MeO}^-$. It has been proposed that the alkoxide ion reacts in a similar manner to the amines outlined above in Scheme 8.

$$\text{ArNO}_2 \xrightarrow{h\nu} {}^3(\text{ArNO}_2)^*$$

$${}^3(\text{ArNO}_2)^* + \text{CH}_3\text{O}^- \longrightarrow \text{ArNO}_2^{\bullet} + \text{CH}_3\text{O}^{\bullet}$$

$$\text{ArNO}_2^{\bullet} + \text{CH}_3\text{O}^{\bullet} \longrightarrow \text{ArNO}_2\text{H}^- + \text{CH}_2\text{O}$$

Scheme 9

Electron-transfer is generally regarded as the primary photochemical step in the reduction of nitro aromatics under basic conditions.

v) Photoreductions Under Acidic Conditions

Nitroaromatics are also photoreduced in the presence of hydrochloric acid to give aniline [59] and chlorinated aniline derivatives [60]. An example is shown in equation (18).

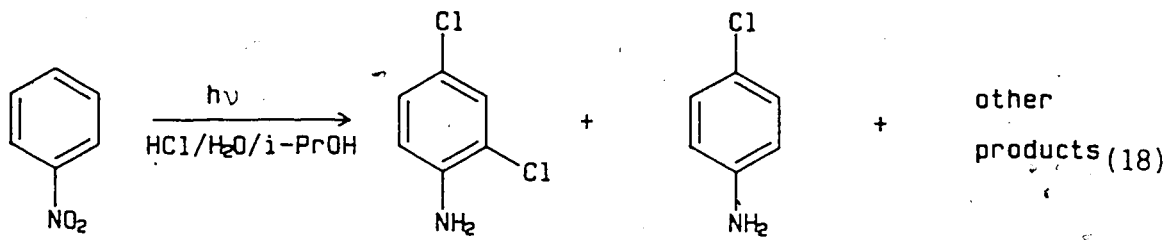

(18)

Addition of HCl causes a marked enhancement in the efficiency of the reactions. From an examination of the HCl catalyzed photoreduction of nitrobenzene by 2-propanol, Wubbels [60] proposed electron transfer from the chloride ion to the photoexcited nitrobenzene as the primary process. Flash photolysis of 5-nitroquinoline [61] provided additional evidence that electron transfer is indeed the primary process in the HCl catalyzed photoreduction of nitroaromatics.

Although the presence of the chloride ion is critical, both the acid, and the alcohol, play an essential role in the overall reduction process (Scheme 10).

$$ArNO_2 \xrightarrow{h\nu} {}^3(ArNO_2)^*$$

$${}^3(ArNO_2)^* + Cl^- \longrightarrow ArNO_2^{\bullet-} + Cl^\bullet$$

$$ArNO_2^{\bullet-} + H^+ \rightleftharpoons ArNO_2H^\bullet \quad (pKa\ 3.2)$$

$$(CH_3)_2CHOH + Cl^\bullet \longrightarrow HCl + (CH_3)_2COH^\bullet$$

$$ArNO_2 + (CH_3)_2COH^\bullet \longrightarrow ArNO_2H^\bullet + (CH_3)_2CO$$

$$2ArNO_2H^\bullet \longrightarrow ArNO_2 + ArN(OH)_2$$

$$ArN(OH)_2 \longrightarrow ArNO + H_2O$$

Scheme 10

In summary, electronically excited nitroaromatics are frequently reduced to their nitroso analogue. Under neutral experimental conditions intra- or intermolecular hydrogen abstraction by the excited nitro moiety is the proposed initial step in the photoreduction process. When the reaction medium, on the otherhand, is either basic or acidic, electron

transfer to the excited nitro functionality is the proposed initial photochemical step in the reduction of nitroaromatics. Furthermore, studies have shown that addition of a free radical, R• , to a ground state nitroaromatic molecule can also lead to the nitroso compound. Thus the primary photochemical steps of hydrogen abstraction and electron transfer, or even subsequent free radical addition to a ground state nitroaromatic molecule, are relevant factors that need to be considered when studying the mechanism of photosolvolysis of 10.

D. α -CLEAVAGE REACTIONS OF AMIDES

(i) Introduction

As already indicated above, the N-acyl-2-nitroindolines, 10, seemed especially attractive as photoprotecting groups for a photoactive membrane. While the exact fragmentation mode of these molecules is still unknown an α -cleavage reaction about the amide bond, however, has been established from the preliminary product analysis study reported by Amit [21,22]. Since the fragmentation sequence about the amide bond is a critical step in terms of the photosolvolysis mechanism of N-acyl-2-nitroindolines, it is helpful to present a literature review of the photolytic α -cleavage reactions of amides.

(ii) Photo-Fries Rearrangement of N-Arylamides

The photoinduced Fries rearrangement of aryl esters was first reported in 1960 by Anderson and Reese [62]. Five years later, the photolysis products of N-acylanilides were reported by Stenberg and

co-workers [63]. For example, when benzanilide, 22, is irradiated in ethanol four photoproducts are isolated (19).

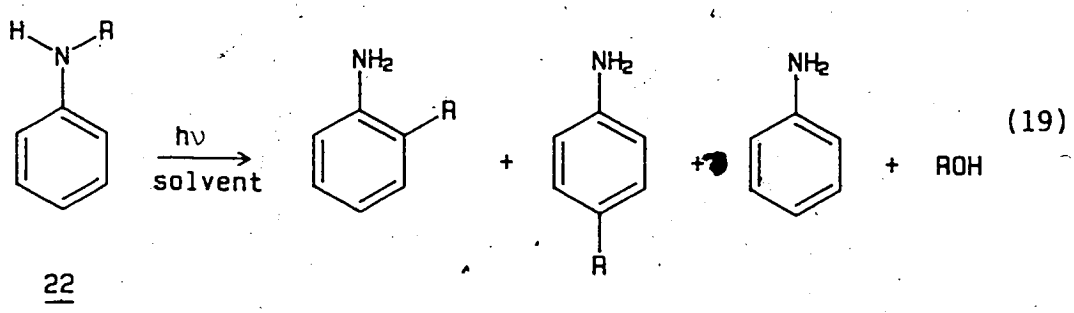

(19)

22

R=COPh	14%	12%	trace	27%

The quantum yield for disappearance of 22, R=COPh in ethanol was reported by Wiley [64] to be $(4.1 \pm .4) \times 10^{-3}$ moles Einstein^{-1}. It is noteworthy that the quantum yield of reactant loss decreases both with increasing solvent polarity, and with increasing wavelength of the incident light. Benzoic acid is produced as one of the minor products. However, while the formation of benzoic acid was reported to occur only in air saturated solutions, oxygen has no effect on quantum yields of disappearance of the starting amide.

A similar photoreaction was observed for N-benzoyl-2,3-dihydro-benzoxazol-2-one, 23. Five photoproducts are produced upon irradiation of 23. Ishida [65] assumed that the reaction proceeded according to Scheme 11.

Both, the primary and secondary photochemical processes of acetanilide, have been extensively studied by Shizuka [66,67]. He reported that the photochemical primary process involves predissociation

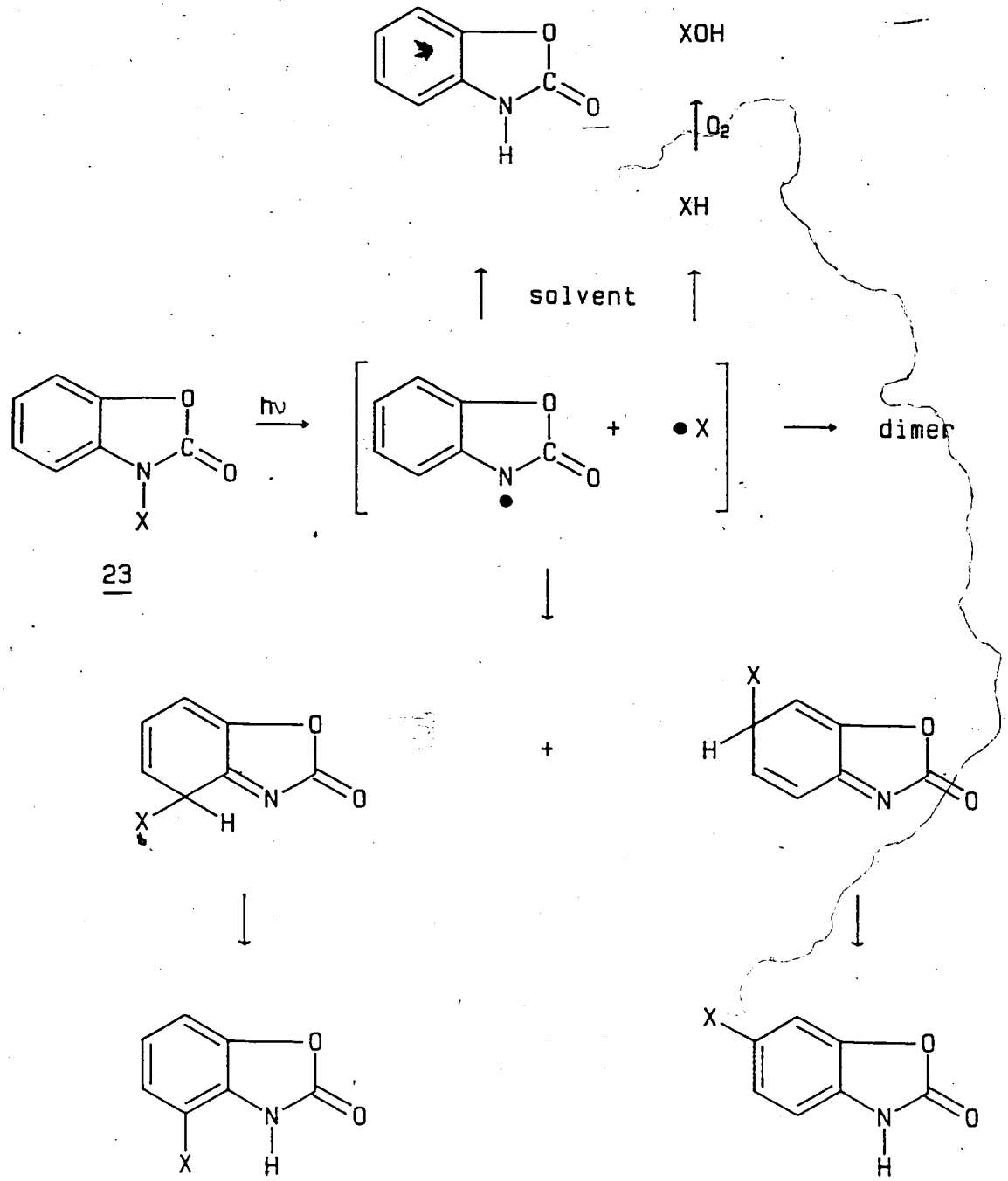

Scheme 11

caused by intersystem crossing $S_1(\pi, \pi^*) \longrightarrow {}^3\delta_0$(N-C) (Fig. 3). Evidence for the involvement of a reactive singlet state was found from flash photolytic studies [68,69]. However, to date there still seems to be some dispute whether the rearrangement occurs from a singlet n, π^* or π , π^* state [65,70].

Some of the radicals formed in the homolytic cleavage diffuse apart, while the remainder of the radicals are kept in the solvent cage long enough to recombine. The odd π electron densities of the anilino radical allows recombination either at the ortho or para sites, or collapse back to starting material [67]. A energy state diagram for acetanilide rearrangement as shown in Fig. 4 was proposed by Shizuka [67].

(iii) Further α -Cleavage Reactions Which Occur Without Rearrangement

Recently Hasegava [71] reported that o-(N-benzylbenzoylamino)-benzophenone, 24, can undergo either deacylation via homolytic cleavage of the CO-N bond or photodealkylation depending on solvent polarity (Scheme 12). Interestingly, no photo-Fries rearrangement products were observed. The quantum yield for deacylation of o-(N-methylacetylamino)-benzophenone reaches a maximum value in methanol and decreases in less polar solvents.

It has been suggested that these results can be understood in terms of relative disposition of the n,π^* and the π , π^* triplet states of the ketone. In general, the reactive energies of π , π^* states of a carbonyl compound are lowered and n,π^* states raised as the polarity and hydrogen bonding properties of the medium is increased.

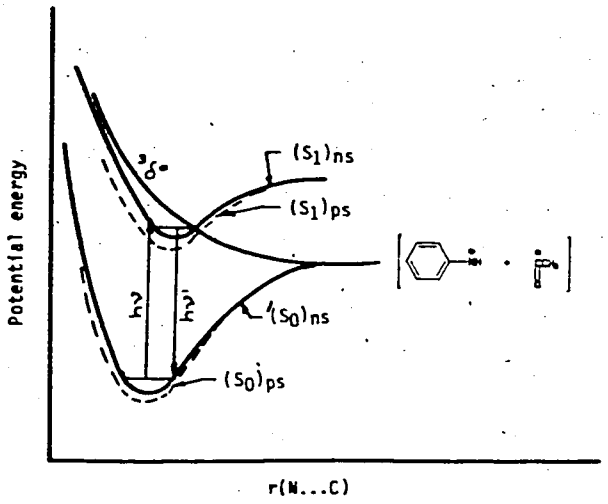

Figure 3: A schematic potential energy diagram for Ph-NH...$COCH_3$ system [67].

ns: nonpolar solvent ps: polar solvent

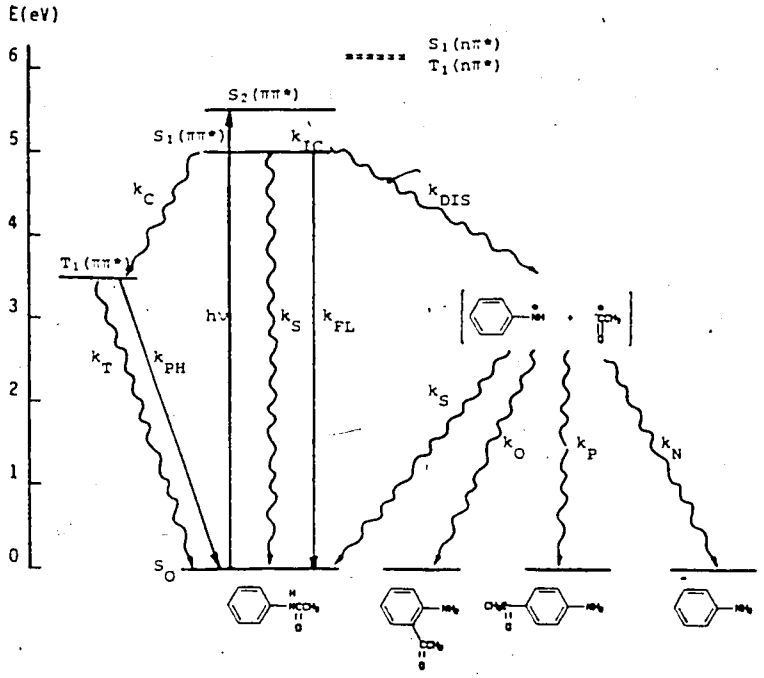

Figure 4: Energy state diagram for acetanilide [67].

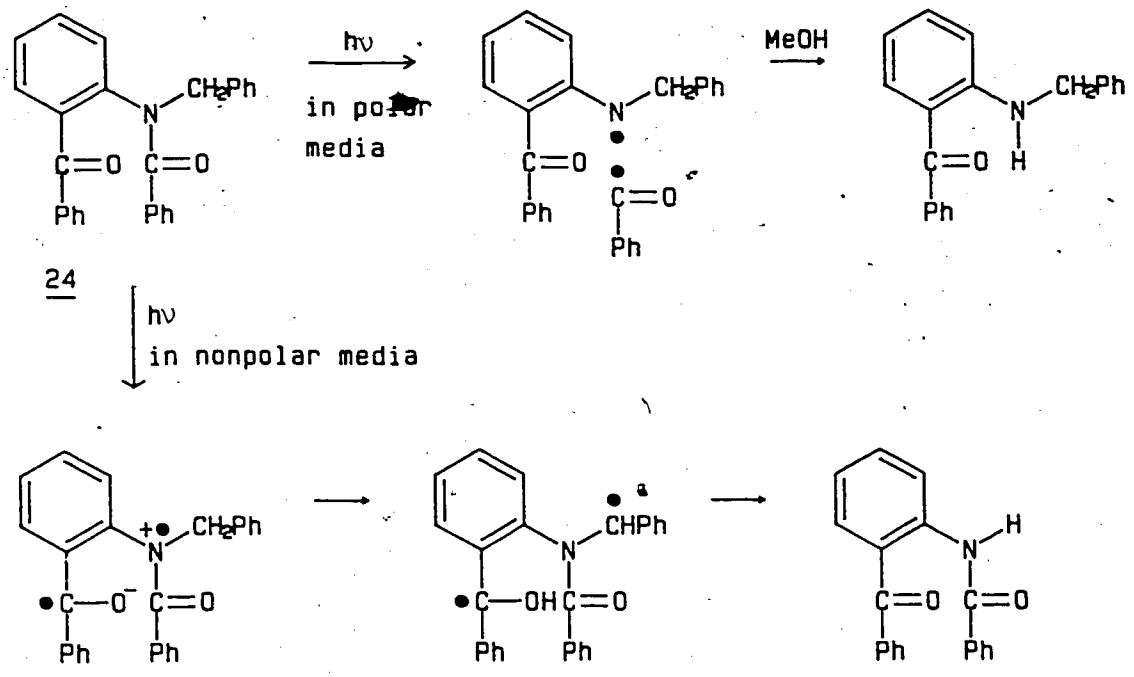

Scheme 12

Thus, in benzene, hydrogen abstraction from the n,π^* triplet is suggested to be the predominant pathway, whereas in methanol photodeacylation is thought to occur from the π,π^* excited state of the benzoylamino-ketone.

Acetoxyacetophenones do not undergo the photo-Fries rearrangement. Miranda [72] attributed the effect to fast intersystem crossing of aromatic ketones to an unreactive triplet excited state.

Various other studies [73,74,21] have also shown that with nitro substituted N-arylamides photo-Fries rearrangement products are not observed. Apparently, the nitro functionality either deactivates the system before CO-N bond homolysis, or the involvement of triplet radical pairs prevent in-cage radical recombination to afford rearrangement

products.

Generally, experimental evidence for N-arylamides confirms the homolytic nature of the fragmentation step and suggests a singlet character of the excited state precursor of the radical pair. Because solvents and/or substituents can enhance intersystem crossing, fragmentation about the CO-N bond of N-arylamides has also been reported from the triplet excited state. As a result, homolytic α -cleavage of N-arylamides may, in principle, be observed from either the singlet or the triplet excited state.

E. STATEMENT OF PROBLEM AND OBJECTIVE

A key feature in the development of a charge-mosaic membrane is the photochemical activation of the anionic, cationic and neutral domains. The N-acyl-5-bromo-7-nitroindoline photoprotecting group, 10, seemed particularly attractive for this project, in as much as the photosolvolysis reactions of interest occur in near quantitative yields, using long wavelength UV (> 350 nm). In principle, the protecting group can be recycled (Scheme 13).

Because of the photoprotecting groups pivotal nature a comprehensive knowledge of the fragmentation process and its efficiency is imperative. However, no definitive mechanistic information has to date appeared in the literature. Therefore, the aim of this research project was to shed some light on both the mechanism and efficiency of this unique photolysis reaction. The compound chosen for this investigation was N-benzoyl-5-bromo-7-nitroindoline, 10a.

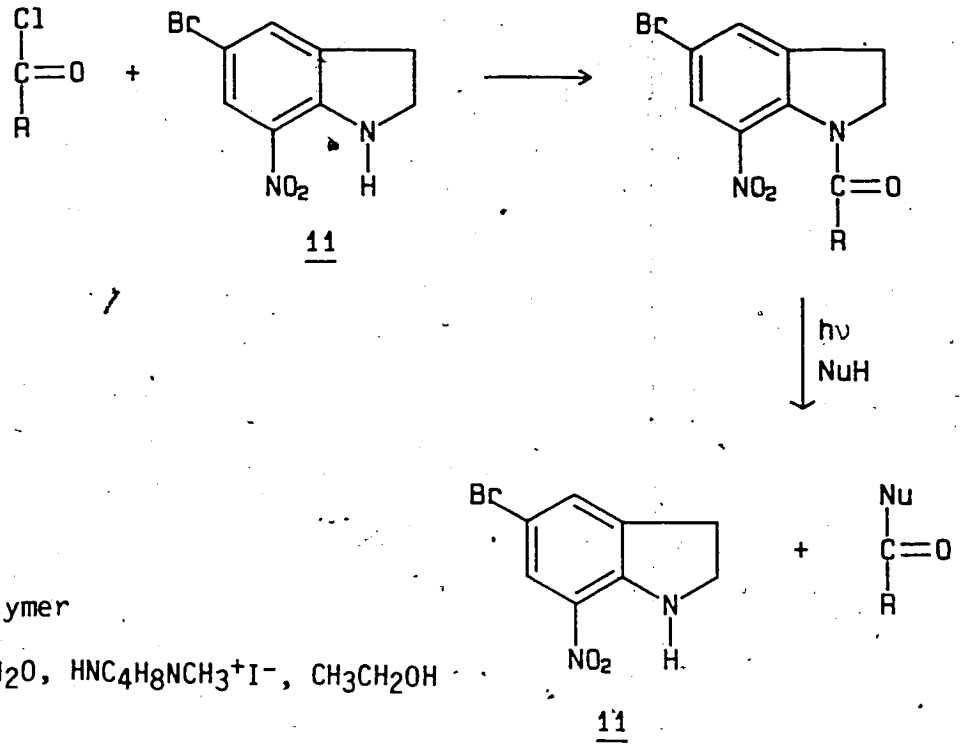

R = Polymer

NuH = H_2O, $HNC_4H_8NCH_3^+I^-$, CH_3CH_2OH

Scheme 13

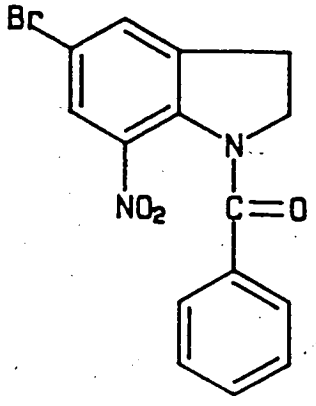

10a

CHAPTER II

RESULTS AND DISCUSSION

A. INTRODUCTION

This mechanistic study of N-benzoyl-5-bromo-7-nitroindoline photofragmentation falls into five major categories: (i) Synthesis and electronic spectra of reactant; (ii) Photoproduct analysis; (iii) Solvent and pH effects; (iv) Photofragmentation study; and (v) Quantitative analysis. The results obtained on each topic are presented and discussed separately. Each discussion attempts to integrate the results obtained in this study with those of other workers in terms of a mechanism consistent with experimental evidence. In the conclusion, a complete mechanism for the photofragmentation of N-benzoyl-5-bromo-7-nitroindoline will be suggested. The generality of this mechanism for other N-acyl-2-nitroanilide photofragmentations is examined.

B. SYNTHESIS

N-benzoyl-5-bromo-7-nitroindoline and its substituted derivatives used for the linear free energy relationship study, were synthesized via a five step procedure from indoline. The synthetic pathway is outlined in Scheme 14.

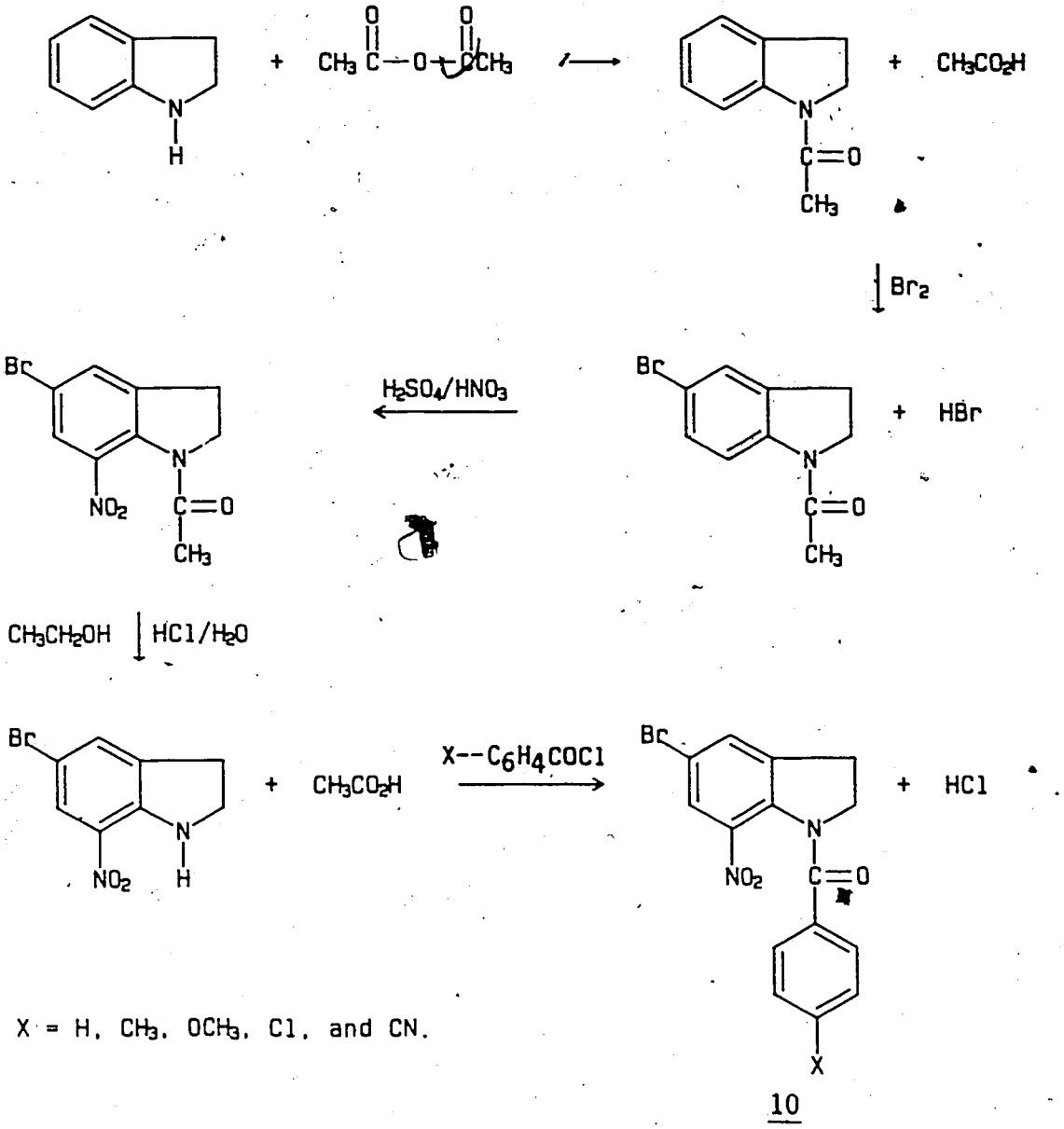

10

Scheme 14

All of the N-acyl-5-bromo-7-nitroindolines prepared were characterized by ^{1}H NMR, ^{13}C NMR and mass spectroscopy, and UV spectrophotometry. Preparative and analytical details are given in the experimental chapter.

C. ELECTRONIC SPECTRA OF 1-BENZOYL-5-BROMO-7-NITROINDOLINE

(i) Introduction

Important information concerning the energetics and dynamics of electronically excited states of organic molecules can be obtained from radiative transition measurements. From the absorption and emission spectra, for example, state electronic energies and multiplicities are often readily inferred. In some cases analysis of the spectra allows the deduction of equilibrium nuclear geometry and dipole moments, and gives evidence for the formation of excited molecular complexes.

(ii) Results

(a) UV-Spectra

The UV-spectrum of 10a in acetonitrile was characterized by four intense absorption bands at 215, 234, 260, and 352 nm (ε = 3564 cm^{-1} M^{-1}) (Figure 5). (The λ_{max} of the lowest energy absorption bands and corresponding molar extinction coefficients of 4'-substituted 10a are given in Table 4 pg 80). A slight bathochromic shift of the absorption spectrum, and considerable broadening of bands, was revealed in going from a non-polar solvent (cyclohexane : CH_3CN, 49:1) to a polar (CH_3CN:H_2O, 2:3) solvent medium. The red shift of the lowest energy band corresponds to 1.9 kcal/mole lowering of the first excited singlet transition (λ_{max} non-polar = 346 nm, λ_{max} polar = 354 nm).

(b) Fluorescence Spectra

A broad structureless emission band at 555 nm was recorded when 10a in CH_3CN was excited at 354 nm and monitored between 400-650 nm

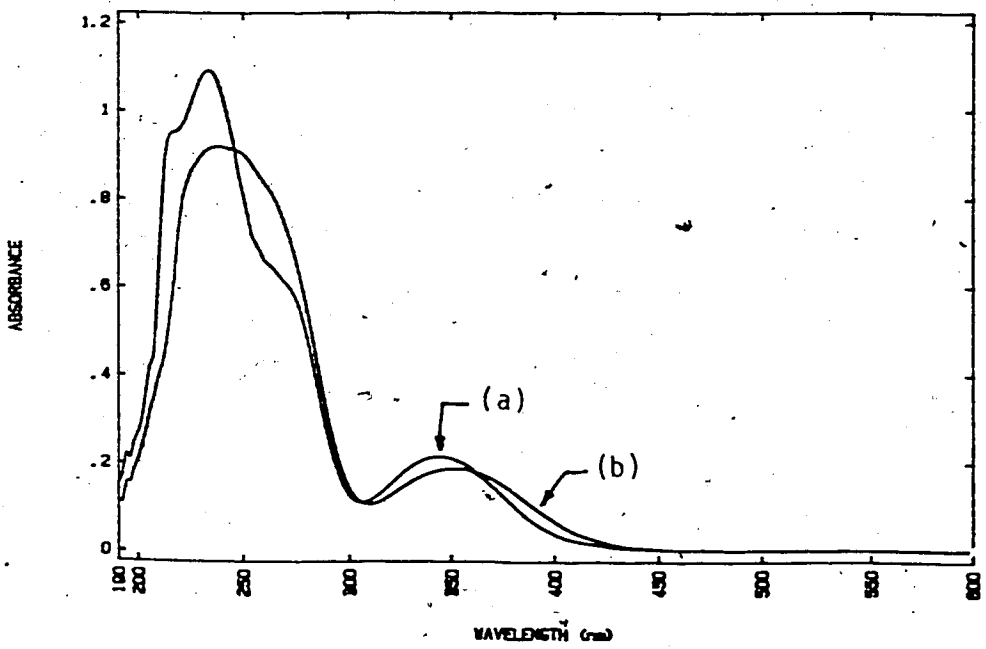

Figure 5 : UV-absorption spectrum of 10a in (a) acetonitrile-cyclohexane (1:49) and (b) acetonitrile-water (2:3).

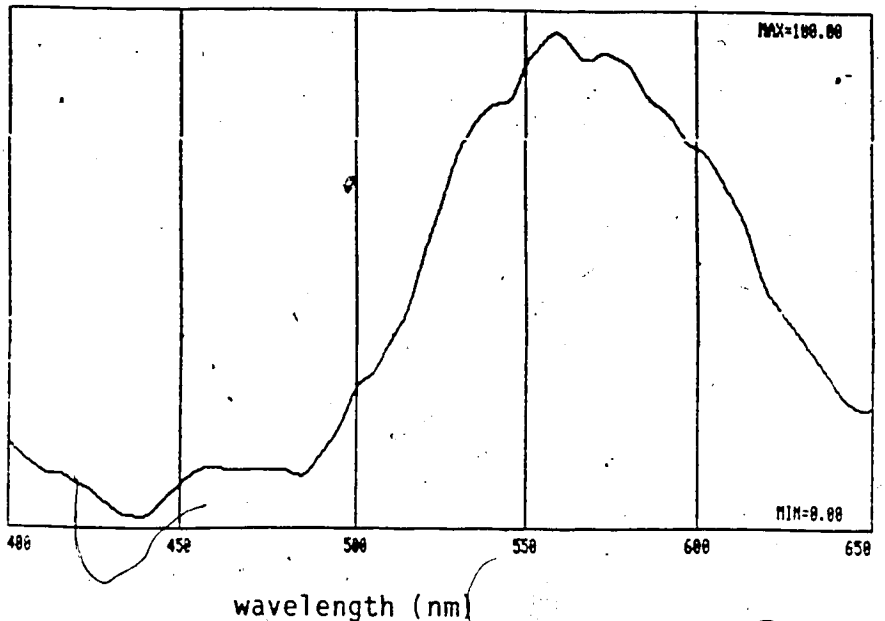

Figure 6 : Fluorescence-emission spectrum of 10a in anhydrous acetonitrile.

(Figure 6). The presence of oxygen in solution had no noticeable quenching effect on the emission spectrum. Identical spectra were obtained in aerated or argon degassed solutions. No fluorescence emission was observed when 10a was dissolved in aqueous CH_3CN (mole fraction of water = .66) and excited at 354 nm.

(c) Phosphorescence Spectra

Phosphorescence measurements of 10a in a 2-methyltetrahydrofuran glass (77 K) showed radiative light emission from at least two distinct species (Fig. 7). With delay times between 1.0×10^{-5} and 5.0×10^{-5} s, a rapid decay of the shorter wavelength emission band at 515 nm was noted. The longer wavelength emission band at 545 nm could still be detected as long as 1.0×10^{-3} s after excitation of 10a. A five fold dilution of 10a in the 2-methyltetrahydrofuran glass matrix caused a reduction in the total emission band intensity, but principally in the shorter wavelength radiative emission region. When the glass matrix of 10a was examined immediately after emission measurement the area of light impingement was distinctly yellow. In order to exclude the possibility of luminescence due to solvent impurity the neat solvent glass was also excited at 354 nm but no emission was recorded.

Two emission bands were also detected when 5-bromo-7-nitroindoline, 11a, was excited at 354 nm. The shorter wavelength band at 520 nm again rapidly decayed ($< 5.1 \times 10^{-5}$ s), whereas the longer wavelength emission at 545 nm persisted for a considerably longer period of time ($> 7.0 \times 10^{-5}$ s).

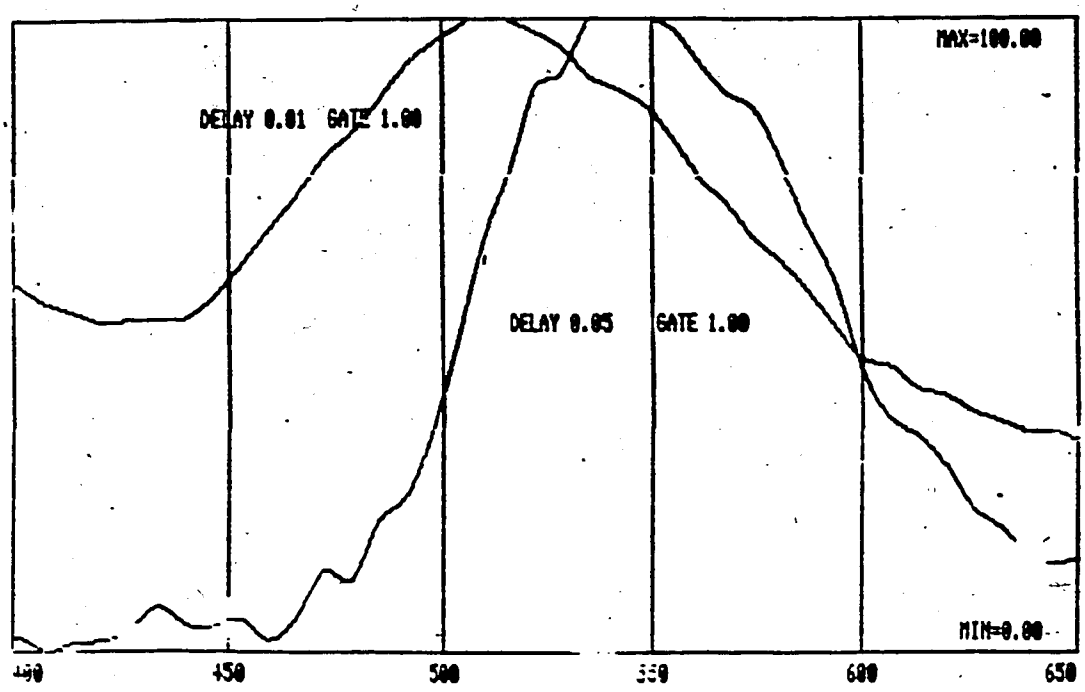

Figure 7: Phosphorescence-emission spectrum of 10a in a 2-methyltetrahydrofuran glass matrix (77 K) with a 0.01 and 0.05 microsecond delay.

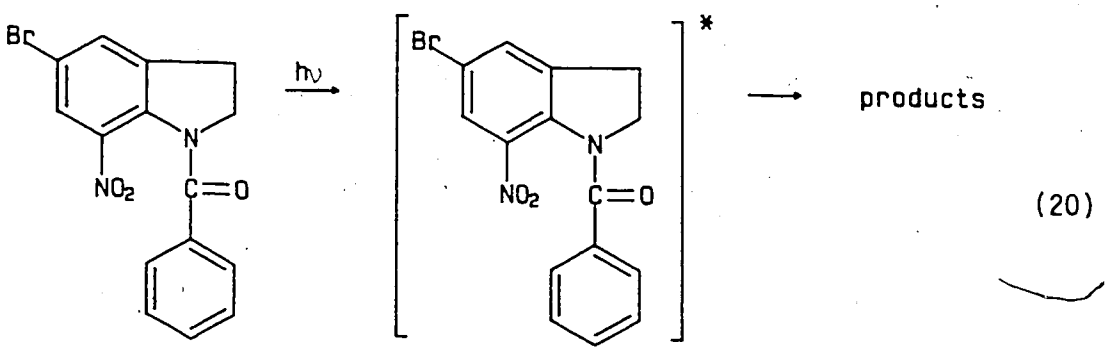

(20)

(iii) Discussion

The objective of this investigation was to probe the excited states of 10a using UV absorbance, fluorescence, and phosphorescence measurements (20).

UV absorption bands for molecules that exhibit a bathochromic shift in going from a non-polar to a polar solution are generally assigned to π, π^* excited states. Such molecules have a larger dipole moment in their π, π^* excited states than in the ground state.

Based on the slight solvent induced bathochromic shift in the UV absorption spectrum of 10a the absorption maximum at 352 nm for 10a can be attributed to a π, π^* transition. With the ortho-heteroatom substituent in 10a, some charge delocalization from the nitrogen through the benzene moiety to the nitro group could conceivably occur.

According to Varma [30] and Capellos [34] the weak n, π^* transition of nitrobenzene and its derivatives is severely overlapped by the much more intense π, π^* absorption bands. The n, π^* and π, π^* states of nitrobenzenes, which can be distinguished clearly in gas phase spectra, are relatively close in energy. It is also likely that 10a has two close-lying singlet excited states.

The unusually red shifted and structureless fluorescence emission spectrum of 10a in CH_3CN is consistent with a solvent induced inversion of electronic states of different polarity [75] and/or with a polar solvent assisted isomerization of the excited molecule via an internal rotation [76].

Lippert et al [75] in 1962 observed anomalous fluorescence bands in p-cyanodimethylaniline. Excitation in non-polar solvents

resulted in a single fluorescence band. However, in polar solvents a new, red-shifted, fluorescence emission band appeared. Recently Grabowski [76] identified the polar emitting state as an excited rotamer; its electron donating moiety being twisted by 90° with respect to the coplanarity of the aromatic ring (21). Other studies have shown that both a twisted intramolecular charge transfer excited state (TICT) and solvent effects are important [77,78].

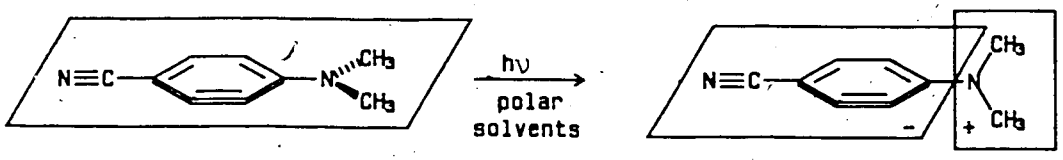

(21)

Due to the rigid geometry of 10a it is difficult to invoke a TICT excited state, originating from an aromatic C-N bond rotation, as the basis for the unusually red shifted fluorescence emission. This suggests that if the TICT mechanism is indeed applicable in the observed fluorescence and phosphorescence of 10a then rotation must occur about the amide C-N bond.

Excited state rotation about the amide C-N bond may prevent effective delocalization of the nitrogen lone pair into the carbonyl moiety thus generating a bifunctional molecule possessing an electron donor and acceptor group; similar to nitroaniline. As a consequence the π, π^* states could decrease in energy giving an intramolecular charge transfer in excited 10a (22).

On the other hand, the lack of detectable fluorescence emission from excited 10a in aqueous acetonitrile, suggests an inversion of close

lying singlet and/or triplet excited states. Because solvents may shift the relative energies of the singlet and triplet states to different extent [79], it is possible that in acetonitrile-water the π,π^* state with intramolecular charge transfer may in fact be the lowest excited triplet state. Since intersystem crossing in nitroaromatics is always very fast if $^1n,\pi^* \longrightarrow {}^3\pi,\pi^*$ and/or $^1\pi,\pi^* \longrightarrow {}^3n,\pi^*$ processes are possible [30], the disappearance of fluorescence in H-bonding solvents could be due to efficient $S_1(n,\pi^*) \longrightarrow T_n(\pi,\pi^*)$ $(n \geq 1)$ intersystem crossing.

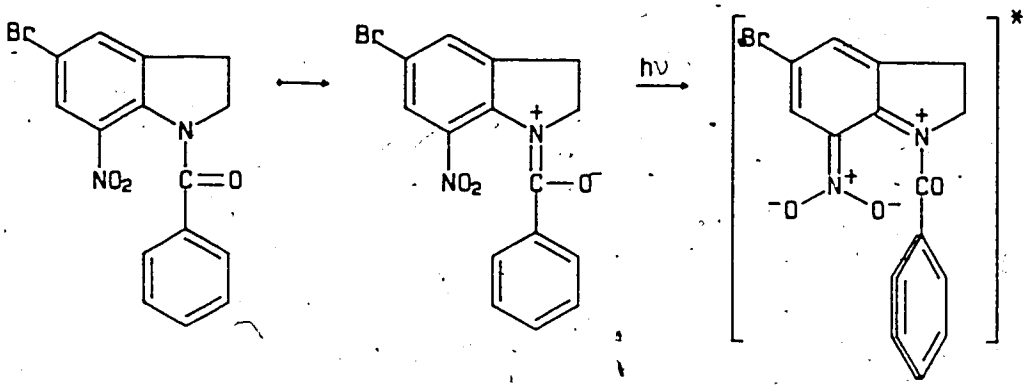

(22)

Support for this solvent induced inversion of the relative energies of excited states comes from the work of Capellos with 2-nitronaphthalene [34]. In non-polar solvents such as hexane the triplet 2-nitronaphthalene state exists as an n,π^* state, while in polar solvents an inversion of states takes place, leaving the charge transfer state as the lowest triplet state.

Since a yellowing of the 10á-2-methyltetrahydrofuran glass matrix after phosphorescence measurement was observed, a concurrent fragmentation process must have also occurred. This observation in

conjunction with the phosphorescence emission spectrum similarity between 10a and 11a, however, raised the question whether the emission assigned to 10a was actually due to a fragmentation product emission.

Clearly, further research is required in order to elucidate the complex photophysical behaviour of 10a.

D. PHOTOPRODUCT ANALYSIS

(i) Introduction

The most definitive information concerning a photoreaction, or any other type of reaction for that fact, is the complete characterization of the reactants, intermediates and products. Important qualitative arguments concerning the mechanism can be based on those considerations alone. Therefore, a complete photochemical mechanistic study must include a knowledge of all the significant reaction products. Since mechanistic pathways can be, and often are, governed by the reaction medium, product distribution in various pure and binary solvent systems need to be scrutinized. With this in mind, the products formed upon irradiation of 10a were examined in detail in a variety of solvents.

(ii) Results

(a) Isobestic Point

Irradiation of 10a with 350 nm Rayonet lamps resulted in a decrease in intensity of its 354 nm band, and concomitant increase in intensity at 422 nm in CH_3CN-H_2O solvent mixtures (Fig. 8) or 436 nm in CH_3CN only (Fig. 9). Continued irradiation established the presence

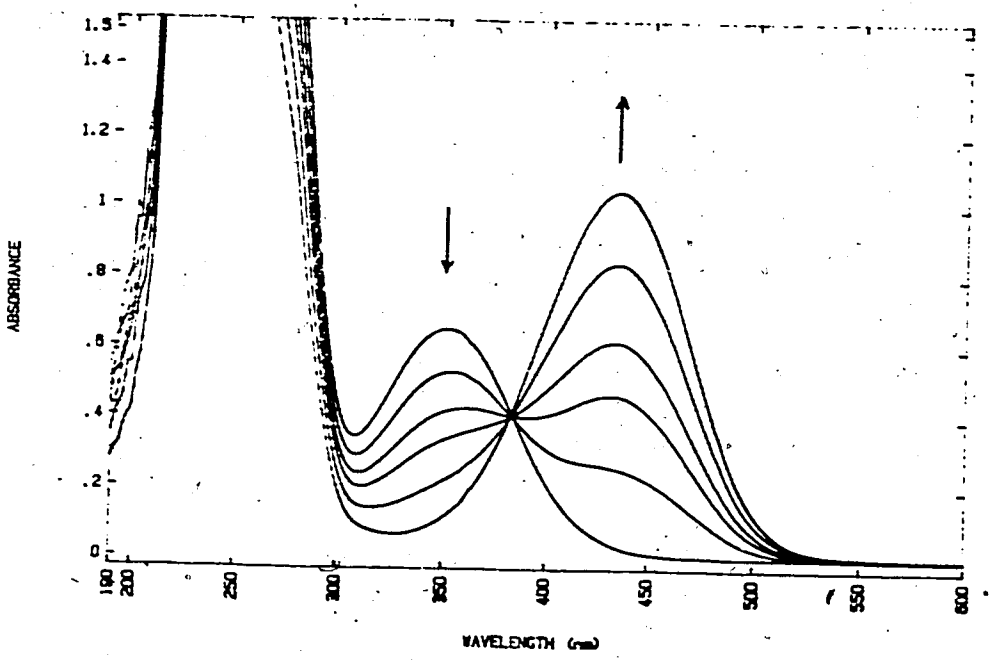

Figure 8: UV absorption spectrum of 10a in acetonitrile after 0, 30, 60, 90, 150 and 450 seconds irradiation in the Rayonet UV-reactor (RPR 3500 lamps)

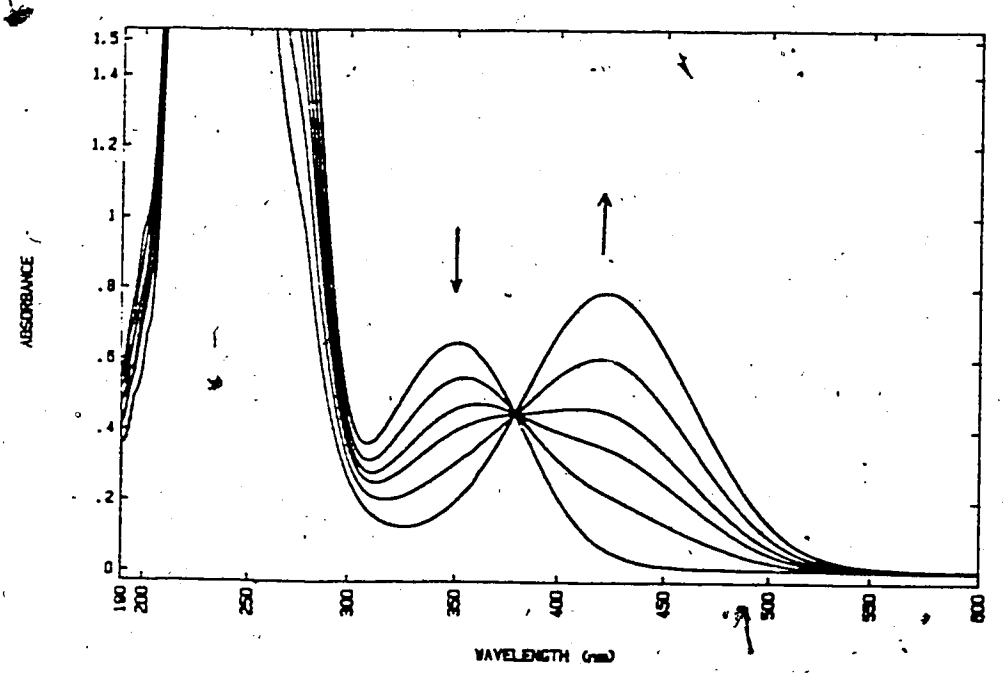

Figure 9: UV absorption spectrum of 10a in acetonitrile-water after 0, 30, 60, 90, 150 and 450 seconds irradiation in the Rayonet UV-reactor (RPR 3500 lamps)

of an isobestic point at 380 nm which was maintained for the complete conversion of 10a. Similarly, an isobestic point was recorded when 10a was irradiated in THF and THF-H_2O solvent media. It should be noted that when the solvents (CH_3CN or THF) were used without prior purification no isobestic point was observed.

(b) In Anhydrous Acetonitrile as Solvent

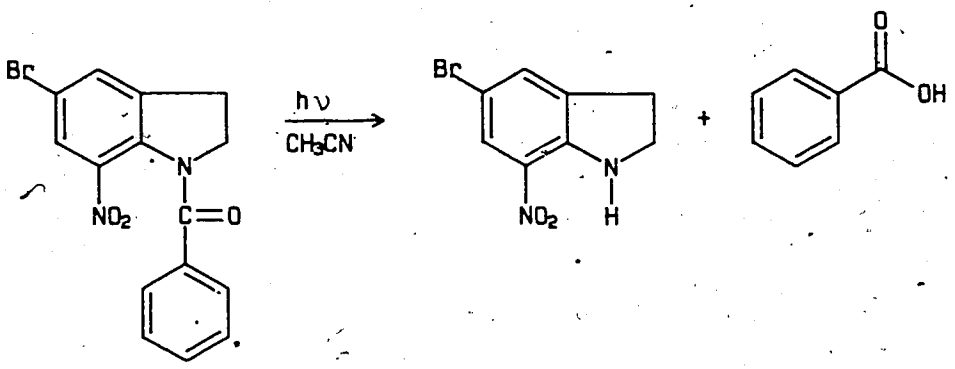

(23)

10a 11a 12a

Photolysis of 10a in anhydrous CH_3CN yielded two photoproducts. The ^1H NMR and mass spectrum of the solid obtained by base extraction from the reaction mixture, were in complete agreement with this product being benzoic acid [80], 12a. 5-Bromo-7-nitroindoline, 11a, was recovered from the CH_2Cl_2 phase, after the benzoic acid extraction. The ^1H NMR and mass spectrum of the solid were idential to those of 5-bromo-7-nitroindoline.

(c) In Acetonitrile-Water as Solvent

When 10a was photolyzed in CH_3CN-H_2O a third photoproduct, besides 11a and 12a, was formed. On the basis of UV, NMR and high resolution mass spectrum the structure of the photoproduct was identified as 5-bromo-7-nitrosoindole, 25.

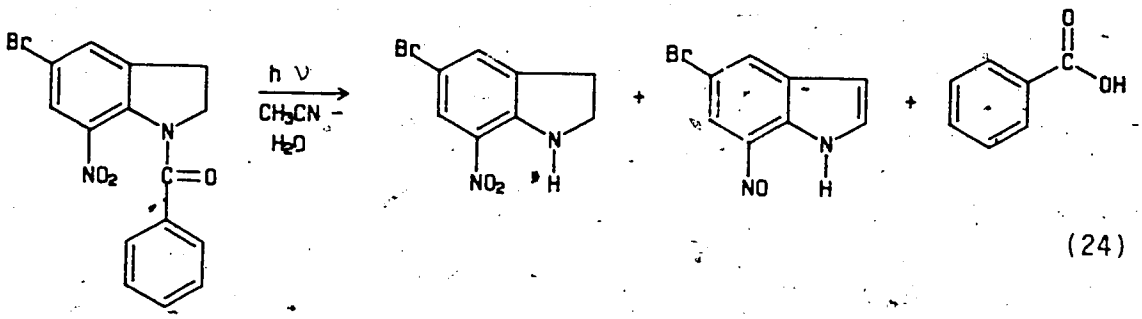

(24)

10a 11a 25 12a

The UV spectrum of 25 in CH_3CN showed the presence of a nitroso moiety. At low concentrations absorption maxima were observed at 214 and 406 nm with a point of inflection at approximately 270 nm. The weak n, π^* transition of the nitroso group was found at 734 nm.

The ^1H NMR spectrum of 25 was relatively simple (Figure 10). It consisted of five resonance peaks in the region from δ 6.5 to δ 12. Four of the five resonances were centered at δ 6.66, δ 7.53, δ 8.31 and δ 9.19. The fifth peak at δ 11.7 was broad, and clearly was due to a proton attached to a nitrogen. The two vinyl resonances at δ 6.66 and δ 7.53 were in close agreement with the chemical shifts of indole (δ 6.45 H3 and δ 7.26 H2) [81].

Proton decoupling experiments were carried out. Irradiation of H1 at δ 11.7 brought about the collapse of the multiplet at δ 7.53 and δ 6.66 into two doublets. The coupling constant J_{23}, 2.8 Hz, was consistent with H2-H3 coupling of indole systems [81]. On the other hand, irradiation of the doublet at δ 9.19 collapsed the doublet at δ 8.31 into a single sharp line. Considering the N=O proximity, the resonances at δ 9.19 and δ 8.31 were assigned to H6 and H4, respectively,

and coupled to each other with a coupling constant (J_{46}) of 1.4 Hz.

From the low resolution mass spectrum a parent peak at m/e 224 was obtained. A strong P+2 peak (98%) indicated the presence of a single bromine atom. The molecular formula, $C_8H_5BrN_2O$, for compound 25 was derived from the high resolution mass spectrum.

The most prominent peaks observed in the low resolution mass spectrum of 25 were accounted for by Scheme 15.

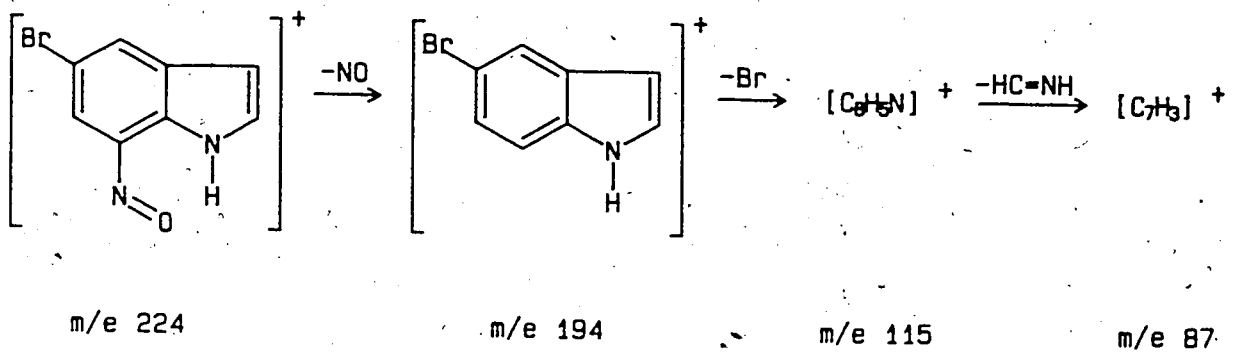

Scheme 15

The ^{13}C proton decoupled NMR spectrum of 25 is shown in Figure 11 with chemical shifts given in Table 1. In addition to the assigned peaks the spectrum showed four extraneous resonance peaks, (extraneous peaks are indicated with an asterisk in Figure 11). When the residue, obtained by evaporation of the solution used for the ^{13}C NMR spectrum, was recrystallized from acetone, a dark brown amorphous solid was obtained. The J modulated spin echo ^{13}C NMR spectrum of the

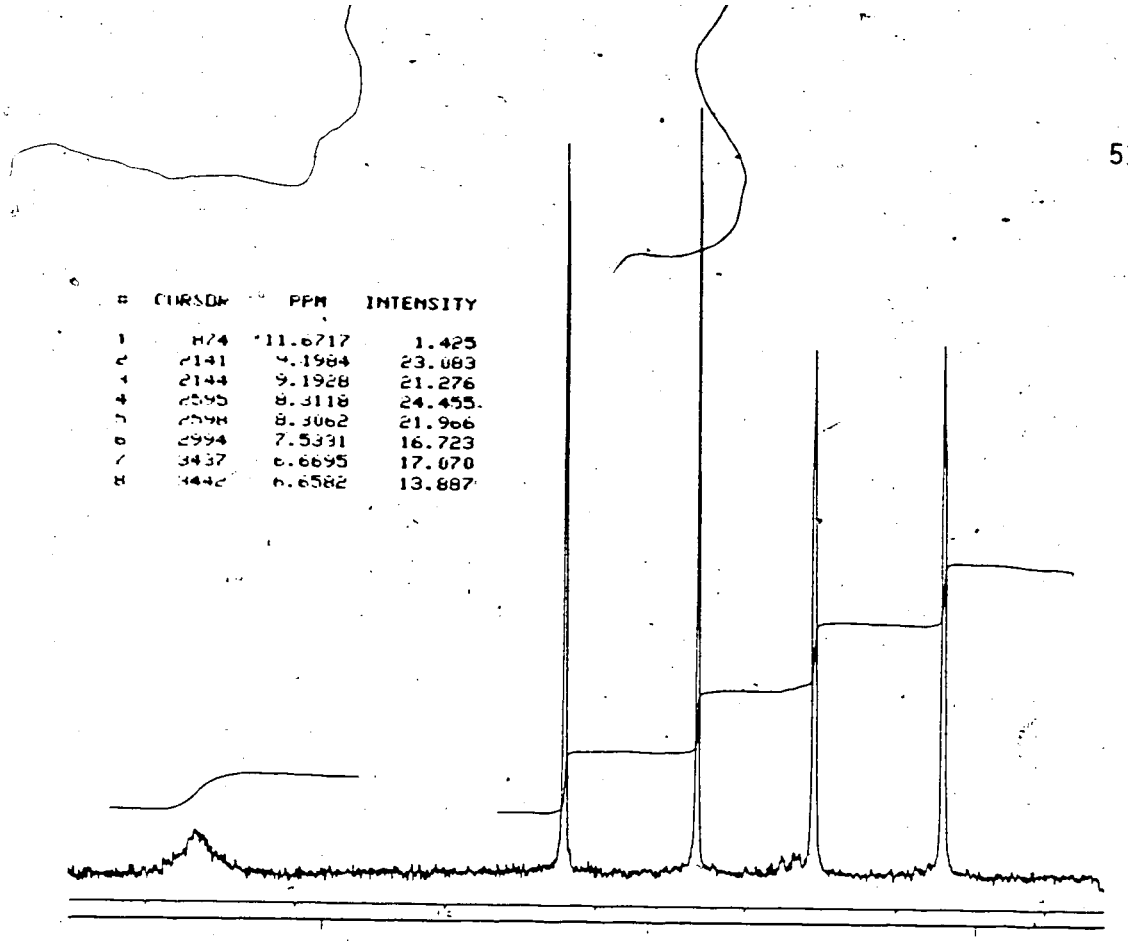

Figure 10: ^{1}H NMR spectrum of 25.

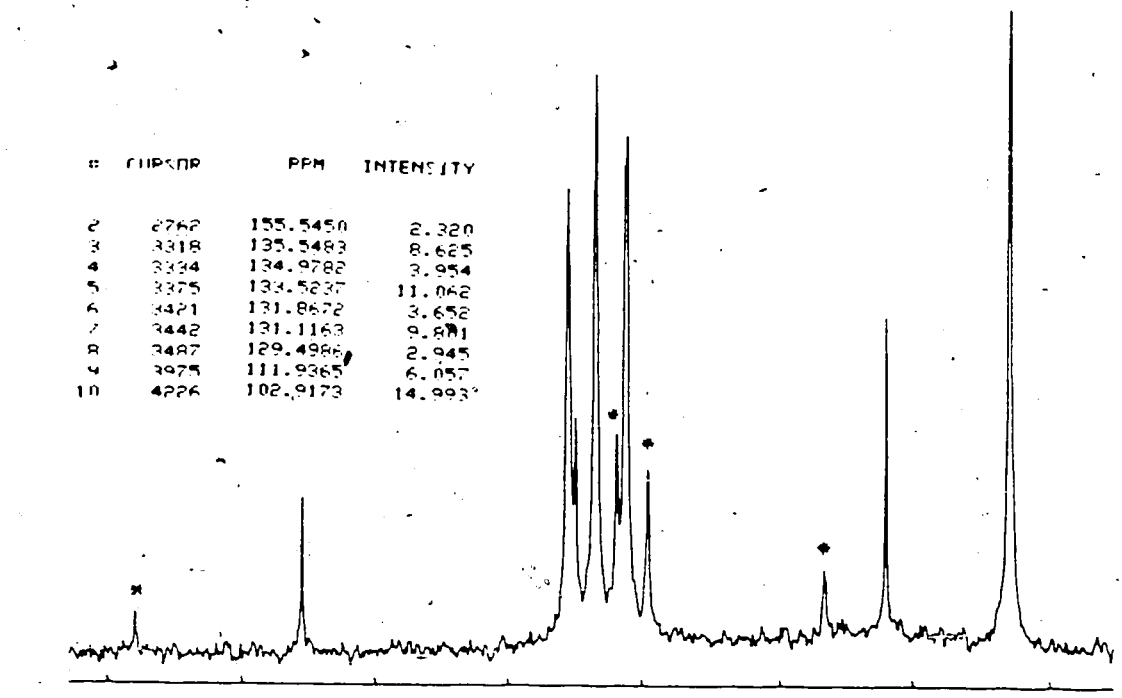

Figure 11: ^{13}C proton decoupled NMR spectrum of 25.

recrystallized solid in acetone d_6 still displayed similar resonance peaks observed in the proton decoupled ^{13}C spectrum, however, resonance peaks labelled with an asterisk in Figure 11 were now either completely absent or just noticeable.

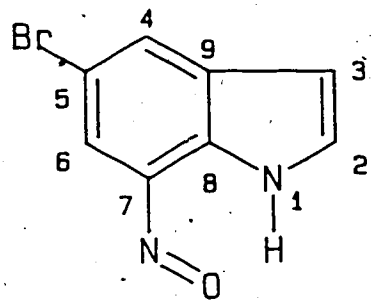

25

TABLE 1 Observed and Calculated ^{13}C NMR Chemical Shifts of 5-bromo-7-nitrosoindole, 25.

Carbon #	Chemical Shift[a,b] (observed)	Chemical Shift[a,c,d] (calculated)
2	131	124
3	103	102
4	134	132
5	112	118
6	136	116
7	156	152
8	135	130
9	112	127

[a] In ppm downfield from TMS.

[b] Resonance peaks in vicinity of calculated value.

[c] For ^{13}C NMR chemical shifts of indole see page C-160 ref. 81.

[d] For substituent effect see page C-120 and C-125 ref. 81.

On the bases of the calculated chemical shifts for 5-bromo-7-nitrosoindole, 25, a tentative assignment of the observed resonance peaks was made (Table 1).

The solution IR spectrum of the nitroso compound, 25, also suggested the presence of a mixture rather than a single component. The strong absorption bands observed in the range 1400-1175 cm^{-1} are typical of dimeric nitrosocompounds. Aromatic trans dimers show a characteristic -N=N-O band in the range 1300-1250 cm^{-1}. A medium band was observed at 1260 cm^{-1} in the solution IR of 25. However, bands were also observed at 1379 and 1425 cm^{-1} near to the reported value of cis dimers (approx. 1395, 1410 cm^{-1}) [81]. The strong, sharp band at 3470 cm^{-1} was consistent with the N-H stretching vibration of an indole. Complete infrared absorption data are found in the experimental chapter.

The spectral evidence given clearly indicates that the additional photoproduct produced in aqueous CH_3CN is 5-bromo-7-nitrosoindole. It is also clear that this component either slowly decomposes forming a secondary product, or in solution exists in equilibrium with the dimer.

The composition of the photoproduct mixture in aqueous CH_3CN was determined by HPLC. Relative product yields are given in equation (25).

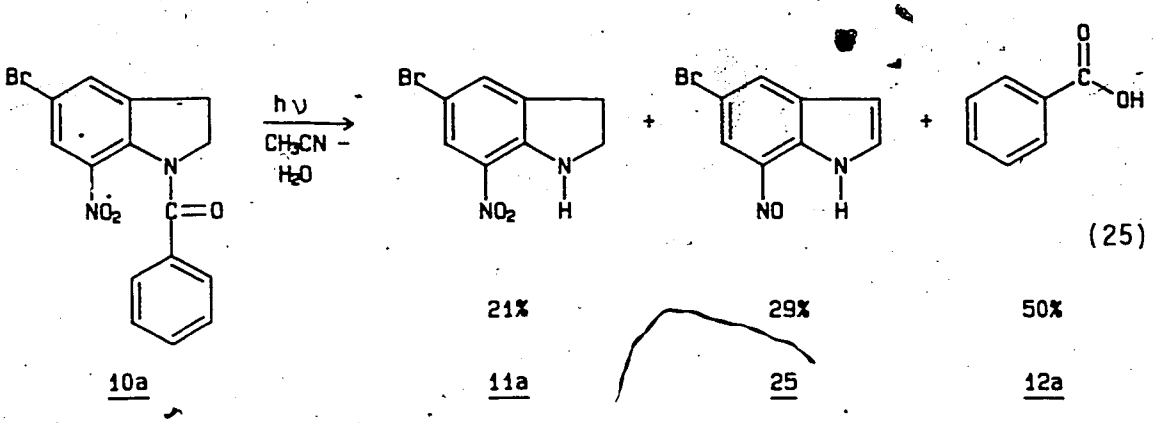

(25)

When a solution of 10a was irradiated for a prolonged period of time (approx. 13 hours) a third non-acidic photoproduct was formed. Only a small amount of this intensely red compound was isolated by TLC. The mass spectrum of this material showed a molecular ion peak at m/e 290. Conspicuously absent from the mass spectrum was a P+2 bromine isotope peak. Due to rapid polymerization of this material, even at -20°C, no other spectral data could be accumulated. On the basis of only the mass spectrum it is possible that this photoproduct is a dimer of nitrosoindole.

(d) In Anhydrous Tetrahydrofuran as Solvent

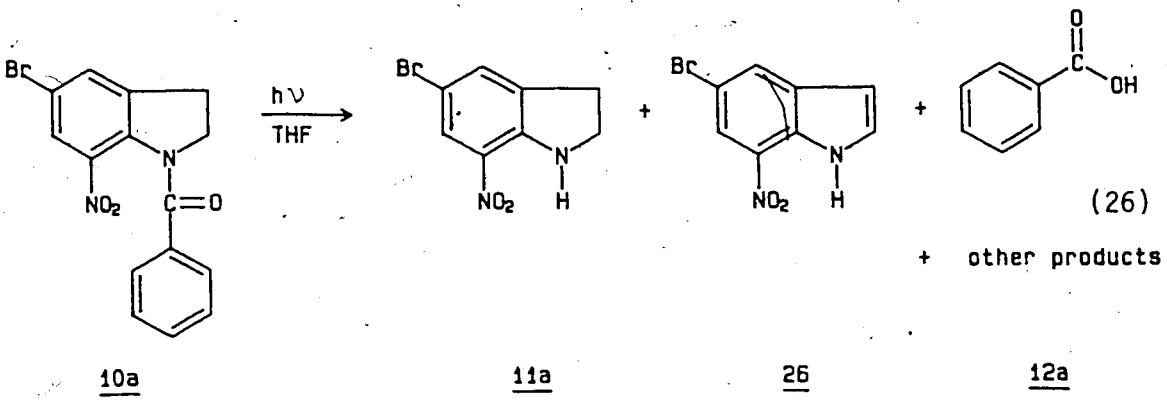

(26)

+ other products

A ^1H NMR spectrum of the products resulting from irradiation of 10a in anhydrous tetrahydrofuran indicated a rather complex reaction mixture. Three products out of this mixture could be identified. Benzoic acid and 5-bromo-7-nitroindoline were readily identified by their respective R_f values and ^1H NMR spectra, when compared against known samples. The third product was established as 5-bromo-7-nitroindole, 26, by its low resolution mass spectral fragmentation peaks, the observed mass from the high resolution mass spectrum, and the ^1H NMR spectrum.

The 500 MHz ^1H NMR spectrum of the third photoproduct displayed resonances which were similar to those of 25. Quartets were centered at δ 8.29, δ 8.10, δ 7.42, and δ 6.68. Because the spectrum possessed a similarity to that of 25, the resonances centered at δ 8.10 and δ 8.29 were assigned to indole protons located at C-4 and C-6 respectively. A coupling constant of 1.6 Hz was found between these two protons. The two quartets centered at δ 7.42 and δ 6.68 were in agreement with the reported chemical shifts of indole vinyl protons, and accordingly were assigned to H-2 and H-3 respectively. The coupling constant between the two vinyl protons was 3.0 Hz. Since each vinyl proton resonance is observed as a doublet of a doublet, further coupling to the N-H proton would seem to take place. The broad N-H resonance peak was centered at δ 9.91.

The low resolution mass spectrum of the third photoproduct was in agreement with 5-bromo-7-nitroindole. The parent peak was observed at m/e 240, with an intense P+2 peak indicating the presence of a single bromine. In addition, the most prominent peaks, aside from the parent peak, were identical with m/e values due to 25. The molecular formula of

the third product, 26, was shown to be $C_8H_5BrN_2O_2$ from the high resolution mass spectrum.

(e) In Tetrahydrofuran-Water as Solvent

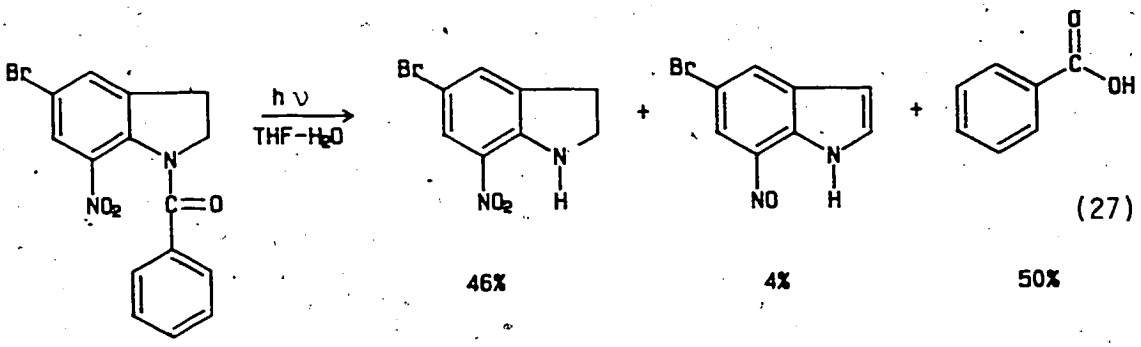

(27)

46% 4% 50%

10a 11a 25 12a

A ^1H NMR spectrum of the crude reaction mixture obtained from irradiation of 10a in aqueous THF had resonance peaks due to only three components. The major components were 5-bromo-7-nitroindoline, 11a and benzoic acid 12a. About 4% of 5-bromo-7-nitrosoindole, 25, was also identified in the reaction mixture.

(f) In Ethanol as Solvent

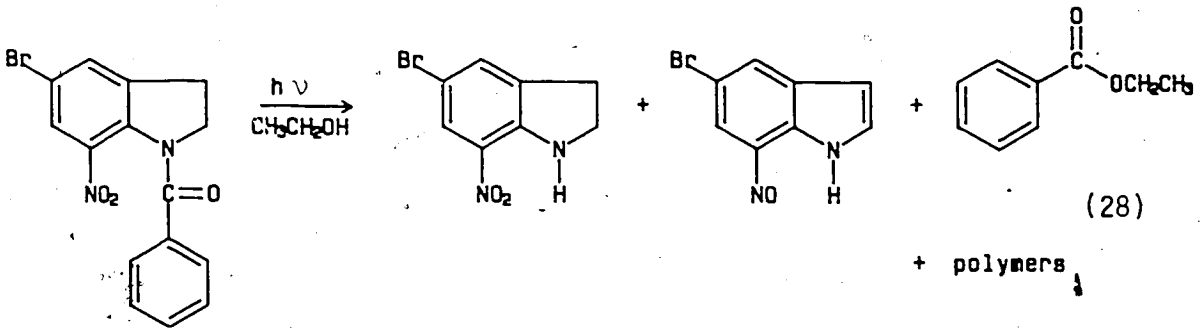

(28)

+ polymers

10a 11a 25 27

Analysis of the photoproduct mixture, obtained in ethanol as a solvent, by ^1H NMR revealed besides some polymeric material the presence of only three components. The major component was 5-bromo-7-nitroindoline. 5-Bromo-7-nitrosoindole was identified as a minor constituent (approximately 4% relative to 5-bromo-7-nitroindoline). Instead of benzoic acid, as observed in previous studies, ethylbenzoate, 27, was produced.

(g) In Anhydrous Acetonitrile and 1,3-Cyclohexadiene

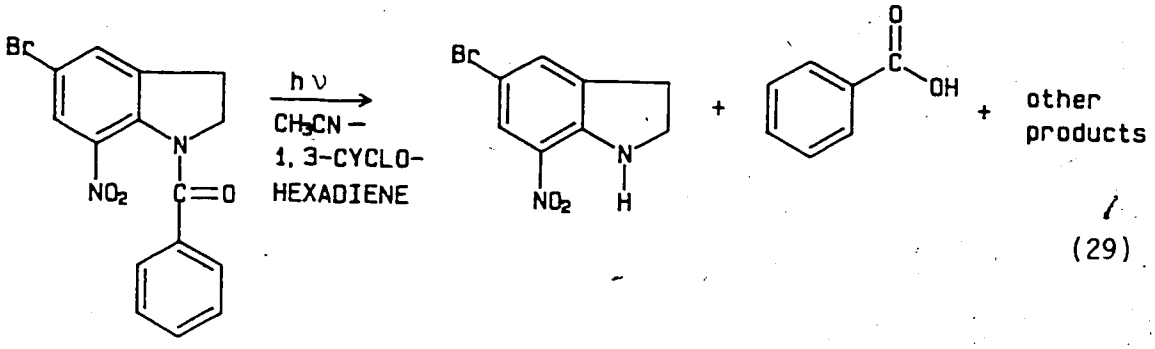

(29)

10a 11a 12a

Separation of crude reaction mixture, obtained from irradiation of 10a in CH_3CN and .16 moles/litre of 1,3-cyclohexadiene, by thin layer chromatography, (TLC) showed that 5-bromo-7-nitroindoline and benzoic acid were the primary photoproducts. A minor amount of a red solid compound was also separated, but its structure could not be identified. Within one day, at ambient temperature, this red compound turned brown.

(h) In Acetonitrile-Water and 1,3-Cyclohexadiene

As was indicated previously, three major photoproducts, 5-bromo-7-nitroindoline, 11a, benzoic acid, 12a, and 5-bromo-7-nitrosoindole, 25,

(i) Summary of Reaction Product Analysis

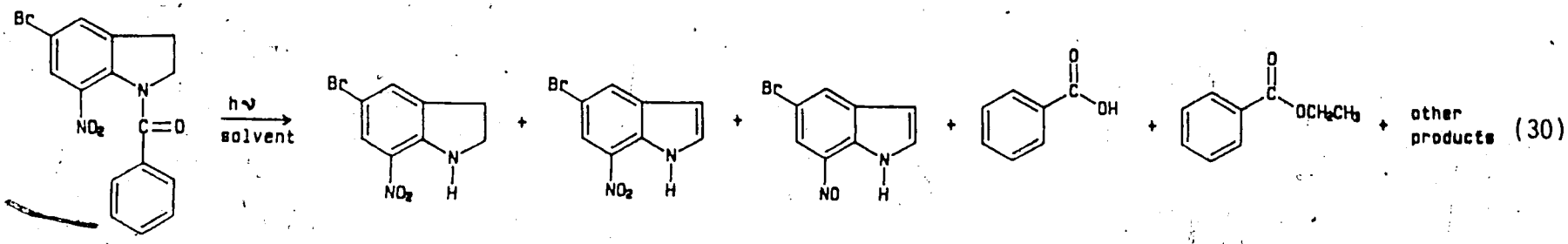

(30)

10a	11a	26	25	12a	27	
CH_3CN	50%	--	--	50%	--	--
CH_3CN-H_2O[b]	21%	--	29%	50%	--	--
THF	a	a	--	a	--	a
THF-H_2O[c]	46%	--	4%	50%	--	--
CH_3CH_2OH	a	--	a	--	a	a
CH_3CN-1,3-Cyclohexadiene	a	--	--	a	--	a
CH_3CN-H_2O-1,3-Cyclohexadiene	--	--	--	--	--	a

Values are relative yields based on ^1H NMR integration and HPLC analysis.

a) Compound present but no quantitative analysis performed.

b) Mole Fraction of Water = .66.

c) Mole Fraction of Water = .75.

are formed when a solution of 10a was photolyzed for 1 hour in CH_3CN-H_2O. Irradiation of a solution of 10a in CH_3CN-H_2O, containing .16 moles/liter 1,3-cyclohexadiene also for 1 hour, led to only partial conversion of 10a. The product mixture contained a significant fraction of photoproduct insoluble in $CDCl_3$. Conspicuously absent, in the ^1H NMR spectrum of the crude photoproducts, were all the resonance peaks attributable to 25. Extension of the irradiation time from 1 hour to 2 hours, followed by TLC separation, gave large amounts of black insoluble solid material. Two minor photoproducts were also separated, but could not be identified.

When 1,3-cyclohexadiene was added to a mixture of photoproducts (11a, 12a, and 25) obtained from photolysis of a solution of 10a in CH_3CN-H_2O and the mixture irradiated for another hour, 5-bromo-7-nitrosoindole disappeared. 5-Bromo-7-nitroindoline, on the other hand, seemed photolytically and thermally stable, and unreactive towards the diene. This was shown by ^1H NMR analysis of the crude reaction mixture after evaporation of the solvents.

(iii) Discussion .

Cohen and Fischer [82] indicated that in simultaneous reactions such as:

$$A \text{ ------> } B \qquad (31)$$

$$A \text{ ------> } C \qquad (32)$$

where the ratio of the amount of C to that of B remains constant throughout the reaction, an isobestic point should be observed. In such a system, therefore, the concentrations of the species present are all

linear functions of one another. Therefore, the presence of a well-defined isobestic point, or point of constant absorbance, indicates that the reaction proceeds without side reactions.

Photolysis of 10a in anhydrous CH_3CN furnishes benzoic acid and 5-bromo-7-nitroindoline, 11a, in nearly quantitative yield. However, in aqueous acetonitrile, where the mole fraction of water = .66, 5-bromo-7-nitrosoindole, 25, was shown to be formed as a third, previously unreported, major photoproduct. Amit [22], in the photolysis of 10a in CH_2Cl_2-dioxane-H_2O (5:10:0.5) or CH_3CN-H_2O (25:1) reported benzoic acid and 5-bromo-7-nitroindoline as the only photoproducts.

Amit [22] postulated that the excited 7-nitro group activates the amide bond to nucleophilic attack. A mechanistic scheme such as shown in Scheme 16, based on intramolecular nucleophilic attack of the amide bond by the nitro-oxygen, is consistent with the formation of photoproducts 11a and 25 in non-hydrogen-donating solvents such as CH_3CN and CH_3CN-H_2O. The complex reaction mixture observed in anhydrous tetrahydrofuran, however, cannot be adequately explained by only a nucleophilic addition pathway.

As was presented in the introduction to this thesis, the photoreduction of nitroaromatics has been reported to occur by different processes to give the corresponding nitrosoaromatic [83,84]. It may be formed by direct reduction of the nitro functionality (33-36), air oxidation of phenylhydroxylamine (37), or by decomposition of an alkoxyarylaminyloxide (38 and 39).

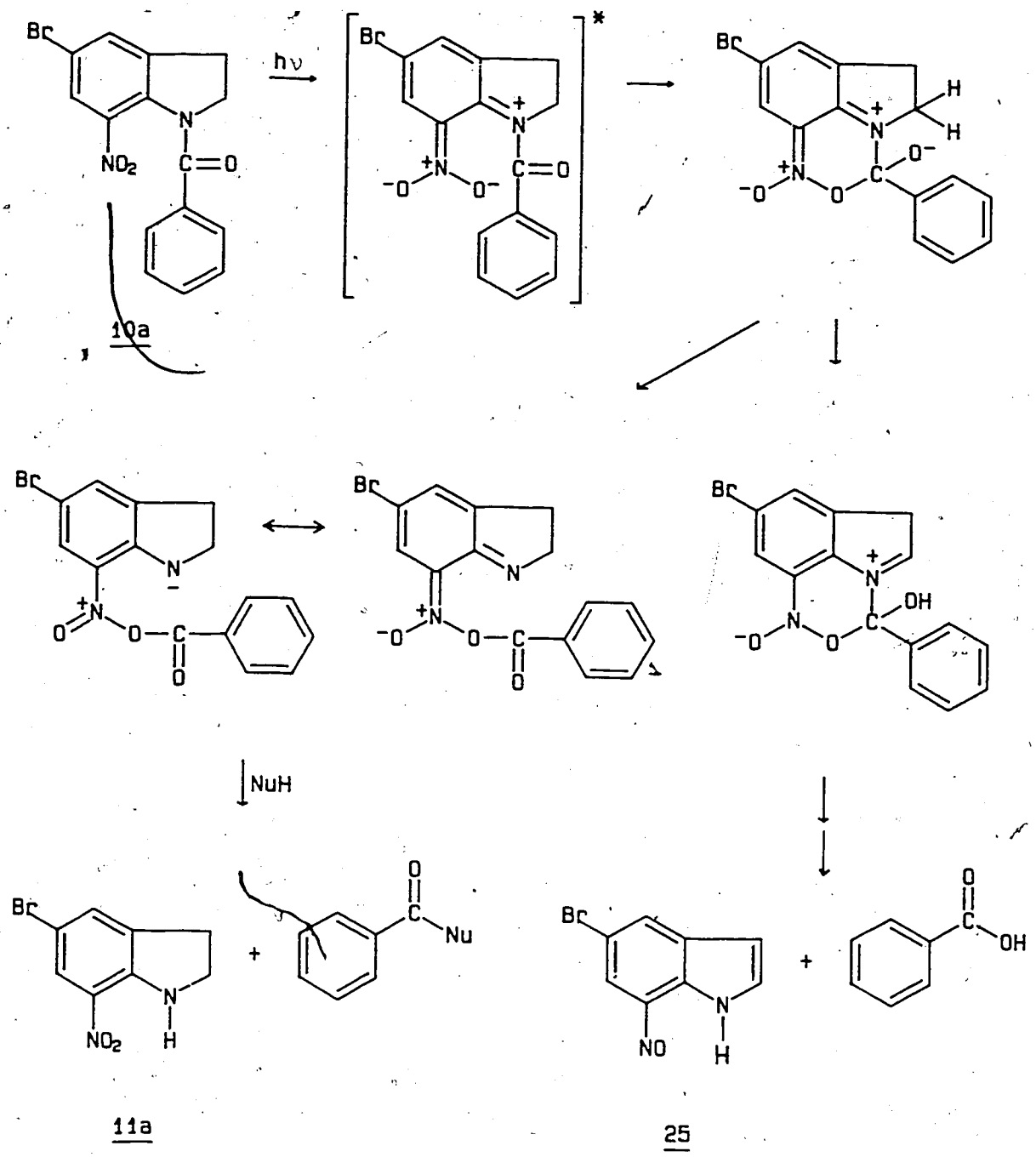

Scheme 16

$ArNO_2$			--->	$^3(ArNO_2)^*$		(33)
$^3(ArNO_2)^*$	+	$R\text{-}CH_2O\text{-}R'$	--->	$ArNO_2H\cdot$	+ $RCHOR'\cdot$	(34)
$ArNO_2H\cdot$	+	$R\text{-}CH_2O\text{-}R'$	--->	$ArN(OH)_2$	+ $RCHOR'\cdot$	(35)
$ArN(OH)_2$			--->	ArNO	+ H_2O	(36)
ArNHOH	+	1/2 O_2	--->	ArNO	+ H_2O	(37)
$ArNO_2$	+	$R\cdot$	--->	$ArNO_2R\cdot$		(38)
$ArNO_2R\cdot$			--->	ArNO	+ $OR\cdot$	(39)

Formation of 5-bromo-7-nitrosoindole, 25, in degassed non-hydrogen-donating solvent systems such as $CH_3CN\text{-}H_2O$ would exclude the direct reduction and air oxidation routes, and suggests that the reaction proceeds via a radical spin trapping pathway. The reactant itself can be safely excluded as a likely hydrogen donating source due to the low concentration of 10a used in reaction solution and the typically very short lifetimes of excited nitroaromatics [24].

A plausible alternative to the mechanism outlined in Scheme 16 which is consistent with the experimental results, would be homolytic cleavage of the N-C bond with subsequent spin trapping of the benzoyl radical, 28, by the nitro moiety 29 (Scheme 17). Such a proposed photolytic homolysis of the amide C-N bond has been documented by Shizuka [66,67] and others [71,72]. Electronic rearrangement of the biradical intermediate 30 may subsequently form a nitronic carboxylic acid anhydride 31.

Acetonitrile has a high affinity for water, and as a result it is an extremely difficult solvent to completely dry. The residual water content in acetonitrile after distillation from CaH_2, the drying

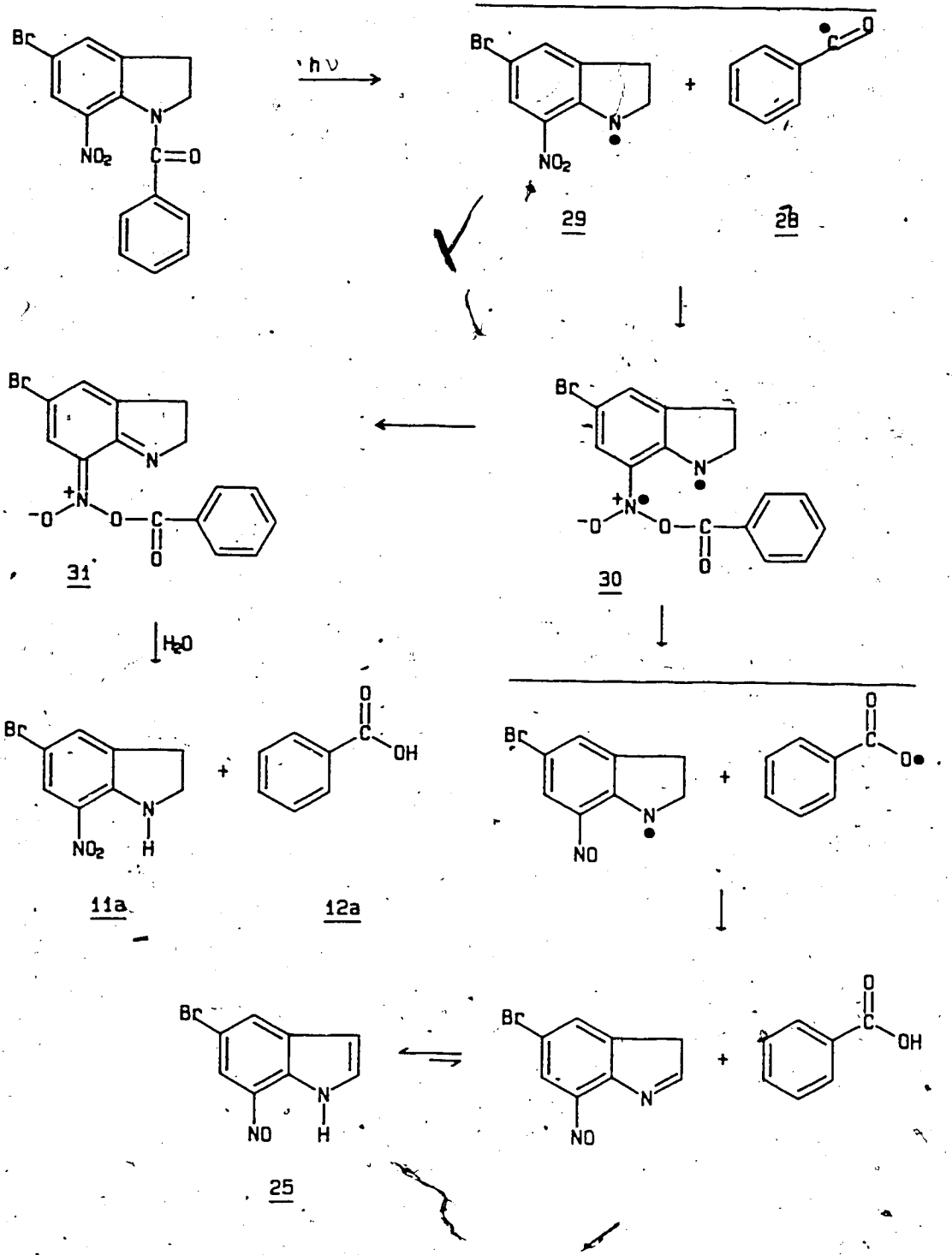

Scheme 17

procedure used in this work, is reported to be circa 1900 ppm [85]. There is no doubt that such a high concentration of water in CH_3CN could rapidly hydrolyze the nitronic carboxylic acid anhydride to yield photoproducts 11a and 12a.

If α-scission of the biradical intermediate 30 can compete effectively with electronic rearrangement then decomposition of the biradical reduces the nitro group to a nitroso function. The benzoyloxy radical would be able to abstract a hydrogen from C-2 of the nitroso radical before escape from the solvent cage or loss of CO_2.

Products containing the tetrahydrofuran moiety were formed as part of the photoproduct mixture when 10a was irradiated in neat THF. Such photoproducts can be accounted by considering the mechanistic pathway outlined in Scheme 17. Following homolytic amide bond fission, hydrogen abstraction from the tetrahydrofuran solvent becomes an additional radical decomposition mode. As in acetonitrile, no 5-bromo-7-nitrosoindole was observed in "anhydrous" tetrahydrofuran photolysis mixture. When 10a was irradiated in aqueous tetrahydrofuran (mole fraction of water = .75) a minor amount of 5-bromo-7-nitrosoindole was identified, and no products ascribable to H-abstraction from solvent were noticed.

It was anticipated that quenching of excited 10a with 1,3-cyclohexadiene would provide a useful qualitative tool for deciding if any, or all, of the heterocyclic products were formed from a triplet state. However, neither 11a nor 25 was indentified as a photoproduct when 10a was irradiated in aqueous acetonitrile containing 1,3-cyclohexadiene.

The failure to observe any 5-bromo-7-nitrosoindole may result

either from the selective quenching of excited 10a, or from oxazine formation via a dark reaction of 25 and the diene. Aromatic nitroso compounds are very reactive dienophiles and add smoothly to substituted dienes at room or lower temperatures to give the corresponding oxazine derivatives. For example, nitrosobenzene when treated with 2,3-dimethyl-1,3-butadiene has been reported to yield N-phenyl-3,6-dihydro-4,5-dimethyl-1,2-oxazine [86] (40).

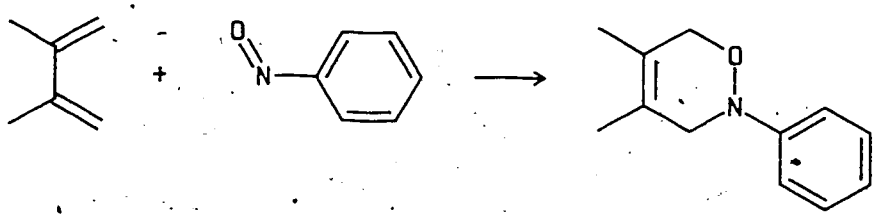

(40)

That photoproduct 25 indeed readily combines with 1,3-cyclohexadiene was demonstrated when 10a in CH_3CN-H_2O was irradiated for 1 hour before addition of the 1,3-cylohexadiene. Upon addition of this diene and irradiation for another hour resonance peaks attributable to photoproduct 25 were completely absent from the ^1H NMR spectrum. It is, therefore, reasonable to assume that the reaction product is the Diels-Alder adduct 32 (41).

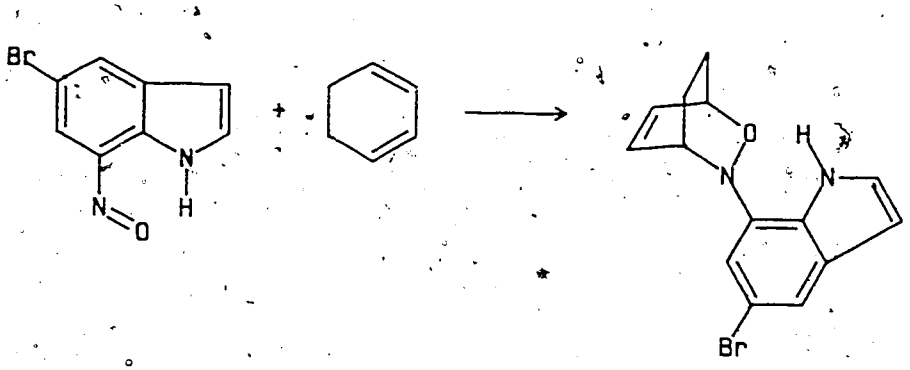

(41)

32

The observation of a preponderance of polymeric material after 2 hours of irradiation may also imply a photochemical reaction of excited 10a with the diene. de Mayo and coworkers [28] have proposed the addition of a triplet excited nitroaromatic to the olefin to give an ozonide-like intermediate which may decompose to form polymeric reaction products.

Therefore, on the basis of the aromatic nitroso's reactivity with dienes and the formation of polymeric material, the experimental test for the assignment of a triplet state product has to be considered as inconclusive.

E. SOLVENT POLARITY AND pH EFFECTS

(i) Introduction

While examining the photoproduct distribution from 10a in various solvents it was noted that product composition was controlled by the nature of the photoreaction medium. The intriguing differences seen in the photoproduct distribution study were therefore probed further by more systematic changes in the medium polarity ($E_T(30)$ values) and pH.

(ii) Results

(a) Photoproduct Distribution as a Function of Solvent Polarity $E_T(30)$

The $E_T(30)$ solvent polarity values for binary mixtures, were estimated according to the equation and parameters given in reference 87. These values are tabulated against the amount of photoproduct 25 observed in a range of pure and binary solvent systems, Table 2.

TABLE 2 Medium Effects on the Formation of 25 in the Photofragmentation of 10a.

SOLVENT	MOLE FRACTION OF WATER	$E_T(30)$	% 25 [a,b]	log 25 [d]
CH_3CN[e]	--	46	0 ± 2	--
CH_3CN-H_2O[f]	.24	51.7	6 ± 2	-1.22, +0.12/-0.18
CH_3CH_2OH[e]	--	51.9	4 ± 2	-1.40, +0.18/-0.30
$THF-H_2O$[c,e]	.75	53.5	8 ± 2	-1.10, +0.10/-0.12
CH_3CN-H_2O[f]	.42	54.9	14 ± 2	-0.85, +0.05/-0.07
CH_3CN-H_2O[f]	.66	56.4	35 ± 2	-0.46, +0.03/-0.02
CH_3CN-H_2O[f]	.81	57.2	36 ± 2	-0.44, +0.02/-0.03

a) % 25 based on $25/(25 + 11a) \times 10^2$

b) Determined by ^1H NMR method

c) Parameters E_D and C* for water-dioxane binary solvent mixture were used for E_T (30) calculation [87]

d) Log of mole fraction of photoproduct 25

e) Ambient temperature irradiation of 10a reaction solution

f) 10a solution temperature maintained at 7°C during irradiation

The temperature at which the irradiation was carried out was found to significantly influence the product composition formed in aqueous CH_3CN. In CH_3CN-H_2O with mole fraction of water = .66 and at a solution temperature of 7°C 35% of 25 was recorded. At ambient temperature irradiation, where the solution temperature reached 45°C at end of irradiation

and similar solvent system, the yield increased to 47%. Still higher yields were measured in the product analysis study (58%), where reactant conversion possibly occurred at higher solution temperatures.

(b) Photoproduct Distribution as a Function of NaOH Concentration

Based on the initial hypothesis that nucleophilic addition of the nitro oxygen to the carbonyl moiety is the primary photochemical step it was anticipated that the presence of NaOH in aqueous CH_3CN would accelerate the photofragmentation of 10a via proton removal from C-2 of intermediate 33. The photoproduct distribution should also be changed as base is added (42).

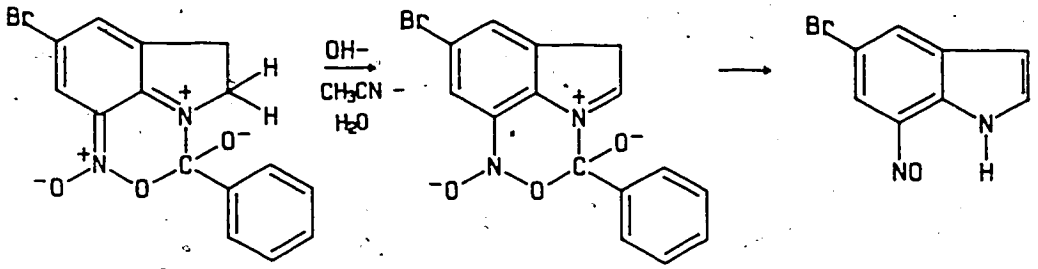

33 (42)

The ratio of 11a vs. 25 produced was found to be a function of the concentration of NaOH. As the NaOH concentration increased the amount of the nitrosoindole 25 formed increased while 11a decreased, (Table 3); although at higher NaOH concentration a decrease in 25 was observed. The variation in photoproduct 25 with sodium hydroxide is shown in Figure 12, with mole % of 25 plotted against pH of water.

A subsequent mass balance on 0.010 g of reactant with no added

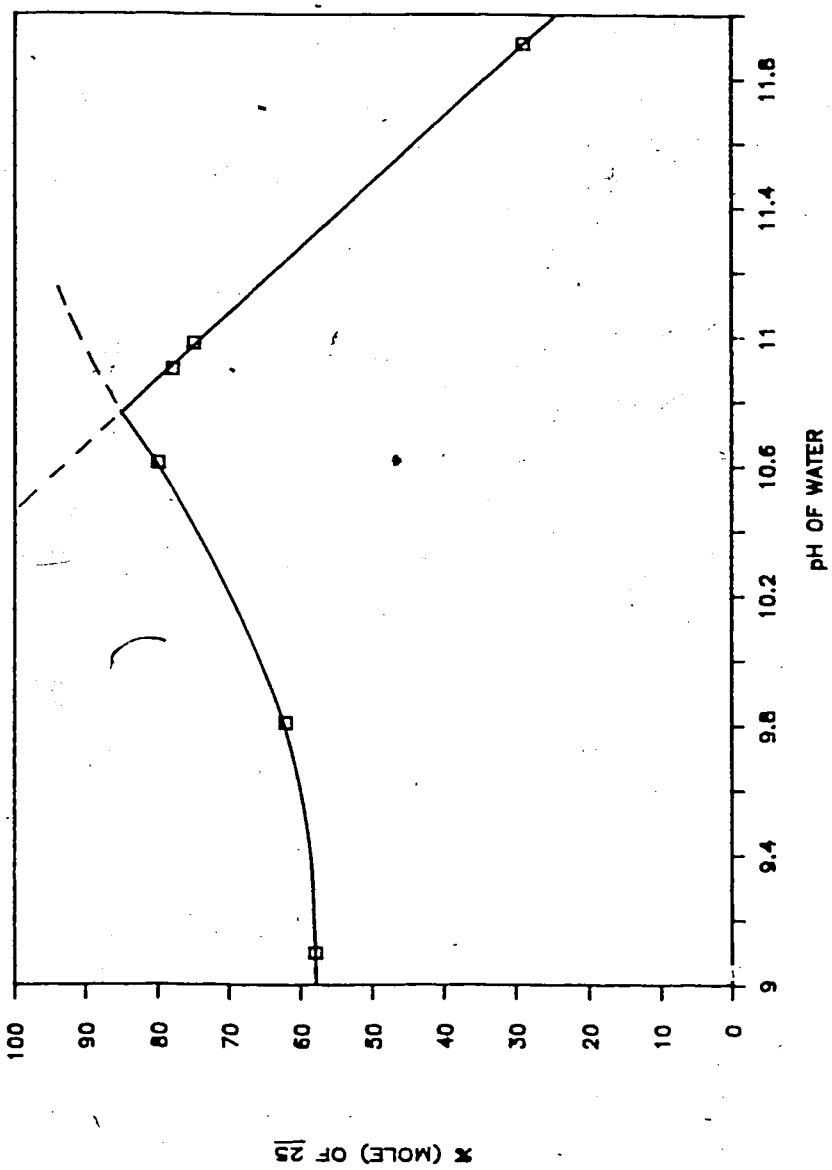

Figure 12: Variation of photoproduct 25, % (mole) 25, with the pH of water used for CH_3CN-H_2O solvent mixture.

NaOH in aqueous solution showed that 88 ± 12 % of theoretical photoproduct yield was recovered. No solid residue was observed in either the base wash or methylene chloride layers during the separation of the benzoic acid photoproduct. With the pH of water at 11.92 and identical experimental conditions only 56 ± 2% of product was recovered. The base wash of photoproduct mixture at higher pH values contained a solid suspension which did not partition into methylene chloride layer. The mass spectrum of this black solid displayed fragmentation peaks as high as m/e 446; considerably above the parent peaks for 11a, 25 or even 10a. None of the fragmentation peaks matched the parent peaks for 11a or 25.

TABLE 3 pH Effects on Photoproduct 25 in the Photofragmentation of 10a[a] in CH_3CN-H_2O.

[NaOH] in H_2O	pH of H_2O[b]	% (mole) 11a[c]	% (mole) 25[c]
0	9.10	42 ± 1	58 ± 1
1.0×10^{-4}	9.81	38 ± 1	62 ± 1
5.0×10^{-4}	10.61	20 ± 1	80 ± 1
8.0×10^{-4}	10.90	22 ± 1	78 ± 1
1.0×10^{-3}	10.98	25 ± 1	75 ± 1
1.0×10^{-2}	11.91	71 ± 1	29 ± 1

a) 10a in CH_3CN-H_2O (mole fraction of water = .66)

b) Measured on Radiometer pH meter at 23°C

c) Determined by HPLC method

Given the reactivity of nitroso compounds it is likely that at higher NaOH concentrations not only the formation, but also the decomposition of 25 was catalyzed. It is likely that dimeric nitroso, or other coupling products (azo- or azoxybenzene), arise from base-catalyzed condensation of the nitrosoindole 25.

(iii) Discussion

It is apparent from the data presented in the previous section that the product distribution obtained upon irradiation of 10a is dependent on the solvent used. The range of solvents used include polar aprotic solvents (THF and CH_3CN) as well as polar protic solvents. Anhydrous tetrahydrofuran and acetonitrile are solvents with good cation solvating power but with little ability to solvate anions [88]. Ethanol and water are polar protic solvents which can solvate both anions and cations [88]. In order to understand the variation in products with change in solvent, correlations with solvent polarity parameters were sought.

Many empirical parameters have been developed for determining the solvent polarity effect on rate and position of equilibrium in chemical reactions. Several scales are based on the solvatochromism of dyes [89]. The most widely used of these is the $E_T(30)$ scale based on the solvatochromic dye pentaphenylpyridiniumphenolate, 34 [90].

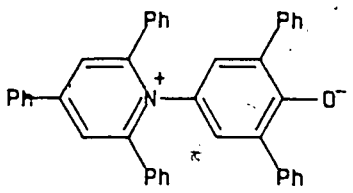

34

The polar behaviour of binary liquid mixtures has recently been described quantitatively as a function of their composition. According to Langhals [87,91], the nonlinearity of the $E_T(30)$-composition calibration curve of solvent mixtures can be linearized by using equation (43).

$$E_T(30) = E_D \times \ln (C_P/C^* + 1) + E_T^\circ(30) \qquad (43)$$

In equation (43) $E_T(30)$ is the polarity of the binary liquid mixture, C_P the molar concentration of the more polar component, and $E_T^\circ(30)$ is the $E_T(30)$ value of the pure less polar component. Because the $E_T(30)$ polarity values are based on the dipolar nature of excited 34, equation (43) responds not only to the polarity of the medium, but also to its hydrogen bonding/donor character.

As is shown in Figure 13 there is a linear correlation between $E_T(30)$ values and log 25. Since the empirical solvent polarity parameter can be understood as the result of a linear free-energy relationship [92], a correlation of experimental data from a new reaction series with those of a known series can indicate a mechanistic similarity between the two series. Thus the exceptionally marked increase in yield of 25 with increasing $E_T(30)$ values suggest the solvation of a dipolar species during the photofragmentation process leading to 25.

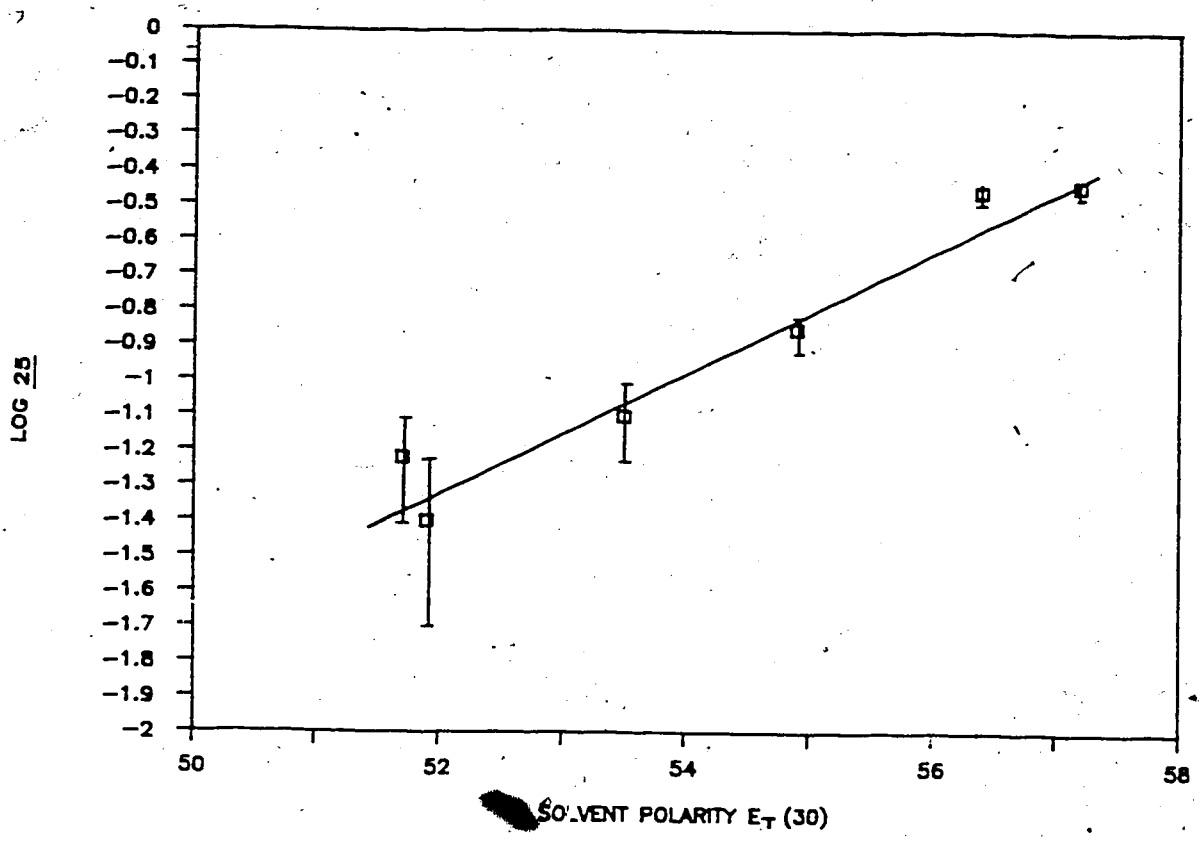

Figure 13: Variation of photoproduct 25, log 25, with the solvent polarity value $E_T(30)$ in the photofragmentation of 10a.

Such a solvent dependence for formation of 25 could originate with solvation effects on the excited or even ground state of 10a. The relative order of excited states in substituted nitroaromatics is strongly dependent on the solvent system [30]. As suggested on pg. 45 the lowest excited triplet state of 10a may be either n,π^* or π,π^* depending on the solvent system. In strongly H-bonding solvents such as water, and to a lesser extent ethanol, the highly dipolar excited π,π^* state may thus become the state of lowest energy. Highly polar protic solvents may interact with the negatively polarized oxygen atom in the nitro group. At an area of low electron density both protic and

aprotic solvents can function as electron pair donors [88]. By each of these interactions the dipolar nature of excited 10a could be effectively stabilized (Scheme 18).

In contrast, aprotic solvents such as tetrahydrofuran and acetonitrile are poor anion solvators, and in those solvents the absence of 25 may be interpreted by a lowest excited n,π* state in 10a due to a reduction in dipolar interaction by the solvent.

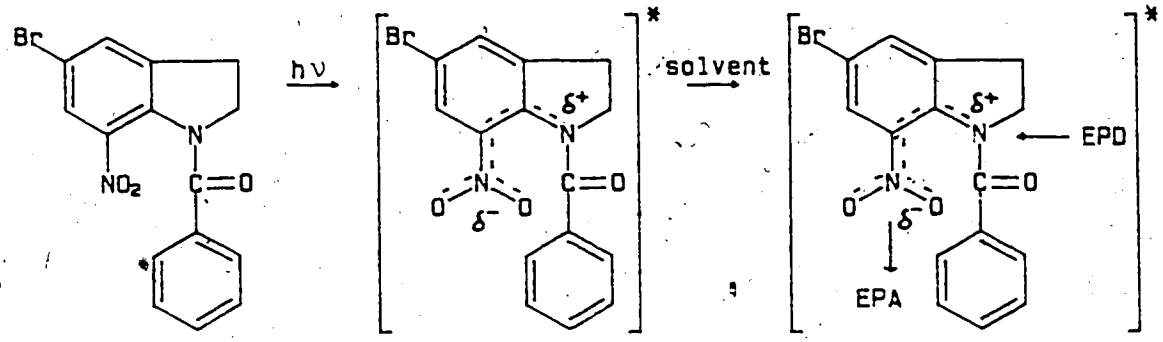

EPA = Electron pair acceptor

EPD = Electron pair donor

Scheme 18

In the CH_3CN-H_2O solvent system the maximum attainable mole percent of 25 was 58. But, in a CH_3CN-H_2O-NaOH solution the mole percent of 25 exceeded 80. As was observed, the relative distribution of photoproduct 25 in the CH_3CN-H_2O-NaOH solvent system is consistent with a hydroxide catalyzed proton removal. However, in light of the product distribution in THF solvent (pg. 54), and the correlation of 25 formation with $E_T(30)$ values, salt effects rather than base catalyzed proton removal from the C-2 carbon should be considered.

In order to corroborate the increase of 25 to a change in ionic strength of the solvent medium, salts such as $LiClO_4$ or $(n\text{-}Bu)_4NClO_4$, in lieu of NaOH, should be considered for future studies.

F. FRAGMENTATION STUDY

(i) Introduction

A homolytic fragmentation process has been proposed from the photoproduct analysis of 10a (Section (D)). Established experimental methods such as electron spin resonance (e.s.r.) measurements, free radical trapping, and substituent effects can corroborate the presence of free radical intermediates in a mechanistic sequence.

(ii) Results

(a) Electron Spin Resonance Measurements

A spectrum was gradually obtained when a deoxygenated solution of 10a in CH_3CN or CH_3CN-H_2O was irradiated as a solid matrix at 120-195 K in an e.s.r. spectrometer cavity with a glass or quartz high pressure mercury lamp. The spectrum obtained consisted of a triplet with lines of unequal intensities, and a hyperfine splitting of 31.8 G (Figure 14).

In contrast to the consistent reproducibility of the low temperature e.s.r. spectra of 10a, the ambient temperature e.s.r. spectra, recorded after warming the irradiated samples of 10a to 25°C, seemed to be very much a function of the type of lamp, and, perhaps, solvent system used for the solid matrix irradiation.

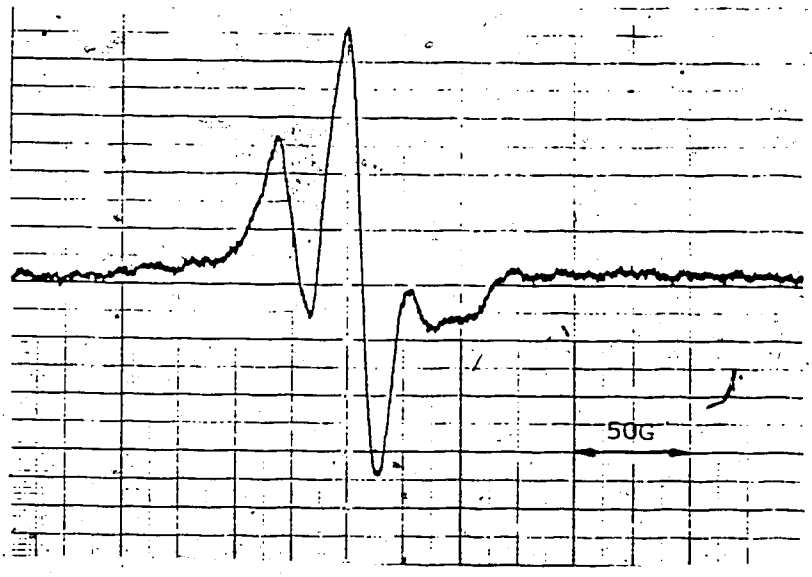

Figure 14: Solid matrix (120 K) e.s.r. spectrum from 10a irradiation in an e.s.r. cavity.

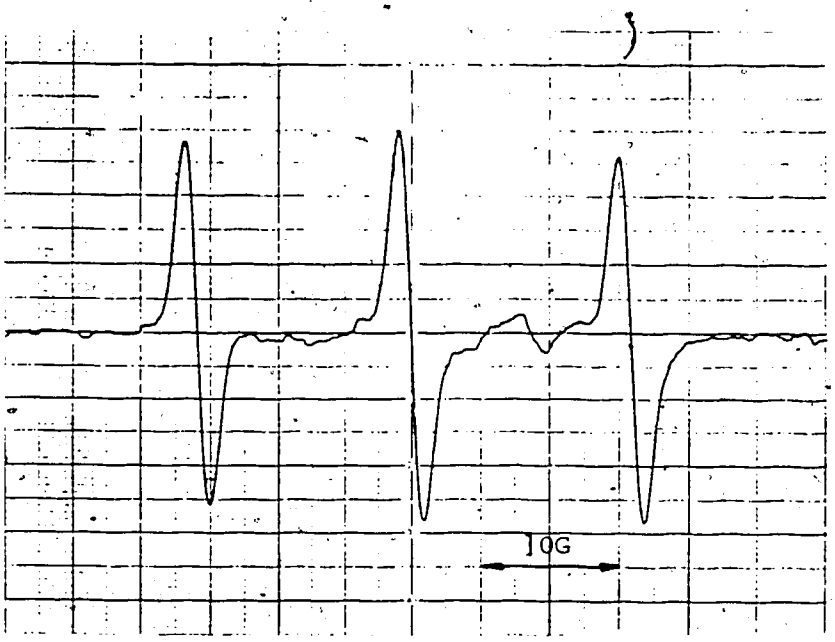

Figure 15: Ambient temperature e.s.r. spectrum after 10a irradiation at 120 K in an e.s.r. cavity and then warmed to ambient temperature.

When 10a in CH_3CN was irradiated at low temperatures with a high pressure quartz mercury lamp the resulting ambient temperature e.s.r. spectrum exhibited a widely spaced set of triplets. This spectrum was the result of a single nitrogen hyperfine interaction of 16.9 G and a g value of 2.0067 (Figure 15). When a similar solution of 10a in CH_3CN or CH_3CN-H_2O was irradiated at low temperature with a high pressure glass mercury lamp no ambient e.s.r. spectrum was observed.

As a control experiment, a degassed sample of 11a in CH_3CN was monitored for e.s.r. signals before freezing to a solid matrix and UV-irradiation. The spectrum recorded was identical to the ambient temperature e.s.r. spectrum obtained after the low temperature photolysis of 10a with the high pressure quartz mercury lamp (Figure 16).

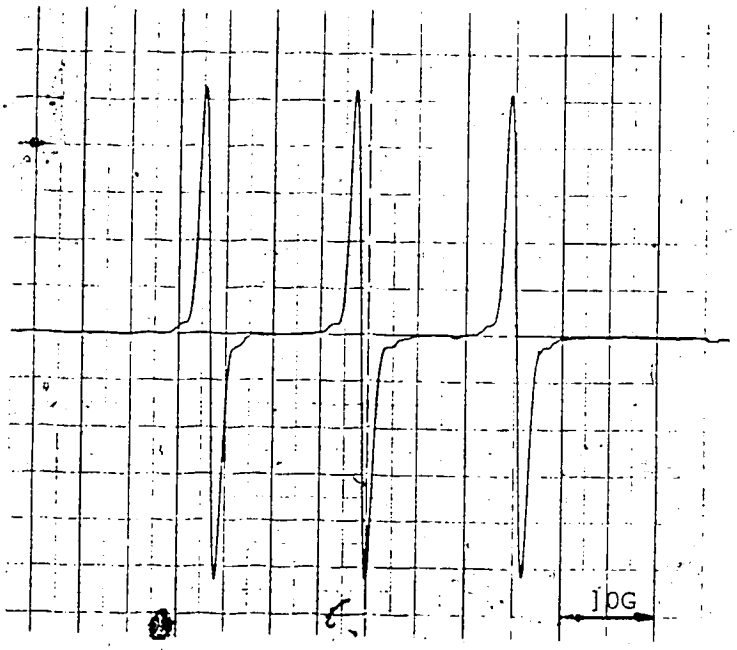

Figure 16: Ambient temperature e.s.r. spectrum from 11a exposed only to visible light.

Subsequent cooling of the degassed sample of 11a to 120 K and recording its e.s.r. spectrum depicted a triplet, however, of unequal spacing and peak intensity; quite unlike the low temperature e.s.r. spectrum observed for irradiated 10a (Figure 17). Irradiation of 11a in the solid matrix did not change the e.s.r. spectrum.

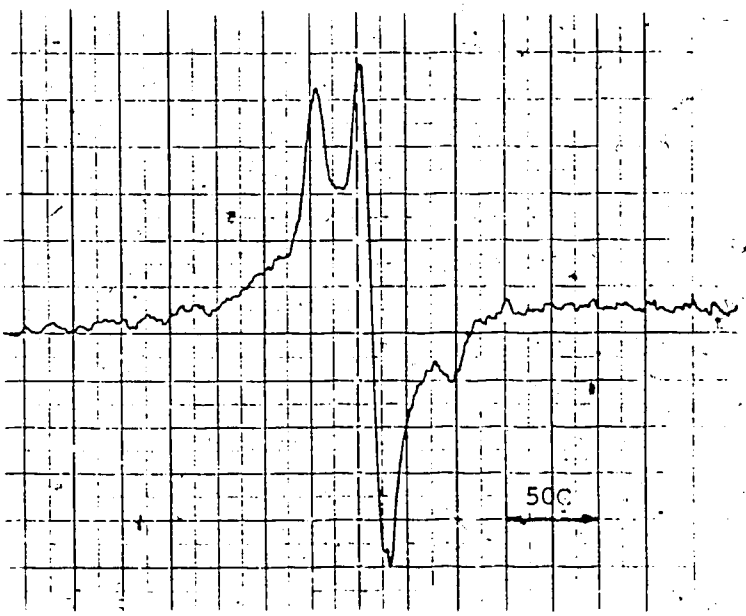

Figure 17: Solid matrix e.s.r. spectrum of 11a.

(b) Free Benzoyl Radical Interception

In order to check for possible diffusion of benzoyl radicals from the solvent cage, subsequent to homolysis of 10a in CH_3CN. the degassed reaction mixtures were analyzed for benzaldehyde, benzil, and in the presence of $^{18}O_2$, for labelled benzoic acid.

When thoroughly degassed CH_3CN solutions of 10a were irradiated for .5 and 14 hours and immediately analyzed via gas chromatography no benzaldehyde was observed. Also the TLC of the photolyzed mixture

revealed no component with an R_f value similar to benzil.

Irradiation of 10a for 1 hour in freshly distilled CH_3CN containing $^{18}O_2$ afforded a mixture composed primarily of photoreactant. Mass spectrometry of the residue, obtained after evaporation of the solvent was conducted such that benzoic acid was exclusively vapourized and ionized. It showed a single parent peak for benzoic acid (m/e 122). When a new sample was prepared, and the irradiation time extended to 6 hours, the mass spectrum of the mixture displayed a small peak at m/e 124; indicative of ^{18}O benzoic acid. The benzoic acid was separated by TLC. The mass spectrum of this separated material again displayed a small m/e 124 ion peak (15% relative to m/e 122). This peak, however, was completely absent in the mass spectrum of benzoic acid separated from a mixture photolyzed in the absence of $^{18}O_2$.

(c) Hammett-Linear Free Energy Relationship

In the early stages of the mechanistic study it was anticipated that a linear free energy relationship would provide a valuable insight into the fragmentation mode of 10a. A satisfactory correlation of $\log \Phi_X/\Phi_H$ with a $\sigma^{\cdot}$ radical substituent constant would be considered an indicator of a homolytic fragmentation of the amide linkage.

Quantum yields for disappearance of 4'-substituted 10a were determined for aerated tetrahydrofuran-water (mole fraction of water = .33) solutions at room temperature. The quantum yields and recorded UV spectral measurements, are summarized in Table 4.

When the $\log (\Phi_X/\Phi_H)$ values for X = H, Cl, Me, OMe and CN are plotted against their corresponding Jackson $\sigma^{\cdot}$ values [93], and

values for X = H, Cl, Me and CN only are considered, a straight line with a slope of 1.3 is obtained (Figure 18). The correlation coefficient for that slope is 0.94.

TABLE 4 Quantum Yields for Disappearance of 4'-substituted 10a in Tetrahydrofuran-Water as a Function of Substituent.

X	λ_{max} (nm)	ε [a] (cm^{-1} M^{-1})	$\Phi \times 10^2$ [b,c]	$\log(\Phi_X/\Phi_H)$	σ [d]
H	352	3712	1.2 ± .1	0	.04
Cl	350	4288	2.6 ± .1	.34	.15
Me	352	3905	3.9 ± .1	.51	.32
OMe	354	4166	2.2 ± .2	.26	.45
CN	350	4648	4.9 ± .1	.61	.47

a Estimated error is ± 3%

b Errors are deviations from average based on 2 runs

c Measured relative to the photodecomposition of potassium ferrioxalate [94]

d Ref. 93.

(iii) Discussion

Each of the three experiments considered, the e.s.r. study, $^{18}O_2$ capture, and $\sigma^{\cdot}$ correlation, provide evidence in favour of a homolytic fragmentation of the benzoyl moiety.

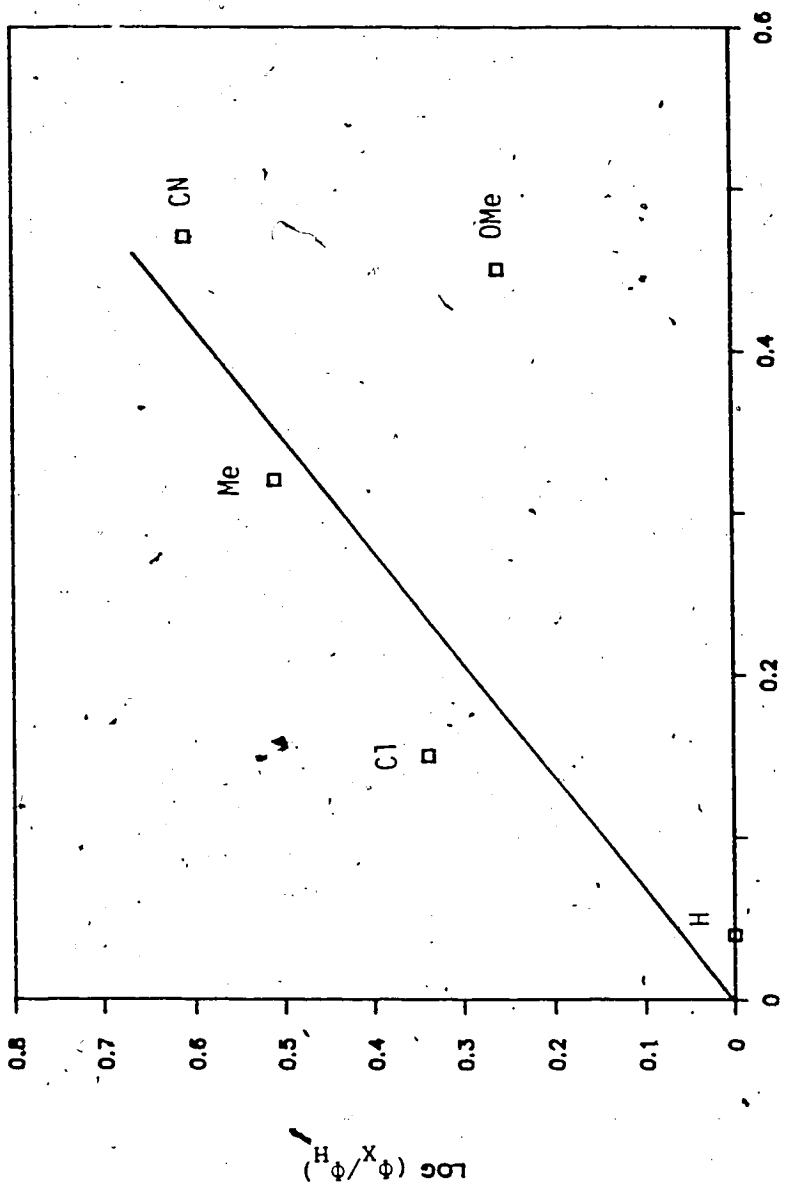

Figure 18: Log (Φ_X/Φ_H) versus σ

The e.s.r. spectrum obtained upon irradiation of 10a in a glass matrix (Figure 14) was assigned to the homolytic α-cleavage products 28 and 29 (44). The skewed triplet of this low temperature e.s.r. spectrum of 10a is ascribed principally to 29 superimposing a broad single peak due to 28.

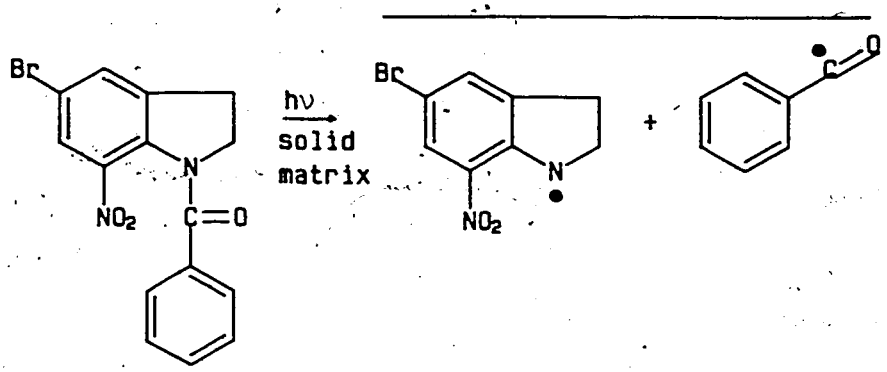

(44)

10a 29 28

The immobilized state of 10a in a glass matrix, the difference in the low temperature e.s.r. spectra from 10a and 11a irradiation (Figure 14 vs. Figure 17), and the photoproduct distribution of 10a in THF are facts which suggest that the e.s.r. peaks observed from the low temperature irradiation of 10a are due to intermediates 28 and 29.

Benzoyl radicals have been studied in solid matrices by Schmidt et al [95]. The e.s.r. spectrum of benzoyl radicals on a cold finger at 70 K was a single broad line with a width (peak-peak) of 15.5 G. When slowly warmed the orange-red colour and e.s.r. signal disappeared at 120 K.

Most aminyl radicals are rather short-lived, and are often only observed by e.s.r. at reduced temperatures [96]. As a result the ambient temperature e.s.r. spectrum shown in Figure 15 is assigned to a secondary reaction product. The observation of identical ambient temperature e.s.r. spectra from 10a or 11a irradiation corroborates the above hypothesis.

The $^{18}O_2$ capture experiment provides evidence for the presence and fate of a benzoyl moiety diffused from the solvent cage. Previous studies have shown that benzoyl radicals have the propensity to diffuse from the solvent cage during the photo-Fries rearrangement [64,97].

Formation of ^{18}O labelled benzoic acid corroborates a homolytic α-cleavage in the photofragmentation process of 10a. The large m/e 122 peak relative to m/e 124 implies that intramolecular spin trapping predominates, and relatively few radicals diffuse from the solvent cage. The radicals that do diffuse from the solvent cage are scavenged by the O_2 forming benzoic acid probably via the pathway suggested by Kan and Furey [98]. The authors suggested that the benzoyl radicals which escape the solvent cage will be scavanged by O_2 to give benzoic acid, probably via the UV-unstable perbenzoic acid (45-48).

$$\mathrm{PhC}(=O)\cdot + O_2 \longrightarrow \mathrm{PhC}(=O)\text{-}OO\cdot \qquad (45)$$

$$\mathrm{PhC}(=O)\text{-}OO\cdot \xrightarrow{\text{solvent}} \mathrm{PhC}(=O)\text{-}OOH + \text{solvent}\cdot \qquad (46)$$

$$\mathrm{PhC(=O)\text{-}OOH} \xrightarrow{h\nu} \mathrm{PhC(=O)\text{-}O^{\bullet}} + {}^{\bullet}\mathrm{OH} \qquad (47)$$

$$\mathrm{PhC(=O)\text{-}O^{\bullet}} \xrightarrow{\text{solvent}} \mathrm{PhC(=O)\text{-}OH} + \text{solvent}^{\bullet} \qquad (48)$$

The observation of a relatively intense peak at m/e 122 could be ascribed to either traces of water in CH_3CN, or intramolecular oxygen transfer from the nitro group. Since no nitroso photoproducts were recovered when 10a was photolyzed in CH_3CN, hydrolysis, of perhaps an intermediate such as 31 shown in Scheme 17, has to be assumed.

In the photo-Fries rearrangement of N-benzoyl-2,3-dihydro-benzoxazol-2-ones, Matsui [65] attributed the formation of benzoic acid (17.2%) to hydrogen abstraction by benzoyl radicals from the solvent (CH_3CN) followed by air oxidation of the intermediate benzaldehyde. When thoroughly degassed CH_3CN solutions of 10a were irradiated for .5 and 14 hours and immediately analyzed via gas chromatography no benzaldehyde was observed.

Non-cage recombination of benzoyl radicals leads to the formation of benzil [99]. However, thin layer chromatography of a photolyzed mixture of degassed 10a in CH_3CN revealed no component with an R_f value similar to benzil.

In view of the $^{18}O_2$ and e.s.r. experiments it was anticipated that the Hammett-Linear Free Energy Relationship would further strengthen the homolytic fragmentation hypothesis.

In the past, several scales of Hammett-type substituent constants for free radicals have been proposed [100,101]. In nearly

every case, the radical substituent parameter has been defined after assumption of some polar contribution. Jackson and coworkers [93] have put forward a $\sigma^{\bullet}$ scale in which the decomposition of substituted dibenzylmercury forms the standard reaction. In the dual-parameter treatment (49), the polar substituent constant chosen by Jackson was σ^{o} (Taft's inductive substituent parameter).

$$\text{Log}\left(\frac{k_x}{k_H}\right) - \rho\sigma^{0} = \sigma^{\bullet} \qquad (49)$$

The dibenzylmercury model reaction for defining the $\sigma^{\bullet}$ scale involves the virtually complete formation of a free benzyl radical in the transition state, with associated stabilization by para substituents [93].

The close correlation of $\sigma^{\bullet}$ from the benzylic model with the 10a fragmentation process indeed implies a somewhat similar substituent effect in both transition states (Figure 18).

An important exception to the $\sigma^{\bullet}$ kinetic radical substituent scale is 1-(4'-methoxybenzoyl)-5-bromo-7-nitroindoline, 35. The methoxy-substituent differs significantly from the benzylic correlation (Figure 18). As Weller [102] has reported, aromatic ethers are typical electron-donor quenchers with relatively low oxidation potentials. Photochemical CIDNP studies have clearly demonstrated the occurrance of an electron transfer process between anisoles and nitrobenzene derivatives [103]. The lower quantum yield of disappearance of 35 could thus be ascribed to quenching of excited 35 by either a ground

state 35 or perhaps via intramolecular exciplex formation.

G. QUANTITATIVE MEASUREMENTS

(i) Introduction

There are many kinds of experimental information that can be used to construct a reaction mechanism. In addition to structural knowledge, kinetic measurements and excited state dynamics provide a valuable set of data.

(ii) Results

(a) Quantum Yield Measurements in CH_3CN and CH_3CN-H_2O

TABLE 5 Quantum Yields for Disappearance of 10a in CH_3CN and CH_3CN-H_2O.

Mole Fraction of H_2O	Quantum Yield x $10^{2a,b}$	
	Aerated	Degassed
0.00	2.3 ± 0.3	2.4 ± 0.2
0.11	1.8 ± 0.2	1.9 ± 0.1
0.24	1.5 ± 0.1	1.8 ± 0.2
0.42	1.4 ± 0.2	1.7 ± 0.1
0.66	1.2 ± 0.1	1.6 ± 0.2
0.81	1.1 + 0.2	---

a Errors are standard deviations of at least 3 runs.

b Measured relative to the photodecomposition of potassium ferrioxalate [94].

Quantum yields for the disappearance of 10a in CH_3CN and various CH_3CN-H_2O solvent systems were obtained. Measurements were performed both on air saturated and degassed samples. The results of the measurements are given in Table 5.

(b) Quantum Yield Measurements in Tetrahydrofuran and Tetrahydrofuran-Water

TABLE 6 Quantum Yields for Disappearance of 10a in Tetrahydrofuran and Tetrahydrofuran-Water.

Mole Fraction of H_2O	Quantum Yield x $10^{2a,b}$ Aerated	Degassed
0.00	1.4 ± 0.2	1.6 ± 0.0
0.08	1.3 ± 0.2	---
0.16	---	0.8 ± 0.1
0.33	1.0 ± 0.1	0.8 ± 0.0
0.53	1.6 ± 0.1	1.2 ± 0.0
0.75	2.9[c]	2.6 ± 0.3
0.82	2.9 ± 0.2	---
0.87	---	3.2

a Errors are deviations from average based on 2 runs.

b Measured relative to the photodecomposition of potassium ferrioxalate [94].

c Value obtained with water used for photolysis of 10a in degassed CH_3CN and CH_3CN-H_2O solution (Table 5).

The "Photoproduct Analysis" study (Section D, pg. 46) has demonstrated that the product distribution is a function of the solvent system. Therefore, it was deemed as informative to also measure the quantum yield of 10a disappearance in THF solvent media (Table 6). Again, as in CH_3CN or CH_3CN-H_2O solvent media, the possible effect of dissolved oxygen was examined.

(c) Electron Transfer Quenching

TABLE 7 Quantum Yields for Disappearance of 10a in CH_3CN as a Function of 1,4-Dimethoxybenzene.

1,4-Dimethoxybenzene (moles/liter)	Quantum Yield x 10^2 [a,b] (aerated)	Φ°/Φ
0.00	2.6 ± 0.1	1.0 ± 0.1
0.0092	2.6 ± 0.1	1.0 ± 0.1
0.0160	2.5 ± 0.0	1.0 ± 0.1
0.0258	2.6	1.0 + 0.1

a Errors are deviations from average based on 2 runs.

b Measured relative to the photodecomposition of potassium ferrioxalate [94].

To probe the excited state dynamics of 10a in both CH_3CN and CH_3CN-H_2O the quantum yield for disappearance of 10a, in the presence of various amounts of an electron donor quencher, was measured. 1,4-Dimethoxybenzene was selected as the electron donor because of its

non-basic nature, low oxidation potential, $E(D/D^+)$ = 1.34 V, [102] and UV transparency above 320 nm. Quantum yield measurements for disappearance of 10a were made on aerated samples in both CH_3CN and CH_3CN-H_2O (mole fraction of water = .66). For the CH_3CN solvent system the results are displayed in Table 7, and for the corresponding aqueous solution in Table 8.

TABLE 8 Quantum Yields for Disappearance of 10a in CH_3CN-H_2O as a Function of 1,4-Dimethoxybenzene (mole fraction of water = .66).

1,4-Dimethoxybenzene (moles/liter)	Quantum Yield x $10^{2a,b}$ (aerated)	Φ°/Φ
0.00	1.66	1.00 ± 0.20
0.0049	0.914	1.81 ± 0.36
0.0101	0.910	1.82 ± 0.36
0.0155	0.597	2.77 ± 0.55
0.0215	0.411	4.03 ± 0.81
0.0248	0.363	4.56 + 0.91

a Measured relative to the photodecomposition of potassium ferrioxalate [94].

b Estimated error is ± 10%.

(d) Triplet State Quenching

The electron transfer quenching study of 10a in CH_3CN-H_2O suggested the involvement of both a triplet and singlet excited state. In order to corroborate this observation the quantum yields for

disappearance of 10a were measured in the presence of different concentrations of 1,3-cyclohexadiene. Diene quenchers reportedly interact only with the triplet excited state [37]. Similarly to the electron transfer quenching experiment, a .66 mole fraction of water was selected for the CH_3CN-H_2O solvent media. For this study all samples were degassed before quantum yield measurements were made. The experimental results are summarized in Table 9.

TABLE 9 Quantum Yields for Disappearance of 10a in CH_3CN-H_2O as a Function of 1,3-Cyclohexadiene (mole fraction of water = .66).

1,4-Cyclohexadiene (moles/liter)	Quantum Yield x 10^2 [a,b] (degassed)	Φ°/Φ
0.00	1.53 ± 0.09[b]	1.00 ± 0.20
0.0208	1.32[c]	1.16 ± 0.18
0.0305	1.34[c]	1.14 ± 0.18
0.0460	0.89[c]	1.72 ± 0.27
0.0842	1.00[c]	1.53 ± 0.24
0.1549	0.98[c]	1.56 ± 0.25

a Measured relative to the photodecomposition of potassium ferrioxalate [94].

b Error is standard deviation of 3 runs.

c Estimated error is ± 10%.

(e) Estimated Excited State Lifetimes

The ability to quench excited 10a in CH_3CN-H_2O and the inability to affect the same in CH_3CN clearly demonstrated the lifetime dependency of excited 10a on the solvent media. Since the slope of the straight portion of the Stern-Volmer plot (Figure 19) is equal to $K_q \tau$, and by estimating the quenching rate constant K_q, a value of τ, the lifetime of excited 10a in the absence of the quencher, can be computed.

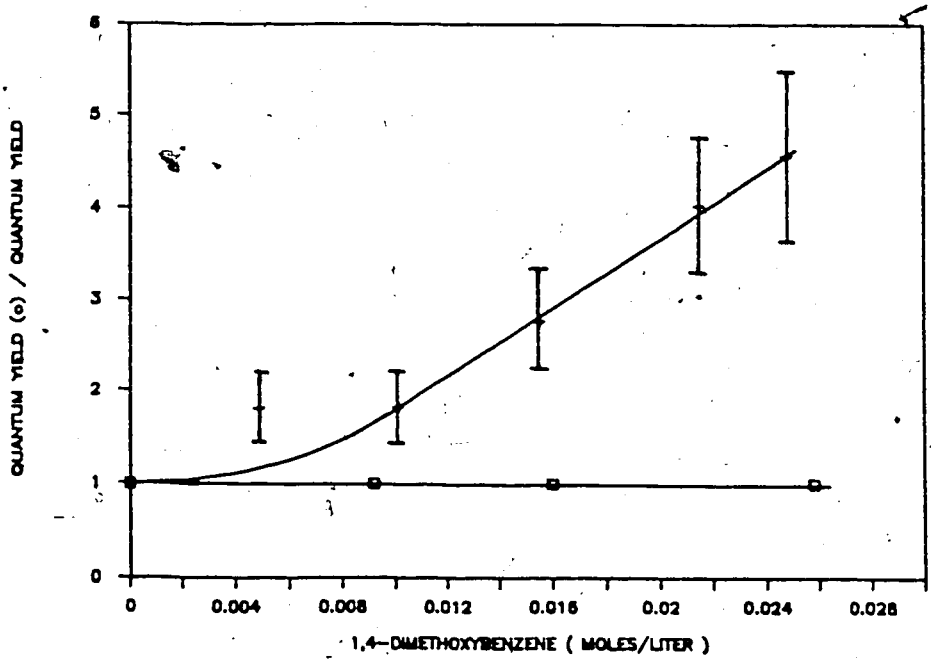

Figure 19: Stern-Volmer plot for disappearance of 10a as a function of 1,4-dimethoxybenzene concentration (▫ in anhydrous acetonitrile, + in acetonitrile-water).

A quenching rate constant can be estimated by considering the free energy value (Δ G) for electron transfer from 1,4-dimethoxybenzene

to excited 10a. According to the Weller equation [102] (50).

$$\Delta G_{ET} = 23.06\ (E_{ox}\ \text{donor} - E_{red}\ \text{acceptor} - e^2/\varepsilon\alpha\ ) - E_{oo} \qquad (50)$$

where for 10a E_{ox} = 1.32 eV [102]

$e^2/\varepsilon\alpha$ = 0.06 eV [104]

E_{oo} ≃ 2.6 eV (estimated from published values of nitroaromatics [68])

The polarographic reduction potential, E_{red} acceptor, for 10a was obtained using Cyclic Voltammetry (Table 10). All reduction potential measurements were carried out on acetonitrile solutions of 10a.

TABLE 10 Cyclic Voltammetric Data for 10a in CH_3CN[a]

Sweep rate (Vs^{-1})	E_{pa} (V)	i_{pa} (μ A)	E_{pc} (V)	i_{pc} (μ A)
.1	-1.06	6	-1.24	6
.5	-1.03	10.3	-1.29	13.8
1.0	-.98	12.5	-1.31	13.8

a 0.1M tetraammonium perchlorate used as supporting electrolyte

For the computation of the ΔG_{ET} value E_{red} of -1.31 eV was selected. Then ΔG_{ET} for the quenching of 10a by 1,4-dimethoxybenzene is approximately 0 kcal/mole.

With ΔG_{ET} = 0 kcal/mole Weller [102] computed in acetonitrile a k_q value of 1.2×10^9 M^{-1} s^{-1}. Therefore, in acetonitrile, where $k_q\tau$ = 0 M^{-1}, the maximum lifetime, τ, is estimated to be $1/k_q = 8 \times 10^{-10}$ s. Assuming that ΔG_{ET} in the CH_3CN-H_2O solvent mixture is also 0 kcal/mole then after viscosity adjustment, from the relative non-viscous solvent acetonitrile (η = 0.0036 poice) to the higher viscosity CH_3CN-H_2O (mole fraction of water = .66) solvent mixture, k_q was calculated as 5×10^8 M^{-1} s^{-1}. In aqueous acetonitrile where $k_q\tau$ = 157 M^{-1} the lifetime of excited 10a is estimated to be 157 $M^{-1}/k_q = 3 \times 10^{-7}$ s.

(iii) Discussion

The changes in slope, when the quantum yields of photolysis of 10a are plotted against the mole fraction of water present in the reaction medium, can be ascribed to changes in the mechanism of the fragmentation process. For example, in THF the initial negative slope at low mole fraction of water changes to a steep positive slope at higher water contents (Figure 20). A mechanistic change also seems to occur for the photoreaction of 10a in acetonitrile and acetonitrile-water (Figure 21).

The product distribution obtained in the different solvent systems is also consistent with a change in the mechanism of 10a photofragmentation. Two photoproducts are observed when 10a is irradiated in CH_3CN, however, in an aqueous acetonitrile solution a third major product was identified. Similarly, the photoproduct distribution in THF

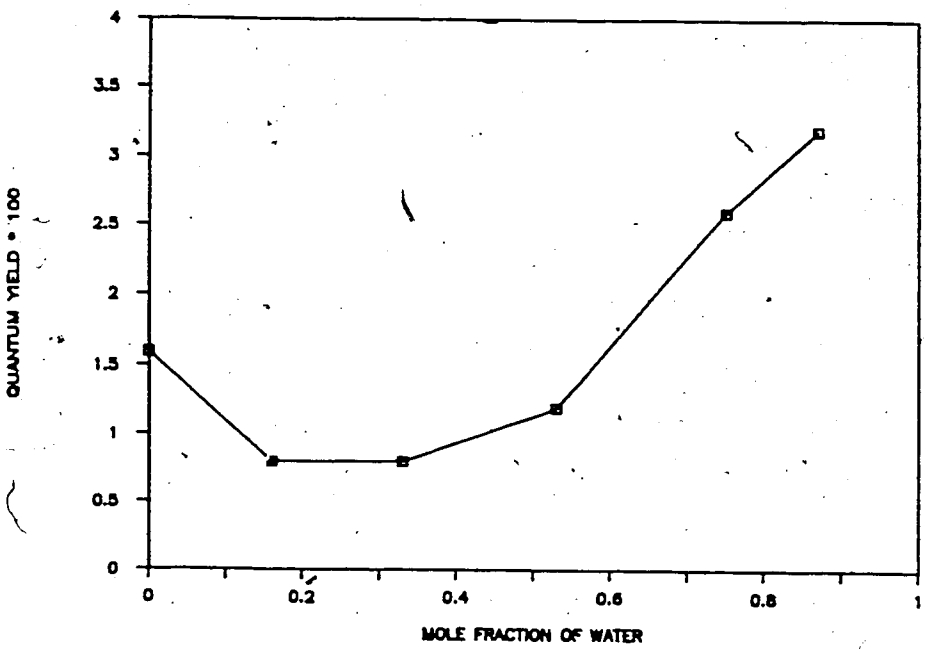

Figure 20: Quantum yield for disappearance of 10a as a function of mole fraction of water in tetrahydrofuran (degassed).

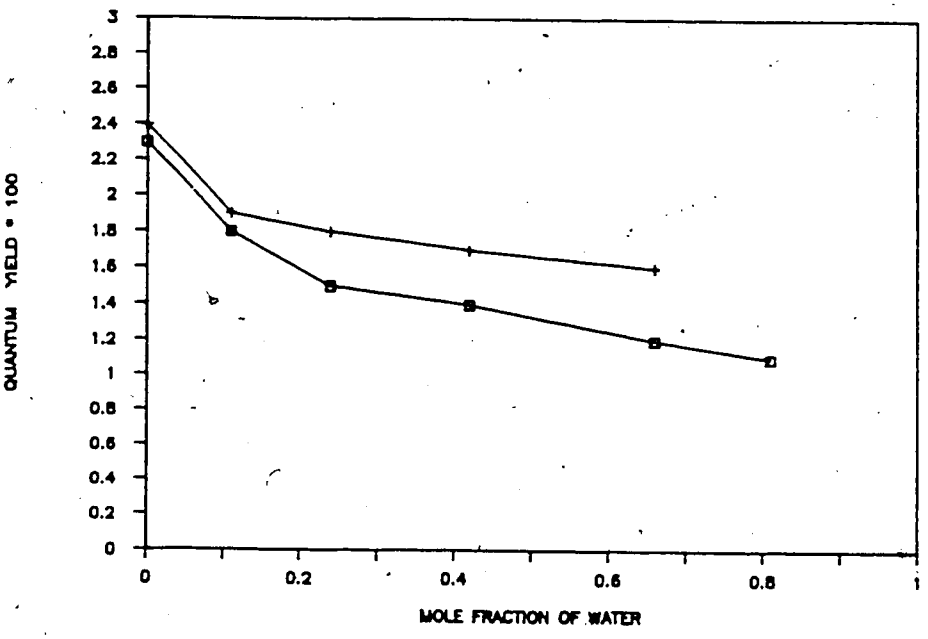

Figure 21: Quantum yield for disappearance of 10a as a function of mole fraction of water in acetonitrile (+ degassed, □ aerated solution).

-H_2O at low water concentrations is different from the distribution found at higher concentrations.

Strong evidence for the mechanistic change originating in the excited state(s) of 10a is obtained from the quenching experiments. In anhydrous acetonitrile 1,4-dimethoxybenzene and molecular oxygen were unable to quench the formation of products (Figure 19). This observation implies that in anhydrous acetonitrile the excited state of 10a has a lifetime equal to or less than 8×10^{-10} s and amide cleavage therefore results from a very short lived excited state. Such short lifetimes are generally associated with singlet states, although on the basis of the available data a short lived triplet state cannot be firmly discounted.

The major argument for a mechanistic change originating in the excited state of 10a rests on the observation of both singlet and triplet excited states of 10a in aqueous acetonitrile. In contrast to the reactions in anhydrous acetonitrile, excited 10a in CH_3CN-H_2O was quenched by O_2 (Figure 21), 1,4-dimethoxybenzene (Figure 19), and 1,3-cyclohexadiene (Figure 22). When considered individually, these quenching experiments might be open to questions, however, taken together they provide strong evidence for a mechanistic change originating in the excited state. From the 1,4-dimethoxybenzene quenching data the lifetime of the triplet excited state of 10a in aqueous CH_3CN (mole fraction of water = .66) was estimated to be 3×10^{-7} s.

In the presence of 1,4-dimethoxybenzene and aqueous acetonitrile the quenching curve for 10a (Figure 19) would appear to increase from its initial value and approach a constant positive non-zero value. This is a

situation commonly encountered when a photochemical reaction occurs through both singlet and triplet excited states, and both are quenched. Selective quenching of the triplet excited state of 10a was shown in the presence of 1,3-cyclohexadiene. The plot Φ_0/Φ_q versus concentration of 1,3-cyclohexadiene (Figure 22) is again typical of a situation in which both the singlet and triplet states can undergo a reaction leading to the loss of starting material.

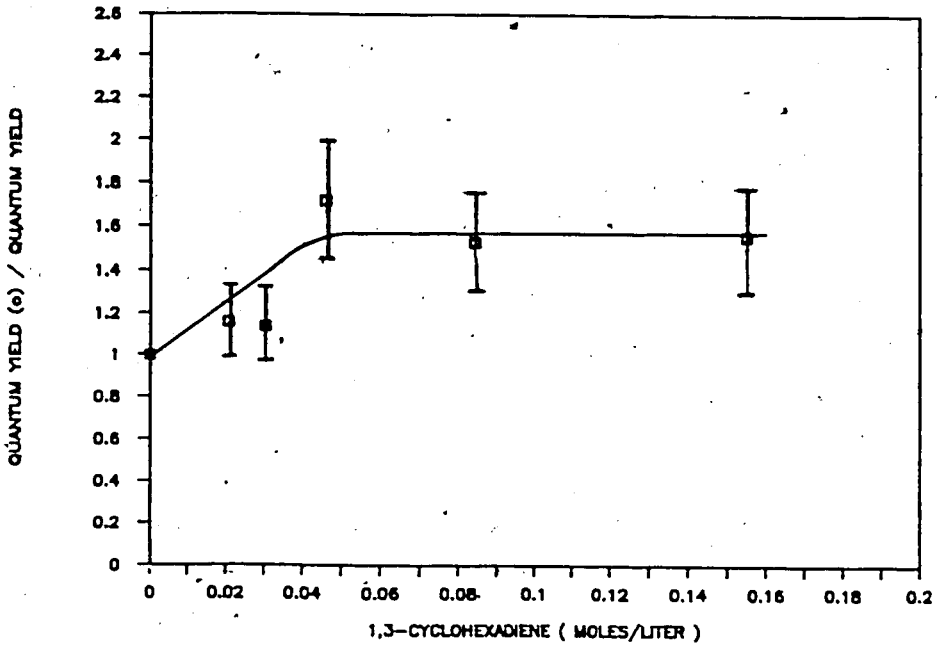

Figure 22: Stern-Volmer plot for disappearance of 10a as a function of 1,3-cyclohexadiene concentration (in acetonitrile-water).

As a result of the Stern-Volmer analysis a kinetic scheme, describing the photofragmentation of 10a to the radical intermediates 28 and 29, in the presence of CH_3CN-H_2O and 1,4-dimethoxybenzene, is proposed (Scheme 19).

$\underline{10a}$	$\xrightarrow{h\nu}$	$^1\underline{10a}$	I
$^1\underline{10a}$	$\xrightarrow{k_{-1}}$	$\underline{10a}$	$k_{-1}[^1\underline{10a}]$
$^1\underline{10a}$	$\xrightarrow{k_{ST}}$	$^3\underline{10a}$	$k_{ST}[^1\underline{10a}]$
$^1\underline{10a} + Q$	$\xrightarrow{k_Q}$	$\underline{10a} + {}^1Q$	$k_Q[^1\underline{10a}][Q]$
$^1\underline{10a}$	$\xrightarrow{k_R}$	$^1[\underline{28} + \underline{29}]$	$k_R[^1\underline{10a}]$
$^3\underline{10a}$	$\xrightarrow{k'_{-1}}$	$\underline{10a}$	$k'_{-1}[^3\underline{10a}]$
$^3\underline{10a}$	$\xrightarrow{k'_R}$	$^3[\underline{28} + \underline{29}]$	$k'_R[^3\underline{10a}]$
$^3\underline{10a} + Q$	$\xrightarrow{k'_Q}$	$\underline{10a} + {}^3Q$	$k'_Q[^3\underline{10a}][Q]$

Scheme 19

The Stern-Volmer equation for the above Scheme is given by:

$$\frac{\Phi^0}{\Phi} = (1 + k_Q\tau_o[Q])(1 + k'_Q\tau'_o[Q])\left(\frac{k_R + k'_R k_{ST}\tau'_o}{k_R(1 + k'_Q\tau'_o[Q] + k'_R k_{ST}\tau'_o)}\right) \quad (51)$$

where $\tau_o = (k_{ST} + k_R + k_{-1})^{-1}$ and $\tau'_o = (k'_R + k'_{-1})^{-1}$

If $k_Q = 0$, that is if the quencher affects only the triplet excited state, the quenching curve tends to a horizontal asymptote given by [106]:

$$\frac{\Phi^0}{\Phi} = \frac{(1 + k'_R k_{ST}\tau'_o)}{k_R} \quad (52)$$

As stated previously, a horizontal asymptote was observed when $\underline{10a}$ was irradiated in the presence of 1,3-cyclohexadiene (Figure 22). However, the form of the quenching curve at lower concentrations ([1,3-cyclo-

hexadiene] < 5.0 x 10^{-2}) could be the result of a depletion of the quencher due to a reaction with the excited reactant or nitroso photoproduct (see "Product Analysis"). Such a depletion of the quencher would make the quantum yield for disappearance of 10a in 1,3-cyclohexadiene a function of time ($\Phi = f(t)$). Thus in the region of low 1,3-cyclohexadiene concentration and high conversion

$$\Phi^0 / \Phi \quad \text{-----> } 1. \qquad (53)$$

At larger quencher concentrations the quenching curve tends to a horizontal asymptote given by equation (52).

Both Shizuka [67] and Wiles [64] have previously observed a solvent polarity effect on the quantum yield of the photo-Fries rearrangement of anilides. Polar solvents decreased the quantum yields of product formation. These results were interpreted by Shizuka in terms of hydrogen bonding between solvent and solute in the excited state. Varma and coworkers [30] in their recent investigation concluded that when 3,5-dinitroanisole is brought into its primary populated π, π^* charge transfer state in hydrogen bonding solvents a single hydrogen bond is formed before any other relaxation occurs.

The drop in quantum yield for disappearance of 10a with increasing mole fractions of water in acetonitrile could be attributed to hydrogen bonding in the excited charge transfer (CT) state. Several factors such as an increase in electron density on the nitro-oxygen in the CT state, steric increase about the nitro group while H-bonding with water, or even a less efficient α-cleavage from the reactive triplet

state might be causes for the decrease in quantum yield for disappearance of 10a.

It is noteworthy that in aqueous THF quantum yields for disappearance of 10a increase with higher mole fractions of water (Figure 20). There seems to be no rationale at hand for such a deviation from the CH_3CN-H_2O solvent system; particularly since, the solvent polarity values of aqueous THF and photoproduct distribution of 10a in THF-H_2O are not significantly different from those observed in the CH_3CN-H_2O solvent. Further research would be required in order to resolve the anomolous photophysical or photochemical behaviour of 10a in THF-H_2O.

H. PROPOSED MECHANISM

(i) Introduction

As indicated in Chapter 1, no systematic mechanistic study of N-acyl-2-nitroanilide photoreduction has been reported to date. Maki [54] as early as 1974 proposed the addition of an excited n,π* nitro group to an anilide carbonyl C=O bond as the primary step in the photodecomposition of N-acyl-2-nitrodiphenylamines, 18. It was suggested that the intermediate 19 so formed would subsequently fragment to an acyloxy- and a nitroso radical (Scheme 6).

Based on the photorearrangement of other N-acyl-2-nitroanilides Amit [20, 21, 22] concluded that only tertiary amides undergo a photo-induced reaction, and the oxygen is transferred from the nitro group to the acyl moiety. Furthermore, he suggested that oxygen transfer from the

nitro group to the acyl unit precedes hydrogen abstraction at the C-2 position of N-acyl-ortho-nitrotetrahydroquinolines.

Of all the N-acyl-2-nitroanilides thus far studied only the 5-substituted N-acyl-7-nitroindolines undergo photosolvolysis rather than photoreduction. Chow [24], in his review on photochemistry of nitro- and nitroso compounds, states: "While the nitro group at the 7-position (of 10) is a requirement, its reaction pattern, and therefore the mechanism, find no analogy in the photochemistry of other o-nitroaromatic compounds".

Recently, Binkley [55] proposed that the mechanistic pathway for the photocleavage of N-acyl-2-nitroanilides is primarily a function of the availability of the hydrogen attached to the carbon α to the amide nitrogen (Scheme 7). According to Binkley's mechanistic proposal, the primary step for the photofragmentation of 5-substituted N-acyl-7-nitroindolines would be the addition of an excited n,π^* nitro group to an amide carbonyl C=O bond, just as was proposed by Maki. However, due to the relatively rigid system of N-acyl-7-nitroindolines the C-2 hydrogen is held too far from the carbonyl group for abstraction and thus a nitronic carboxylic acid anhydride intermediate (pathway B) could be formed which would account for the reported photosolvolysis of 5-substituted N-acyl-7-nitroindolines (Scheme 20).

Since both a nitroindoline and a nitrosoindole compound were isolated after irradiation of N-benzoyl-5-bromo-7-nitroindoline it would appear that something other than C-2 hydrogen availability is the governing mechanistic factor. Considering all the experimental results of this study, in conjunction with the other reported photofragmentation

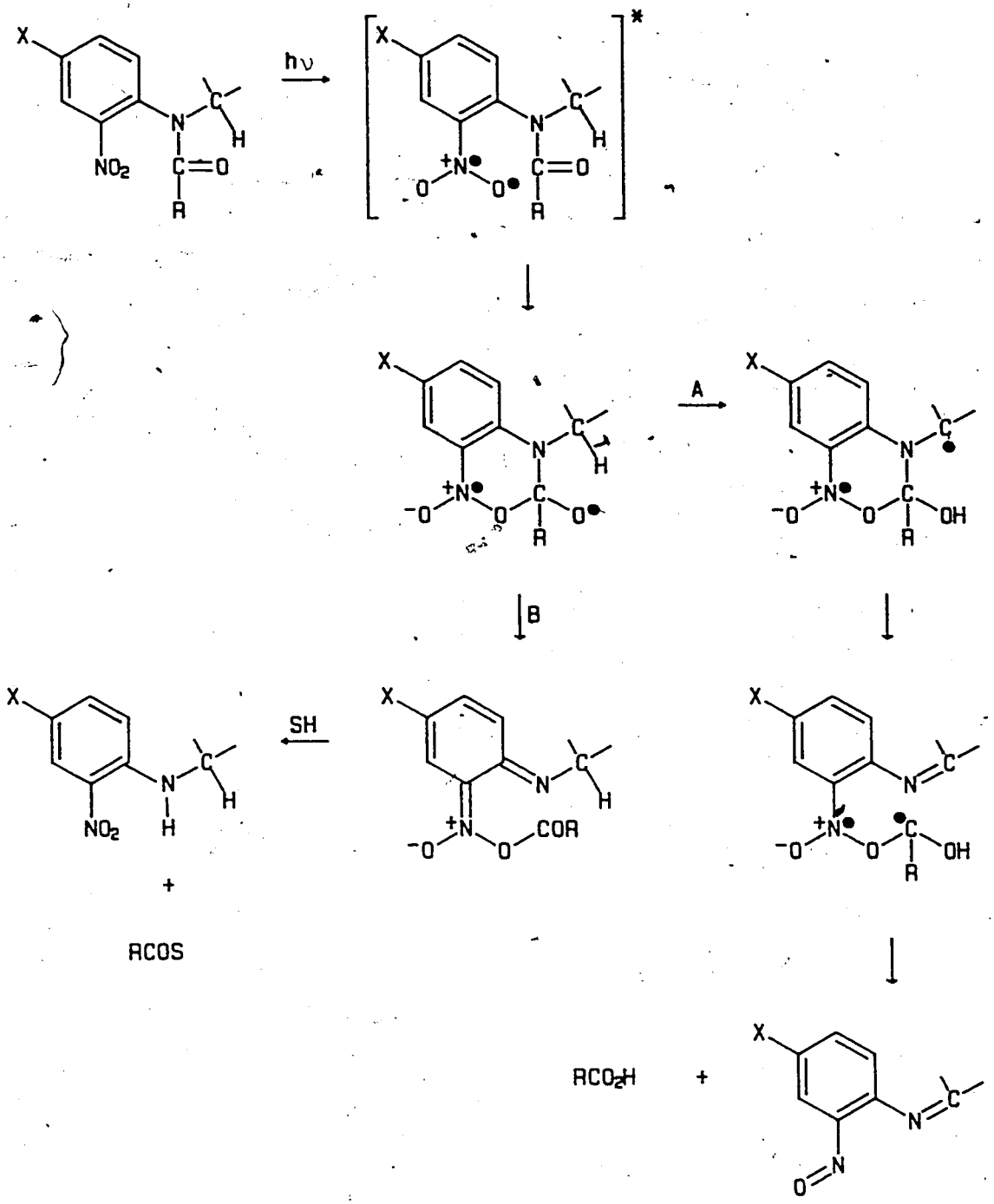

Scheme 20

studies of N-acyl-2-nitroanilides, it is proposed that solvent perturbation of excited states determines the mechanistic pathway of 10a photofragmentation. The solvent influences the yield of fluorescence, the product distribution, quantum yield for disappearance of 10a and the lifetime of excited 10a. Mechanisms which can account for the experimental results are outlined in Scheme 21 and 22.

(ii) Primary Photochemical Process in Aprotic Solvents

Neither molecular oxygen nor 1,4-dimethoxybenzene were able to quench the excited state of 10a in CH_3CN. The failure to quench the excited state in this non-hydrogen-bonding solvent means that this excited state is very short lived ($\tau \leq 8 \times 10^{-10}$ s). Such a short lifetime suggests that the reactive state for 10a in CH_3CN is the singlet excited state. Additional evidence in support of a singlet excited 10a in CH_3CN comes from the observation of fluorescence in CH_3CN and the formation of products through both the singlet and triplet excited states in CH_3CN-H_2O. These results are understandable in terms of the postulate that in non-hydrogen-bonding solvents fragmentation of 10a occurs from an excited singlet n, π^* state localized in the carbonyl chromophore. The postulate presupposes that the singlet n,π^* state, localized on the carbonyl, would be populated with high quantum efficiency and carbonyl photochemistry can compete with deactivation to possibly a lower lying nitro localized state. Therefore, in non-hydrogen-bonding solvents a S_n (n,π^*) ---> ^1D primary process is suggested for 10a.

It should be noted that the proposal of a singlet (n,π^*) --->

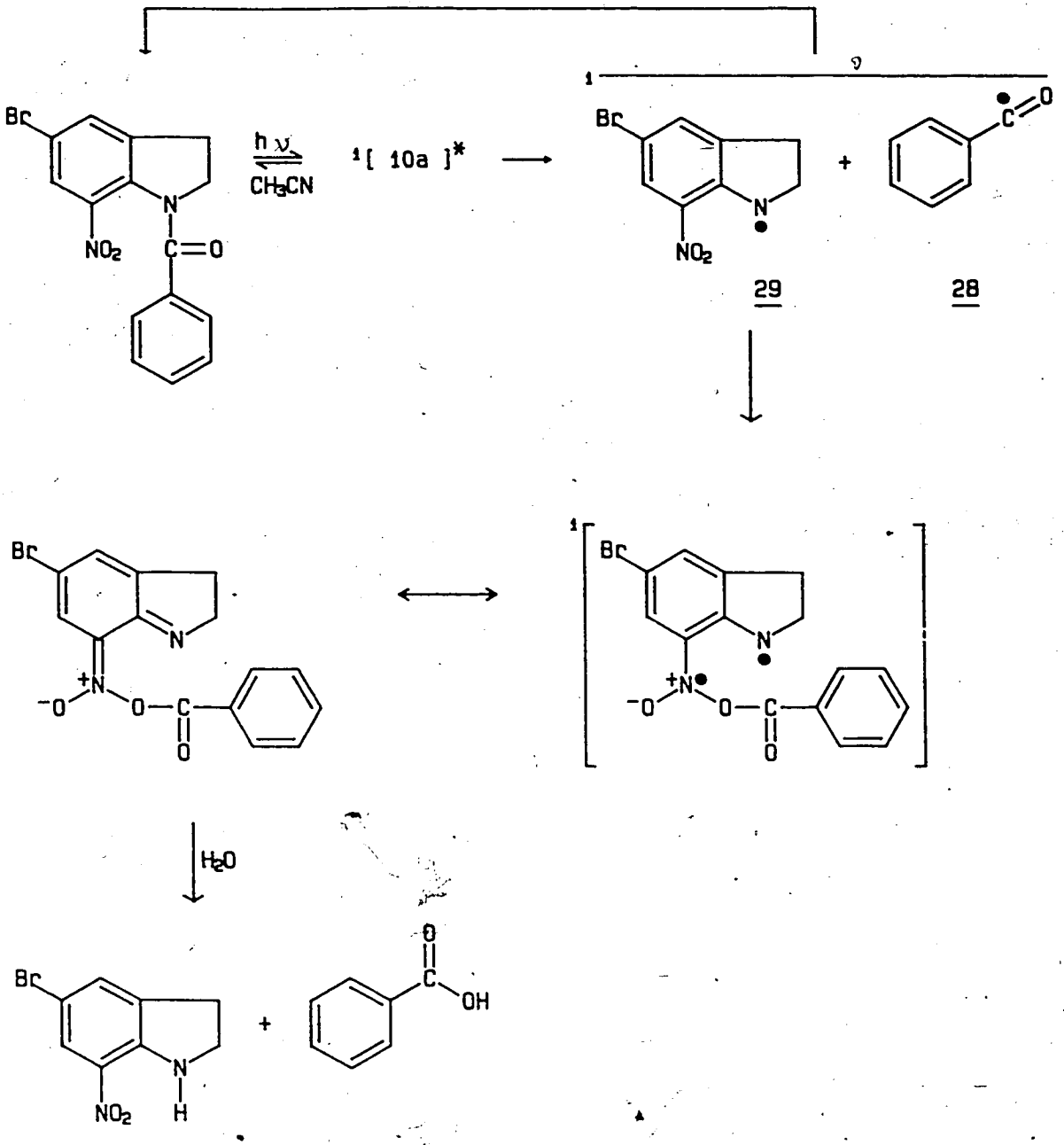

Scheme 21

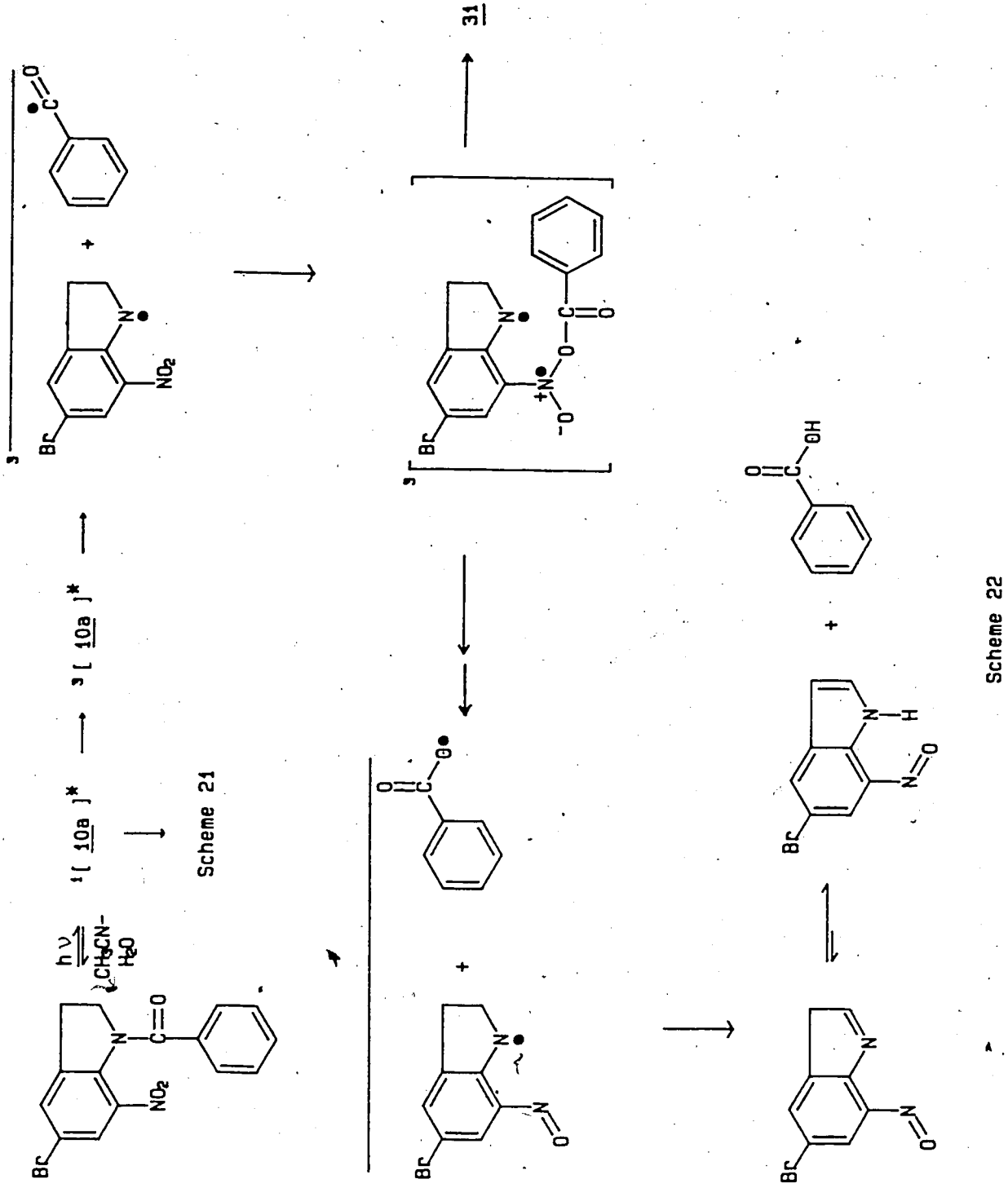

Scheme 21

Scheme 22

^1D primary process for 10a in CH_3CN differs from the generally regarded view that (a) the triplet excited state is the reactive species for nitroaromatics, and (b) a bromine substituent enhances the probability of a radiationless process, such as S_1 ---> T_n and T_1 ---> S_o intersystem crossing. Varma [30] recently demonstrated the complex photophysical behaviour of nitroaromatics in the picosecond and nanosecond kinetic study of excited 3,5-dinitroanisole in CH_3CN and CH_3CN-H_2O.

In spite of a bromine substituent, 10a fluoresces in acetonitrile. This implies that the "heavy atom" effect does not dominate, and bring about very rapid intersystem crossing.

A possible kinetic scheme describing the relaxation of electronically excited 10a in non-hydrogen-bonding solvents is shown in Scheme 23.

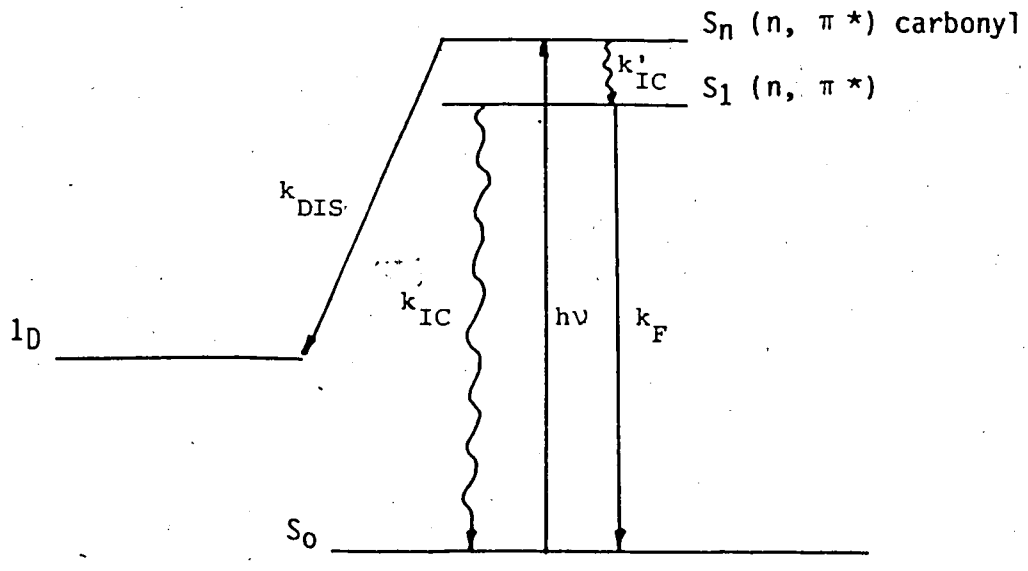

Scheme 23

The homolytic photofragmentation as the proposed initial photochemical transformation is in complete contrast to Binkley's [55] and Maki's [54] proposed mechanism (Schemes 6 and 7). Both of these authors proposed the addition of an oxy-radical to the amide C=O bond as the initial step in the photofragmentation of N-acyl-2-nitroanilides.

Low temperature electron spin resonance studies of 10a in an acetonitrile glass matrix indicated the intermediacy of radicals, but, little structural information could be gleaned from the resulting spectrum. The depicted skewed triplet in the low temperature e.s.r. spectrum could be assigned to either a nitroxide-carboxy biradical, similar to that proposed by Binkley, or to the aminyl radical 29 (Scheme 21).

The observation of ^{18}O enriched benzoic acid in the mass spectrum after photolysis of 10a in an $^{18}O_2$ saturated acetonitrile solution provides supporting evidence in favour of a homolytic cleavage of the amide bond. Both Shizuka [66] and Wiles [64] showed that in the photo-Fries rearrangement of N-arylamides, benzoyl radicals which escape the solvent cage will be scavenged by O_2 to give benzoic acid.

The Hammett-LFER study was also in complete agreement with a homolytic fragmentation mode. The logarithmic value of quantum yield for disappearance of 10a is linearly related to the $\sigma^{\cdot}$ scale proposed by Jackson [93]. Maki [54] in the photolysis of N-acyl-2-nitrodiphenylamines, 18, observed that the conversion of 18 to the photoproduct 20 was most efficient when the acyl group is aromatic and the amide nitrogen substituent is capable of stabilizing a radical intermediate (Scheme 6).

Although the above experimental results clearly support the

notion of a homolytic amide C-N bond fragmentation, they do not prove that this process is the primary photochemical step. However, further weight is added to this proposal since amide C-N bond fragmentation has been amply cited in the literature as the primary step in the photo-Fries rearrangement. On the other hand, there are no known precedents for an oxy-radical addition to an amide C=O bond. The observation of 5-bromo-7-nitroindole as one of the photoproducts in tetrahydrofuran solvent supports the view of primary amide C-N bond homolysis with subsequent H-abstraction by either a benzoyl- or tetrahydrofuran radical (54).

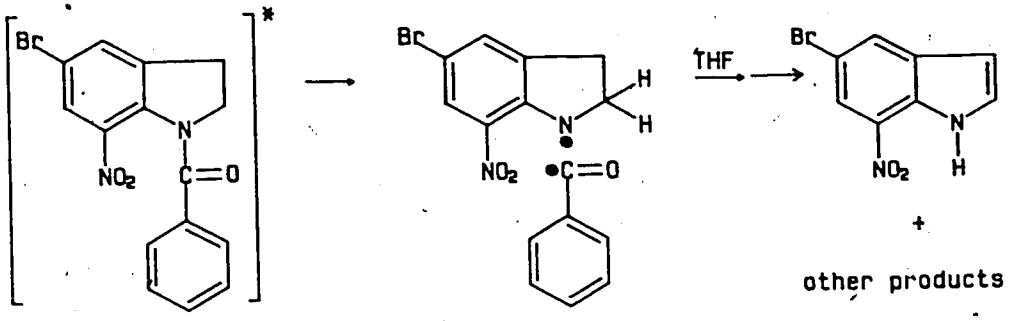

(54)

(iii) Secondary Processes in Aprotic Solvents

After amide bond homolysis, the radicals in the solvent cage can again recombine to starting material, combine to give a nitroxide-arylaminyl diradical, or diffuse from the solvent cage.

There is abundant evidence that nitroaromatics are quite effective spin traps for certain organic radicals [47, 84]. A key step in the proposed mechanism is the coupling of 28 at the nitro functionality of 29 within the solvent cage to form the nitronic carboxylic acid anhydride 31 as shown in equation (55) and Scheme 21.

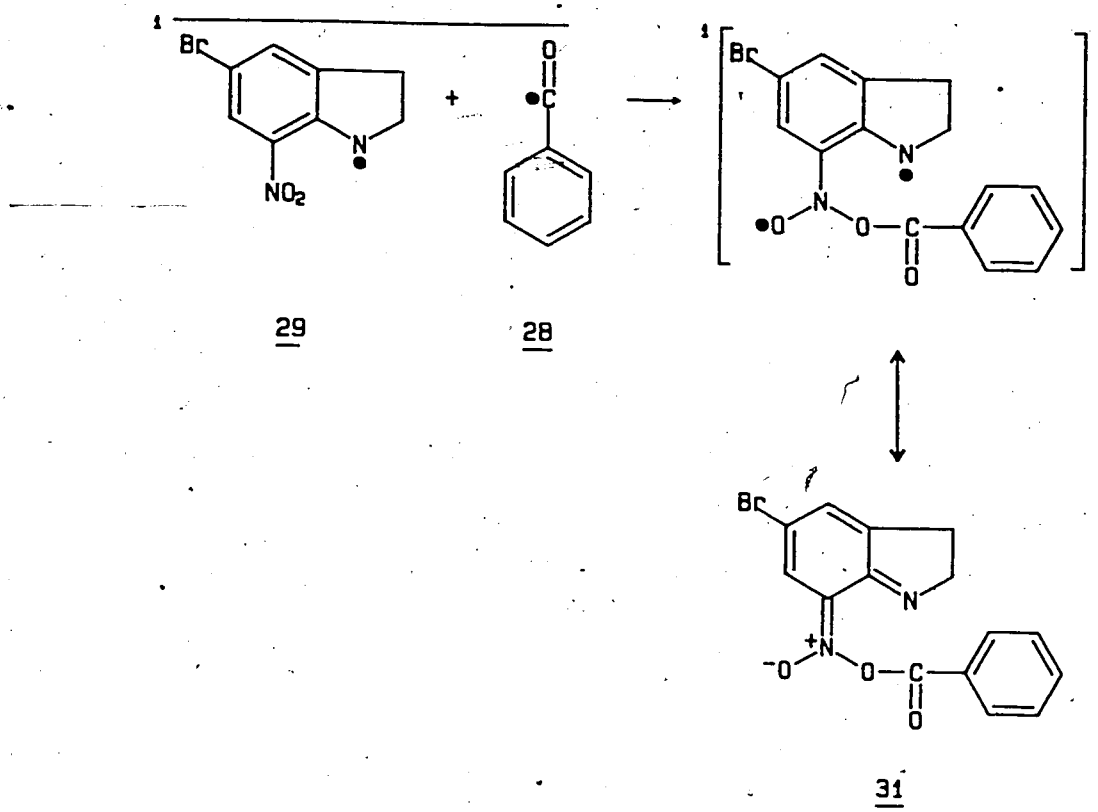

(55)

29 28 31

Shriner [107] in 1937 showed that the hydrolysis of a nitronic carboxylic acid anhydride with aqueous sodium hydroxide led to benzoic acid and a nitro compound, and the reaction with phenylhydrazine led to a hydrazide and a nitro product. This suggests that in the presence of a nucleophile such as water intermediate 31 would be hydrolyzed to 11a and 12a.(57). Clearly, the formation of a low energy, resonance stabilized, photoproduct such as 11a would make the postulated nitronic carboxylic acid anhydride, 31, a very reactive intermediate. However, in the absence of a nucleophile, 31 might be relatively stable.

Unambiguous evidence for a hydrolyzable nitronic carboxylic acid anhydride intermediate comes from the product distribution in the presence of nucleophiles other than water. Irradiation of 10a in ethanol

yielded, for example, ethyl benzoate. Amides and thioesters have also been reported as photofragmentation products [108].

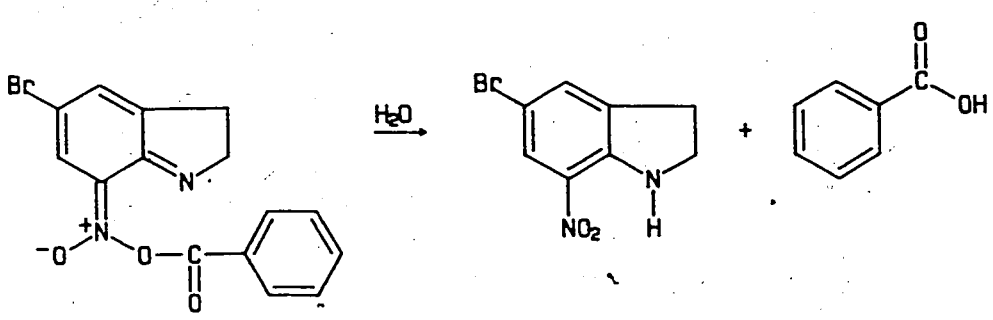

31 11a 12a (57)

The complete mechanism of 10a photolysis in CH_3CN is depicted in Scheme 21.

(iv) Primary Photochemical Process in H-bonding Solvents

Because of the localized excitation character of the nitro n,π* state, Varma [30] concluded that the nitro n,π* states are not very sensitive to the type of aromatic systems to which the NO_2 group is attached. The π,π* charge transfer state, however, is strongly dependent on the type of aromatic system to which the NO_2 is attached, and the solvent medium used. Solvent changes may invert the relative energies of singlet and/or triplet excited states for aryl ketones and nitroaromatics, i.e. n,π* and π,π* may flip-flop energetically. In general, the energy of an n,π* state increases and that of the π,π* decreases with increasing solvent polarity. Furthermore, when the solvents contain a hydrogen bonding component, hydrogen bonding may take place between the ^{1}π,π* charge transfer (CT) state and the solvent

molecule.

The experimental results from the Stern-Volmer quenching analysis (Figure 19) and the disappearance of fluorescence of 10a in aqueous acetonitrile may also be interpreted in terms of hydrogen bonding in the excited state. As already mentioned previously, 1,4-dimethoxybenzene is unable to quench excited 10a in CH_3CN. However, effective quenching of excited 10a with the same molecule occurs in CH_3CN-H_2O (mole fraction of water = .66). The estimated lifetime, τ, of excited 10a in CH_3CN-H_2O increased by almost three orders of magnitude, a phenomena also observed by Varma in his study of 3,5-dinitroanisoles [30]. He described the hydrogen bonded triplet state ($T_{1,\ HB}$) decay as a two step process in which the dissociation reaction is the rate limiting step (58).

$$T_{1\ HB}\ (\pi,\pi^*) \quad \text{---}> \quad T_1,\ (n,\pi^*) \quad \text{---}> \quad S_o \qquad (58)$$

Selective triplet quenching of 10a with 1,3-cyclohexadiene showed that in a polar hydrogen bonding solvent products are possibly formed from both the singlet and triplet excited state.

Given the above experimental results it is proposed that, due to a solvent induced shift of excited states in 10a, intersystem crossing to the triplet excited state effectively competes with fragmentation from the singlet state in polar, protic solvents. The product expected for α-cleavage of 10a from a triplet excited state is a radical pair ^3D.

A kinetic scheme describing the relaxation of electronically excited 10a in polar hydrogen bonding solvents is shown in Scheme 24.

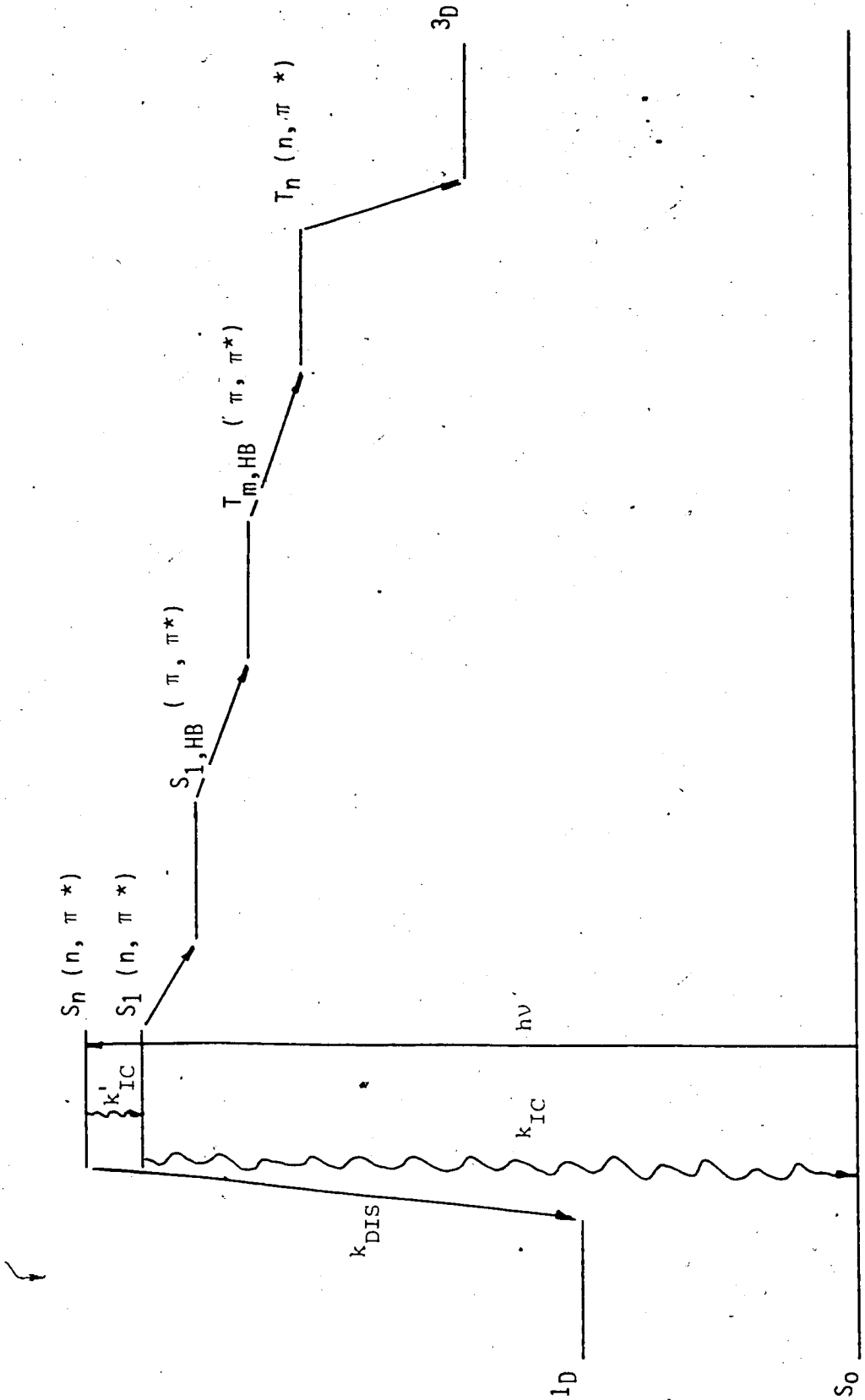

Scheme 24

(v) Secondardy Processes in Polar H-bonding Solvents

In polar H-bonding solvents, spin trapping of the benzoyl radical by the nitro group, within the solvent cage, is proposed. Since amide bond homolysis of 10a seems to occur from singlet and triplet excited states, both a singlet and triplet nitroxide-arylaminyl biradical are predicted in aqueous acetonitrile.

As outlined previously, the singlet nitroxide-arylaminyl biradical 28 and 29 couples to form the nitronic carboxylic acid anhydride 31. Subsequent hydrolysis of 31 in the presence of water would then yield photoproducts 11a and 12a (Scheme 21).

Relatively little is known about the mechanism and rate determining step for the intramolecular decay of triplet biradicals. Current evidence favours intersystem crossing (ISC) to the singlet biradical as the rate determining step in the decay of small, flexible triplet biradicals [109].

The possibility of the decay of a triplet biradical being controlled by hydrogen bonding was suggested by Small and Scaiano [110] in a study of biradicals generated in the Norrish type II reaction. They suggested that the effect of the solvents hydrogen bonding ability probably reflects changes in the interaction between the radical sites in the biradical. This may be due as a result of either a change in the overall conformation, or a communication of the biradical ends involving the solvent. Factors which enhance intersystem crossing in biradical intermediates in organic photochemistry have still not been completely defined.

Buchachenko [111] showed that nitroxides are also capable of

hydrogen bond formation with water. The most probable model he suggested is that in which the hydrogen bond is formed with participation of the lone electron pair of the oxygen atom of the radical. In his σ model, direct π -type overlap between the odd electron orbital and the p_z atomic orbital centered on the oxygen atom of the solvent is assumed to exist (Figure 23).

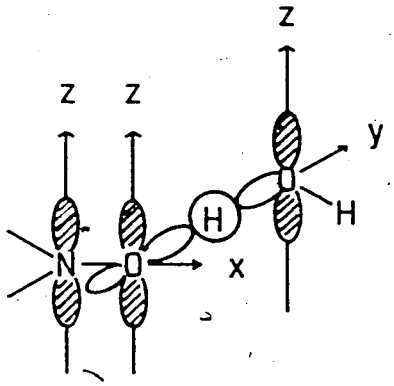

Figure 23: σ Model for nitroxide stabilization via hydrogen bonding.

A solvent stabilized triplet nitroxide arylaminyl biradical could then, either fragment about the N-O bond or intersystem cross to form the singlet nitroxide arylaminyl biradical. N-O bond homolysis would yield a nitroso and a benzoyloxy radical (Scheme 22). Oxygen transfer from the nitro group has been invoked as a major step in the mechanism of photoreactions of nitroaromatic compounds [112]. Direct evidence for an intramolecular oxygen atom transfer from a nitro group has been demonstrated by Amit [21] in the photolysis of N-benzoyl-1,2,3,4-tetrahydro-8-nitroquinoline.

The temperature dependent yield of 11a and 25 in aqueous CH_3CN

would also be consistent with the triplet nitroxide-arylaminyl biradical being a common intermediate for the photoproducts. Since α -cleavage of the N-O bond in the nitroxide arylaminyl biradical possesses a finite activation energy, increased temperatures could lead to a fragmentation rate enhancement. But, an increase in temperature would have no effect on the intersystem crossing rate.

Before escaping from the solvent cage, or losing CO_2, the highly reactive benzoyloxy radical apparently abstracts a hydrogen from the C-2 position of the nitroso arylaminyl radical forming photoproducts 11a and 25 (Scheme 22). This conclusion is supported by Amits report on the photocleavage of N-benzoyl-1,2,3,4-tetrahydro-8-nitroquinolines [21].

Although the postulated mechanism for the photofragmentation of 10a in H-bonding solvents is consistent with the experimental results other mechanistic pathways cannot be discounted. For example, a pathway based on an electron transfer process prior to C-N bond homolysis would also be in agreement with the experimental results.

I. UNIFYING CONCEPT

One interesting observation that comes out of this work is the similarity of 10a phototransformation and other photoreactions. Despite the structural similarity of 9 and 10a, Amit and Patchornik [21,22] assumed a different mechanism for their respective photofragmentations. This conclusion they based on ^{18}O labelling experiments and product analysis.

The apparently unrelated photolysis reactions of 9, 10a, and 18,

however, could be mechanistically consolidated. Since relative excited-state energies can be altered by molecular distortion, and as indicated previously, by solvents, it is proposed that the reactive excited state of the N-acyl-2-nitroanilide, rather than H-availability, determines the photoproduct composition.

On irradiation of N-acyl-2-nitroanilides the primary photochemical step is assumed to be amide bond homolysis from either a singlet or triplet excited state. For 9 [21] and 18 [54], in both H- or non H-bonding polar solvents and 10a in polar H-bonding solvents only a reactive triplet excited state has been postulated. However, for 10a in non H-bonding solvents C-N amide bond homolysis seems to occur from the singlet excited state.

Rapid coupling of the singlet acyl and arylaminyl biradical at the nitro functionality will form a nitronic carboxylic acid anhydride. Solvolysis of this acid anhydride would yield a nitro compound and a carboxylic acid derivative as product of the N-acyl-2-nitroanilide irradiation.

Spin trapping of the triplet acyl and arylaminyl biradical, on the other hand, will lead to a nitroxide-arylaminyl diradical intermediate. Due to the slow intersystem crossing of the triplet diradicals, the triplet nitroxide-arylaminyl diradical, could fragment homolytically about the N-O bond to form an acyloxy and a nitroso-arylaminyl radical. The ensuing reaction steps would produce a nitroso compound either as an intermediate or the final photofragmentation product (Scheme 25).

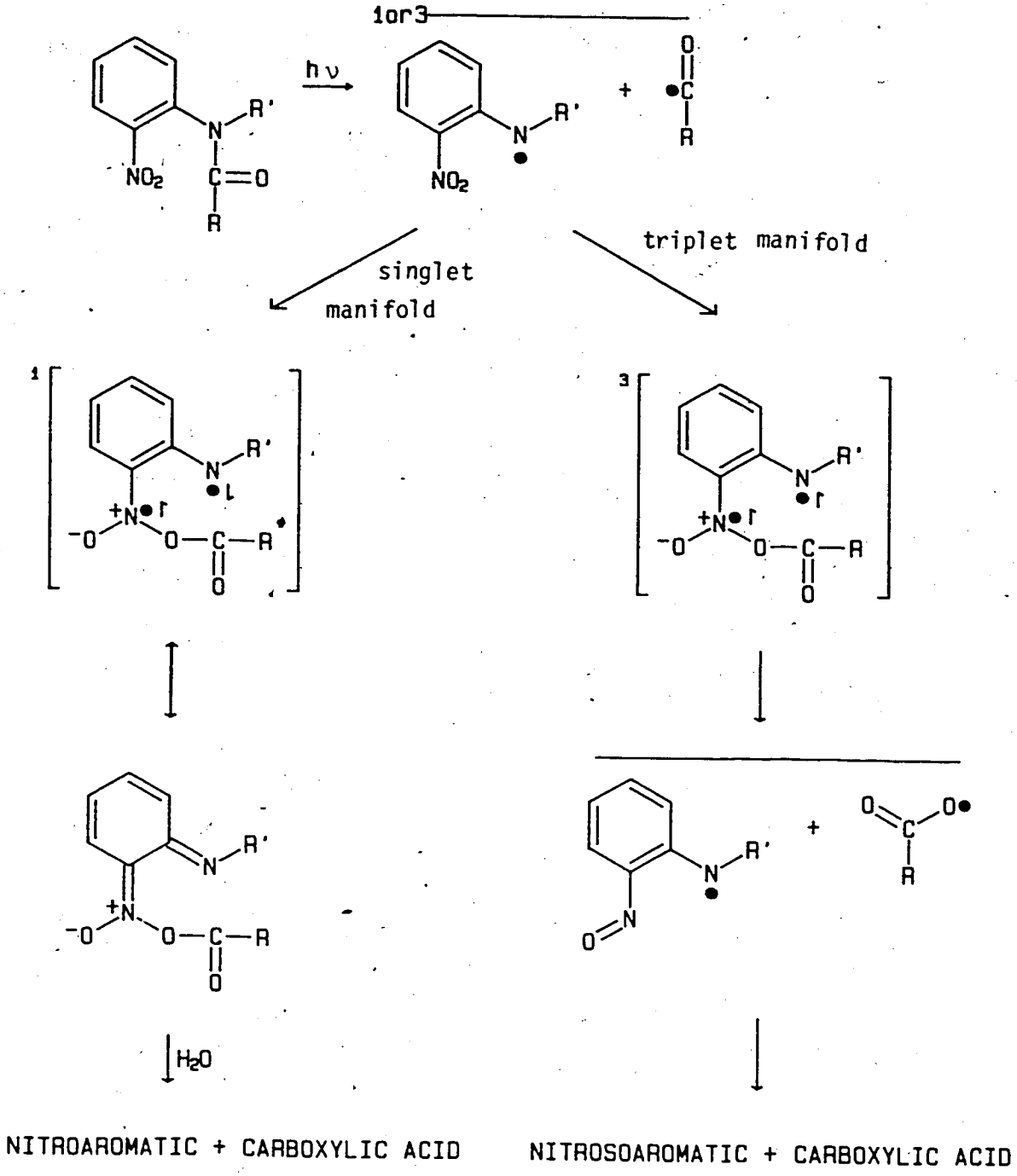
1or3
hν
singlet manifold
triplet manifold
H2O
NITROAROMATIC + CARBOXYLIC ACID
NITROSOAROMATIC + CARBOXYLIC ACID

Scheme 25

J. CONCLUSION

N-Benzoyl-5-bromo-7-nitroindoline photolytically transformed into products with a disappearance quantum yield of 0.01 to 0.05. In CH_3CN, benzoic acid and 5-bromo-7-nitroindoline were the only photoproducts observed. When N-benzoyl-5-bromo-7-nitroindoline was photolyzed in an H-bonding solvent system 5-bromo-7-nitrosoindole, in addition to benzoic acid and 5-bromo-7-nitroindoline, was also identified. Although the photoproduct yields are virtually quantitative its low fragmentation efficiency makes this system unattractive for the photolytic activation of the charge mosaic membrane.

The results from this research led to the suggestion that the unique fragmentation of N-benzoyl-5-bromo-7-nitroindoline is a function of the relative energetics of the excited states rather than availability of C-2 hydrogen as proposed by Binkley [55]. From the absence of excited state quenching by 1,4-dimethoxybenzene, the observation of fluorescence and the product distribution, a singlet reactive state of 10a in CH_3CN was suggested. In the presence of a polar H-bonding solvent system a solvent induced shift of excited states facilitates intersystem crossing to the triplet excited state. This postulate is based on a Stern-Volmer quenching analysis, disappearance of fluorescence, and formation of 5-bromo-7-nitrosoindole.

Whether the reactive state is a singlet or triplet, in each instance homolysis of the C-N amide bond is the proposed primary photochemical process. The singlet biradical could then recombine at the nitro functionality to form a nitronic carboxylic acid anhydride

intermediate, which, in the presence of water, can hydrolyze to 5-bromo-7-nitroindoline and benzoic acid. Spin trapping of the triplet biradical may form a triplet nitroxide-arylaminyl biradical intermediate. A triplet nitroxide-arylaminyl biradical, on the other hand, seems to fragment about the N-O bond. H-abstraction by the benzoyloxy radical from the C-2 position of the nitroso arylaminyl radical, before escape form the solvent cage, would account for the observation of 5-bromo-7-nitrosoindole as the third photoproduct in aqueous CH_3CN.

Homolytic α-cleavage about the RN-COR[1] bond coupled with nitro spin trapping of the acyl radical is proposed as a mechanistic pathway common to all N-acyl-2-nitroanilide photofragmentations.

Although sufficient information has been accumulated to permit discussion of this complex transformation with a certain degree of confidence, further work in some areas of the physical and chemical processes of N-acyl-2-nitroanilides, particularly 10a, is still required. Since the presented evidence advocates a nitronic carboxylic acid anhydride intermediate for 10a phototransformation in non H-bonding solvents it would be of interest to probe further, in an inert solvent system, this elusive intermediate by chemical and spectroscopic means. Also, sensitization experiments might corroborate the triplet excited state as the precursor for 5-bromo-7-nitrosoindole. Finally, the identity of the light emitting species in fluorescence and phosphorescence measurements should be determined by monitoring emission intensities as a function of time and possibly investigate the basis of the dual phosphorescence of N-benzoyl-5-bromo-7-nitroindoline.

CHAPTER III

EXPERIMENTAL METHODS

A. GENERAL

(i) Materials

All of the reagents employed for the syntheses of N-acyl-2-nitroanilides were commercially available and were used without further purification. Acetonitrile was purified and dried by distillation of HPLC-grade solvent from CaH_2, and discarding the first and final 10% of distillate. Tetrahydrofuran used for photoproduct analysis, distribution, and quantum yield studies was distilled from $LiAlH_4$ prior to solution preparation. Both acetonitrile and tetrahydrofuran were stored in glass containers wrapped with aluminum foil, and kept in a N_2 glove bag. Purified water was obtained by filtering distilled water through a paper filter, activated charcoal and finally through an ion exchange column. All other solvents used for the studies were either HPLC-grade, and used without further purification, or reagent grade which were redistilled prior to solution preparation.

Aqueous NaOH solutions were prepared by dilution of a N/10 NaOH solution obtained from BDH Chemicals Ltd. 1,3-Cyclohexadiene, supplied

by Aldrich Chemical Co., was redistilled just prior to solution preparation. For the electron transfer quenching studies 1,4-dimethoxybenzene was purified by recrystallizing the reagent grade material from methanol-water then subliming the recrystallized fraction.

(ii) Melting Points

Melting points were determined on a Reichert Hotplate and are uncorrected.

(iii) ^{1}H NMR Spectra

^{1}H NMR spectra were recorded on either a Varian EM 390, a Bruker WM 250, or a Bruker AM 500 spectrometer. Due to the widely different solubilities of the reaction products, various deuterated solvents were employed. Unless specified, ^{1}H NMR spectra were recorded at 90 MHz on a Varian EM 390 spectrometer, and resonances referenced to internal TMS.

(iv) ^{13}C NMR Spectra

The ^{13}C NMR spectra for photoproduct 25 were obtained at 62.9 MHz on a Bruker WM 250 spectrometer. All other ^{13}C NMR spectra were recorded on a Bruker WP80 spectrometer at 20.1 MHz.

(v) Electronic Absorption Spectra

Absorption spectra were recorded on either a Hewlett Packard 8451 A, or a Perkin-Elmer Lambda 9 Spectrophotometer. All absorption spectra were recorded with a matched pair 1 cm quartz UV cells, and referenced

against the solution solvent system.

(vi) Emission Spectra

The emission spectra of 10a and 11a were measured using a Perkin-Elmer LS-5 fluorescence spectrophotometer coupled to a Perkin-Elmer 3600 data station. The output from this instrument was fed into a Perkin-Elmer 660 printer.

(vii) Infrared Spectra

A Perkin-Elmer 283 IR spectrophotometer was used to obtain the solution spectrum of 25. The spectrum was obtained in $CDCl_3$ with NaCl windows. Initially the KBr disk technique was attempted but no clear intact window could be produced. All other IR spectra were obtained by the KBr disk technique. Only major, and diagnostic bands are reported.

(viii) Gas Chromatography

A Hewlett Packard 5790A gas chromatograph coupled to a 3390A integrator was used for monitoring of photolysis products. The samples were injected into a 1/8" dia. x 10' long stainless steel Fluorad FC 431 column (Chromatographic Specialties Ltd.). Column temperature was maintained at 150°C and the N_2 carrier gas flow rate was set at 21 ml/min.

(ix) Mass Spectra

Electron impact mass spectra were recorded on a VG7070 mass spectrometer (VG Micromass, Altricham, U.K.). Samples were introduced

via a direct insertion probe system. The spectra were acquired, and processed, with a VG 2035 data system.

(x) UV Reactors

All samples of 10a, 4'-substituted 10a and 11a were irradiated in a Rayonet Photochemical Reactor (Model RPR 100, Southern New England Ultraviolet Co.) or a "homemade" UV reactor based on the Rayonet Photochemical Reactor principle. Either RPR 3000 or RPR 3500 lamps (Southern New England Ultraviolet Co.) were used inside the UV reactors for the irradiation of the reactants.

B. SYNTHESIS

(i) 1-Acetylindoline

Acetic anhydride (43.85 g, 0.43 moles) was added dropwise to a stirred mixture of indoline (47.29 g, 0.40 moles) in water (135 ml). The resulting precipitate was filtered. Recrystallization from ethanol (95%) yielded 49.4 g (76.7%) of white needles. NMR ($CDCl_3$): δ 2.15 (s, 3H), 3.05 (t, 1H), 3.90 (t, 1H), 7.1 (m, 3H), 8.15 (d, 1H).

(ii) 1-Acetyl-5-bromoindoline

The title compound was synthesized according to the method of Boekelheide [114]. Bromine (14 ml) was added dropwise to a stirred mixture of 1-acetylindoline (46.4 g, 0.29 moles) in acetic acid (300 ml). The resulting reaction mixture was allowed to stand for another 5 minutes and then was poured into cold water (2.5 l). To the stirred aqueous

suspension just enough sodium bisulfite was added to remove the excess bromine. The solid was collected by filtration. Recrystallization from methanol yielded 55.7 g (81%) of colourless crystals. NMR ($CDCl_3$): δ 2.20 (s, 3H), 3.05 (t, 1H), 4.05 (t, 1H), 7.3 (m, 2H), 8.10 (d, 1H).

(iii) 1-Acetyl-5-bromo-7-nitroindoline

The title compound was synthesized according to the method of Boekelheide [114]. N-Acetyl-5-bromoindoline (41.5 g, 0.146 moles) was added in small portions to a stirred cold mixture (0-5°C) of fuming nitric acid (9.7 ml), acetic acid (50 ml) and concentrated sulfuric acid (62 ml). During the addition of N-acetyl-5-bromoindoline and subsequent 15 hours, the temperature of reaction mixture was maintained between 0 and 5°C. At the end of the 15 hour reaction time the mixture was poured onto cracked ice and the precipitated solid was filtered, washed with water and dried. Recrystallization from 200 ml of methanol-acetone mixture (1:2.3) yielded 8.2 g (20%) of yellow needles, m.p. 200-201°C (lit. [114] 197-198°C). ^1H NMR ($CDCl_3$): δ 2.20 (s, 3H), 3.25 (t, 1H), 4.25 (t, 1H), 7.55 (t, 1H), 7.80 (d, 1H). IR (KBr): 1531 cm^{-1} (NO_2), 1675 cm^{-1} (CO).

(iv) 5-Bromo-7-nitroindoline

A solution of 1-acetyl-5-bromo-7-nitroindoline (10.0 g, 0.035 moles), ethanol (16 ml) and 6N HCl (42 ml) was boiled under reflux for 6 hours. The mixture was then filtered, made basic with aqueous ammonia, and the solid precipitate collected. Recrystallization from acetone-methanol (1:1) yielded 5.84 g (69%) of orange-red crystals, m.p.

131-132°C. ^1H NMR ($CDCl_3$): δ 3.16 (t, 2H), 3.90 (t, 2H), 6.80 (s, 1H), 7.25 (t, 1H), 7.90 (d, 1H). Mass spectrum m/e 244 (P+2), 242 (P), 198, 196, 117, 89.

(v) 1-Benzoyl-5-bromo-7-nitroindoline

A solution of 5-bromo-7-nitroindoline (5.53 g, 0.023 moles), and benzoyl chloride (9.53 g, 0.068 moles) in dry pyridine (55 ml), was heated to reflux under a nitrogen atmosphere. After 13 hours of reflux water (110 ml) was added to the reaction mixture. The slurry was then poured into 200 ml cold 5% aqueous NaOH, stirred for 3 minutes and filtered. Recrystallization from 360 ml methanol-acetone (1:2.6) yielded 5.84 g (73%) of yellow needles, m.p. 214-215°C. ^1H NMR (CD_3CN): δ 3.16 (t, 2H), 4.21 (t, 2H), 7.48-7.86 (m, 7H). ^{13}C NMR (20.1 MHz; $CDCl_3$): δ 29.60, 53.36, 116.91, 125.89, 128.89, 132.26, 132.40, 134.46, 139.35, 169.98. UV (CH_3CN): λ_{max} 354 nm (ε = 3570 cm^{-1} M^{-1}).

(vi) 1-(4'-Chlorobenzoyl)-5-bromo-7-nitroindoline

A solution of 5-bromo-7-nitroindoline (5.59 g, 0.023 moles) and 4-chlorobenzoylchloride (97%) (15.52 g, 0.086 moles) in dry pyridine (60 ml) was heated to reflux under a nitrogen atmosphere. After 14 hours of reflux, water (100 ml) was added to the reaction mixture, stirred for 25 minutes at ambient temperature, and then filtered. The crude reaction product was redissolved in acetone, filtered, and filtrate concentrated under vacuum. The impure reaction mixture was again added to a solution of pyridine (30 ml) and water (100 ml), refluxed for 2 hours and then

poured into a 2% aqueous NaOH solution (300 ml). After stirring the solution for about 10 minutes at ambient temperature the solid residue was filtered, washed with water and rinsed with methanol. Yield of yellow needles was 7.32 g (83%), m.p. 254-255°C. ^{1}H NMR ($CDCl_3$): δ 3.2 (t, 2H), 4.26 (t, 2H), 7.4-8.0 (m, 6H). ^{13}C NMR (62.9 MHz, CD_2Cl_2): δ 29.81, 117.05, 125.89, 129.34, 130.45, 132.65, 133.19, 135.45, 138.62, 139.92, 141.20, 168.94. UV (THF): λ_{max} 350 nm (ε = 4288 cm^{-1} M^{-1}).

(vii) 1-(4'-Methylbenzoyl)-5-bromo-7-nitroindoline

A solution of 5-bromo-7-nitroindoline (5.59 g, 0.023 moles) and p-toluoylchloride (98%) (13.6 g, 0.086 moles) in dry pyridine (60 ml) was heated to reflux under a nitrogen atmosphere. After 14 hours of reflux water (110 ml) was added to the reaction mixture, stirred for 25 minutes at ambient temperature and then filtered. The crude reaction product was redissolved in acetone, filtered, and filtrate concentrated under vacuum. Recrystallization from methanol-acetone yielded 6.53 g (79%) of yellow needles, m.p. 213-214°C. ^{1}H NMR ($CDCl_3$): δ 2.41 (s, 3H), 3.15 (t, 2H), 4.26 (t, 2H), 7.25-7.93 (m, 6H). ^{13}C NMR (20.1 MHz, $CDCl_3$): δ 21.70, 29.51, 53.36, 116.55, 125.69, 128.91, 129.41, 131.44, 132.19, 135.61, 139.41, 141.01, 143.00, 169.98. UV (THF): λ_{max} 352 nm (ε = 3905 cm^{-1} M^{-1}).

(viii) 1-(4'-Methoxybenzoyl)-5-bromo-7-nitroindoline

A solution of 5-bromo-7-nitroindoline (4.44 g, 0.018 moles) and 4-methoxybenzoylchloride (99%) (11.24 g, 0.066 moles) in dry pyridine

(48 ml) was heated to reflux under a nitrogen atmosphere. After 13 hours of reflux water (110 ml) was added to the reaction mixture. The resulting slurry was then poured into a 2% aqueous NaOH solution (300 ml) stirred for 4 minutes, filtered, and washed with water. The crude reaction product was redissolved in acetone, filtered, and filtrate concentrated under vacuum. Recrystallization from methanol-acetone yielded 5.65 g of yellow crystals, m.p. 201-202°C. ^{1}H NMR ($CDCl_3$): δ 3.16 (t, 2HO, 3.89 (s, 3H), 4.29 (t, 2H), 6.92-7.95 (m, 6H). ^{13}C NMR (20.1 MHz, $CDCl_3$): δ 29.61, 53.52, 55.66, 114.07, 116.48, 125.80, 126.33, 131.07, 132.19, 135.85, 139.27, 140.98, 162.98, 169.72. UV (THF): λ_{max} 354 nm (ε = 4166 cm^{-1} M^{-1}).

(ix) 1-(4'-Cyanobenzoyl)-5-bromo-7-nitroindoline

A solution of 5-bromo-7-nitroindoline (2.43 g, 0.01 mole) and 4-cyanobenzoylchloride (5.01 g, 0.03 moles) in dry pryidine (30 ml) was heated to reflux under a nitrogen atmosphere. After 15 hours of reflux water (50 ml) was added to the reaction mixture, and the slurry poured into a beaker containing water (100 ml). The precipitate was filtered, stirred for 5 minutes in a 2% aqueous NaOH solution, and remaining solid again filtered. The crude reaction product was redissolved in acetone, filtered, and filtrate concentrated under vacuum. Recrystallization from acetone yielded yellow crystals, m.p. 232-233°C. ^{13}C NMR (20.1 MHz, $CDCl_3$): δ 29.58, 53.05, 115.94, 117.72, 126.10, 129.41, 132.72, 138.44, 139.17, 168.03. UV (THF): λ_{max} 350 nm (ε = 4648 cm^{-1} M^{-1}).

C. EMISSION MEASUREMENTS

(i) Fluorescence

Room temperature fluorescence spectra of 10a-acetonitrile, or acetonitrile-water (mole fraction of water = .66) solutions in 1 cm quartz fluorescence cells were recorded. The solutions were either air saturated, or argon degassed prior to measurement. Similarly, fluorescence spectra of 11a in acetonitrile were recorded. An excitation wavelength of 354 nm was employed, and the sample emission was monitored from 400 to 650 nm. The samples were prepared such that they had an absorbance of about 1 at 354 nm. For emission spectrum see Figure 6.

(ii) Phosphorescence

Solutions of 10a or 11a in 2-methyltetrahydrofuran ($\simeq 10^{-4}$ M) were placed in a quartz cell (3 mm O.D.), and cooled quickly in a dewar flask, containing liquid N_2, to form a glass. The sample was then transferred into the liquid N_2 cooled sample compartment of the Perkin-Elmer LS-5 spectrophotometer, excited at 354 nm, and phosphorescence spectra recorded with a gate setting of 1.0 and delay times ranging from 1.0×10^{-5} to 1.0×10^{-3} seconds. For emission spectrum see Figure 7.

D. PHOTOPRODUCT DISTRIBUTION

(i) In Acetonitrile as Solvent

Four ml of a 1-benzoyl-5-bromo-7-nitroindoline-acetonitrile

solution (1.18×10^{-2} M) was transferred into a quartz irradiation vessel and degassed by four freeze-pump-thaw cycles. The sealed sample was irradiated for 14 hours with 7-RPR 3500 lamps. Immediate gas chromatography analysis of irradiated solution using a Fluorad column showed no peak with a retention time typical of benzaldehyde. The acetonitrile was evaporated leaving a reddish-brown solid.

The crude product of two irradiations was dissolved in methylene chloride (5 ml), added to a solution of water (5 ml), and then to saturated aqueous sodium bicarbonate (5 ml). Any non-acidic product was separated from reaction mixture by repeated extractions with methylene chloride (6x5 ml). The methylene chloride extracts were combined, washed with sodium bicarbonate (2x10 ml) then water (10 ml), dried (Na_2SO_4), and solvent evaporated. The ^1H NMR spectrum of the reddish-brown solid indicated the presence of 5-bromo-7-nitroindoline and a minor amount of benzoic acid. Complete separation of methylene chloride extract was achieved on preparative silica gel TLC plates.

The aqueous fraction was neutralized (pH 7) with conc. HCl and extracted with methylene chloride (3x10 ml). The combined methylene chloride fractions were washed with water (10 ml), dried (Na_2SO_4), and solvent evaporated. The ^1H NMR and mass spectrum of the solid extracted were identical with benzoic acid.

(ii) <u>In Acetonitrile-Water as Solvent</u>

A stirred solution of 1-benzoyl-5-bromo-7-nitroindoline (.189 g, 5.43×10^{-4} moles) in acetonitrile (100 ml) and water (50 ml) was irradiated for 12 hours with 10-RPR 3500 lamps. After the

irradiation the solvent was evaporated, the residual solid redissolved in methylene chloride (30 ml), and solution extracted with saturated aqueous sodium bicarbonate (4x30 ml).

The aqueous phase was neutralized with HCl to a pH of 7, and acidic photoproduct extracted with methylene chloride (4x30 ml). The combined methylene chloride extract was washed with water (2x30 ml), dried (Na_2SO_4), and solvent evaported. The ^1H NMR spectrum of the solid residue was identical to benzoic acid.

The methylene chloride phase containing the crude non-acidic photoreaction products was concentrated, and products separated on preparative silica gel thin layer chromatography (TLC) plates using chloroform as eluent.

The band with an intense yellow-orange colour (R_f =.39) was washed from the silica gel with acetone, and solvent subsequently evaporated from the product. A ^1H NMR spectrum of this component indicated the presence of two compounds. Those two compounds were completely separated on preparative silica gel TLC plates via repeated developments using methylene chloride-petroleum ether (1:4) as eluent. The component with the highest R_f value was an orange-yellow solid. ^1H NMR (250 MHz, CD_3COCD_3): δ 6.66 (d, J=2.8 Hz, 1H), 7.53 (d, J=2.8Hz, 1H), 8.31 (d, J=1.4Hz, 1H), 9.19 (d, J=1.4 Hz, 1H), 11.67 (broad, 1H). ^{13}C NMR J modulated spin echo (62.9 MHz, CD_3COCD_3): δ 102.92 (em.), 111.94 (absorp.), 116.60 (absorp.), 131.12 (em.), 133.52 (em.), 134.97 (absorp.), 135.55 (em.), 155.55 (absorp.). UV (CH_3CN): 214 nm, 270 nm (shoulder), 406 nm (ε = 6804 cm^{-1} M^{-1}), 734 nm. Mass spectrum (low resolution) m/e 226 (P+2), 224 (P), 196, 194, 115, 87,

57. Mass spectrum (high resolution) observed mass = 223.9577 ($C_8H_5N_2OBr$). IR ($CDCl_3$) cm^{-1} 3470 (s), 2250 (w), 1480 (m), 1450 (s), 1435 (s), 1425 (s), 1379 (m), 1318 (s), 1260 (m), 1215 (s), 1075 (s), 1052 (s), 1030 (s). The ^1H NMR, and mass spectrum of the other component was identical with 5-bromo-7-nitroindoline.

As a final product a burgundy red band was separated from the silica gel TLC plate. This red photoproduct was only sparingly soluable in chloroform, and gradually changed at -20°C from a burgundy red into a brown insoluable solid. Mass spectrum m/e 290 (P), 248, 149, 105.

(iii) In Tetrahydrofuran as Solvent

100 ml of a 1-benzoyl-5-bromo-7-nitrodindoline-THF solution ($2.9x10^{-4}$ M) was transferred into a quartz vessel and the stirred solution irradiated for 1 hour with 15-RPR 3500 lamps. The reaction solutions of four irradiations were combined, and the solvent evaporated. Immediate gas chromatography (G.C.) analysis of irradiated solution on a 10 ft x 1/8 in. Fluorad column showed no peak with a retention time typical of benzaldehyde. ^1H NMR ($CDCl_3$), TLC (silica gel, CH_2Cl_2 -hexanes (1:1) as eluent) and G.C. analysis revealed a complex reaction mixture. Out of this complex mixture two major non-polymeric components, aside from benzoic acid, were separated on preparative TLC by repeated developments using CH_2Cl_2-hexanes (1:1) as eluent.

The component with the highest R_f value was a pale yellow coloured crystalline solid. ^1H NMR (250 MHz, $CDCl_3$): δ 6.68 (d,d, J=3.0 Hz, 1H), 7.42 (d,d, J=3.0 Hz, 1H), 8.10 (d,d, 1H), 8.29 (d,d, 1H), 9.91 (broad, 1H). Mass spectrum (low resolution) m/e 242

(P+2), 240 (P), 196, 194, 149, 115, 88, 71, 57. Mass spectrum (high resolution) observed mass = 239.9543 ($C_8H_5N_2O_2Br$).

The second separated component from the TLC plates was an orange coloured solid. The ^1H NMR spectrum of this photoproduct was identical to 5-bromo-7-nitroindoline.

(iv) In Tetrahydrofuran-Water as Solvent

A stirred solution of 1-benzoyl-5-bromo-7-nitroindoline (1.08×10^{-2} g, 3.12×10^{-5} moles) in THF (60 ml) and water (40 ml) was irradiated for 1 hour with 15-RPR 3500 lamps. The reaction solution of two irradiations were combined, and the solvent evaported. The 500 MHz ^1H NMR ($CDCl_3$) of crude reaction mixture depicted resonance peaks which could all be assigned to three reaction products; benzoic acid, 5-bromo-7-nitroindoline and 5-bromo-7-nitrosoindole. The relative product composition by peak integration was 92% of 5-bromo-7-nitroindoline and 8% of 5-bromo-7-nitrosoindole. The composition error by NMR peak integration is assumed to be less than $\pm$3%,

(v) In Ethanol as Solvent

100 ml of a 1-benzoyl-5-bromo-7-nitroindoline-ethanol solution (3.9×10^{-4} M) was transferred into a quartz vessel, and the stirred solution irradiated for 1 hour with 15-RPR 3500 lamps. The reaction solutions of two irradiations were combined, and the solvent evaporated. The 500 MHz ^1H NMR ($CDCl_3$) of crude reaction mixture depicted the presence of ethyl benzoate, 5-bromo-7-nitroindoline, 5-bromo-7-nitroso-

indole, and some polymeric material. The relative product composition by peak integration was 96% of 5-bromo-7-nitroindoline and 4% of 5-bromo-7-nitrosoindole.

(vi) In Acetonitrile-1,3-Cyclohexadiene

A 100 ml stirred solution of 1-benzoyl-5-bromo-7-nitroindoline (1.12×10^{-2} g, 3.23×10^{-5} moles) and 1,3-cyclohexadiene (1.25 g, 1.56×10^{-2} moles) in acetonitrile was irradiated for 1 hour with 15-RPR 3500 lamps. After the irradiation the solvent was evaporated. Separation of the crude reaction mixture on preparative silica gel TLC using CH_2Cl_2-hexane (1:4) as eluent yielded 5-bromo-7- nitroindoline and benzoic acid as the primary photoproducts. A minor amount of a red solid compound was also separated but its structure could not be identified since it turned within a day at ambient temperature into a brown solid.

(vii) In Acetonitrile-Water-1,3-Cyclohexadiene,

(a) One stage reaction (without 1,3-cyclohexadiene)

A 100 ml stirred solution of 1-benzoyl-5-bromo-7-nitroindoline (1.12×10^{-2} g, 3.23×10^{-5} moles) in water (40 ml) and acetonitrile was irradiated for 1 hour with 15-RPR 3500 lamps. After the irradiation the solvent was evaporated. The 500 MHz ^1H NMR ($CDCl_3$) spectrum of the crude reaction mixture depicted resonance peaks which could all be assigned to three reaction products; benzoic acid, 5-bromo-7-nitro-indoline, and 5-bromo-7-nitrosoindole.

(b) One stage reaction

A 100 ml stirred solution of 1-benzoyl-5-bromo-7-nitroindoline (1.12×10^{-2} g, 3.23×10^{-5} moles) in water (40 ml), 1,3-cyclo-hexadiene (1.246 g, 1.56×10^{-2} moles), and acetonitrile was irradiated for 1 hour with 15-RPR 3500 lamps. After the irradiation the solvent was evaporated. The 500 MHz ^{1}H NMR ($CDCl_3$) spectrum of the crude reaction mixture depicted resonance peaks ascribable in part to 1-benzoyl-5-bromo-7-nitroindoline, benzoic acid, and 5-bromo-7-nitroindoline. Major peaks at δ 4.4, 4.6 and 6.0 and minor peaks at δ 3.1 and 3.8 could not be assigned to any known photoproduct.

(c) One stage reaction (2 hour irradiation)

Repeat of the above experiment (one stage reaction) with irradiation time extended from 1 hour to 2 hours followed by preparative silica gel TLC separation with CH_2Cl_2-hexane (1:4) as eluent yielded a black insoluable material as the predominant reaction product. Two minor components were, however, separated from the TLC plates, but, could not be identified.

(d) Two stage reaction (without 1,3-cyclohexadiene)

A 100 ml stirred solution of 1-benzoyl-5-bromo-7-nitroindoline (1.12×10^{-2} g, 3.23×10^{-5} moles) in water (40 ml), and acetonitrile was irradiated for 1 hour, left in the dark for 35 minutes and irradiated again for 1 hour with 15-RPR 3500 lamps. After the final irradiation the solvent was evaporated. A 500 MHz ^{1}H NMR ($CDCl_3$) of the crude reaction mixture depicted a spectrum identical to the spectrum obtained

from the one stage reaction (without 1,3-cyclohexadiene).

(e) Two stage reaction

A 100 ml stirred solution of 1-benzoyl-5-bromo-7-nitrodindoline (1.12×10^{-2} g, 3.23×10^{-5} moles) in water (40 ml), and acetonitrile was irradiated for 1 hour. During a dark period of 35 minutes 1,3-cyclohexadiene (1.25 g, 1.56×10^{-2} moles) was added to the irradiated solution, and irradiated subsequently for another 1 hour with 15-RPR 3500 lamps. After the final irradiation the solvent was evaporated. The 500 MHz ^1H ($CDCl_3$) spectrum of the crude reaction mixture confirmed the complete conversion of the starting material. Major resonance peaks could be ascribed to benzoic acid and 5-bromo-7-nitroindole. Although other major resonance peaks again observed at δ 4.4, 4.6 and 6.0 could not be assigned to any known photoproduct.

E. PHOTOPRODUCT DISTRIBUTION

(i) As a Function of Mole Fraction of Water

A 3.04×10^{-4} M solution of 10a in acetonitrile-water solvent mixture with mole fraction of water = 0, .24, .42, .66 and .81 were prepared, 100 ml of the solution was transferred into a cylindrical quartz vessel. The stirred solution was then irradiated for 1 hour with 11-RPR 3500 lamps at 7°C and/or ambient temperature. The ambient temperature samples reached a solution temperature of 45°C at the end of irradiation. After photolysis the solvent was removed under reduced pressure, the residue redissolved in a minimum of $CDCl_3$, and

compositions analyzed on an AM 500 MHz Bruker FT-NMR spectrometer. The mole % of 25 was calculated from the H3 and H6 NMR integration of photoproduct 25 (δ 6.66 H3 and δ 9.19 H6) and H2 and H6 integration of photoproduct 11a (δ 3.90 H2 and/or δ 7.90 H6). Percent conversion of 10a was based on its remaining (δ 4.21 H2), plus the 11a and 25, integration values.

(ii) As a Function of NaOH Concentration

Solutions for photoproduct distribution measurements were prepared by pipetting 10 ml of a 10a-acetonitrile stock solution (2.8×10^{-3} M), and 40 ml of a 0 M, 1.0×10^{-4} M, 5.0×10^{-4} M, 8.0×10^{-4} M, 1.0×10^{-3} M and 1.0×10^{-2} M aqueous NaOH solution into a 100 ml volumetric flask. The system was then diluted to the mark with acetonitrile, transferred into a quartz vessel and the stirred solution irradiated for 1 hour with 11-RPR 3500 lamps. After irradiation the solvent was evaporated, and the residual solid washed (3 times) with methylene chloride (10 ml), and saturated aqueous sodium bicarbonate (10 ml). The combined methylene chloride extract was washed with water (1x10 ml), dried (Na_2SO_4), and solvent evaporated. Methylene chloride (1.5 ml), and hexane (1.5 ml) were syringed back into the round bottom flask. The photoproduct composition was measured on a high pressure liquid chromatography (HPLC) apparatus (Varian 5000 coupled to a Varian Vista 402 data processor) equipped with a SI-5, 15 cm x 4 mm I.D. column, and using a 254 nm UV monitor setting. The HPLC was programmed to have a flow of 1.5 ml/min., and a continuous mobile phase change for the initial 30 minutes (t = 0 minutes 100% hexane, t = 30 minutes 70%

hexane and 30% dichloromethane). From the area count of the peaks for photoproduct 11a and 25 and their respective extinction coefficients at 254 nm their % (mole) values were calculated. The peak area, and extinction coefficient (ε_{254}) values are given in Table 11.

F. ELECTRON SPIN RESONANCE (e.s.r.)

(i) Equipment

The e.s.r. fragmentation study was conducted on a Bruker ER 100D spectrometer equipped with a Te_{102} rectangular cavity. Attached was a Bruker variable temperature unit ER 4111 VT, and a Bruker microwave bridge ER 040 X. To the sample probe a UV light source was attached such that the sample could be continuously monitored for e.s.r. signals while irradiated.

(ii) Irradiation in E.S.R. Probe

About .2 ml of a 1.4×10^{-2} M solution of 10a in acetonitrile or acetonitrile-water was placed in an e.s.r. quartz tube (3 mm O.D., Wilmad Glass Co Inc. 705 PQ) joint to a glass adaptor with a sidearm. The sample in the glass sidearm was degassed with three freeze (77°K)-pump-thaw cycles, sealed, and subsequently transferred into the quartz e.s.r. tube. While the sample was irradiated, for approximately 1 hour (Philips SP 500W glass or quartz lamp), in the e.s.r. probe at 120-195°K, the signals were recorded. After the low temperature irradiation the sample was remove from the cavity, and both sample and e.s.r. probe warmed to ambient temperature. An e.s.r. spectrum of the

Table 11

Raw Data for Photoproduct Distribution as a Function of [NaOH]

[NaOH] in H_2O	Area Count 11a	Area Count 25	ε_{254} 11a	ε_{254} 25	% (mole)[a] 11a	% (mole)[b] 25
0	3739690	2243400	15240	6620	42	58
0	3406560	2042140	15240	6620	42	58
0	3309120	1995440	15240	6620	42	58
1.0×10^{-4}	3737980	2615480	15240	6620	38	62
1.0×10^{-4}	3799770	2722320	15240	6620	38	62
1.0×10^{-4}	3797120	2652210	15240	6620	38	62
5.0×10^{-4}	1437640	2438930	15240	6620	20	80
5.0×10^{-4}	1371690	2417270	15240	6620	20	80
5.0×10^{-4}	1388150	2414140	15240	6620	20	80
8.0×10^{-4}	2440550	3730500	15240	6620	22	78
8.0×10^{-4}	2369160	3640150	15240	6620	22	78
1.0×10^{-3}	2124970	2758700	15240	6620	25	75
1.0×10^{-3}	2077640	2726410	15240	6620	25	75
1.0×10^{-3}	1376550	1796130	15240	6620	25	75
1.0×10^{-2}	2117710	377182	15240	6620	71	29

[a] (area count (11a)/ ε_{254} (11a) (area count (11a)/ ε_{254} (11a) + area count (25)/ε_{254} (25)) $\times 10^2$.

[b] 100 - % (mole) 11a.

previously irradiated sample was again recorded at ambient temperature.

Similarly, a .2 ml solution of 11a in acetonitrile was degassed, irradiated in the e.s.r. probe, and spectrum recorded at low and ambient temperatures.

G. FREE BENZOYL RADICAL INTERCEPTION

Five ml of a 10a-acetonitrile solution (1.39×10^{-2} M) was transferred into an irradiation cell equipped with a micro stirring bar (for description of glassware see "In Acetonitrile-Water as Solvent (degassed)" page 143). Onto a vacuum line both the 100 ml glass bulb containing the $^{18}O_2$ (oxygen-$^{18}O_2$ gas, 92.9 atom % ^{18}O, MSD Isotopes) and the irradiation cell were mounted in a manner appropriate for a bulb to bulb distillation. The 10a-acetonitrile solution in the irradiation cell was then degassed with four freeze (77 K)-pump-thaw cycles, the stopcock to vacuum line closed, and the seal to $^{18}O_2$ bulb broken. While exposed to the $^{18}O_2$ rich atmosphere the solution was stirred vigorously at room temperature for about 10 minutes, cooled to about -70°C, sealed, and $^{18}O_2$ saturated solution irradiated at ambient temperature with 11-RPR 3500 lamps. One sample was irradiated for 1 hour, another for 6 hours.

After irradiation the solvent was evaporated, and the crude reaction product separated on preparative silica gel TLC, using CH_2Cl_2 as eluent. All components with an R_f value of approximate zero were collected, and a mass spectrum obtained.

H. DISAPPEARANCE QUANTUM YIELD MEASUREMENTS

(i) Optical Bench (PRA)

The light source consisted of an Osram high pressure 150W Xenon lamp contained in a Photochemical Research Associate (PRA) lamp housing (ALH 215) and connected to a PRA (M 303) power supply. A water IR filter mounted between the lamp and monochromator (Jobin Yvon H.10) removed the infrared radiation. The entrance and exit slit setting on the monochromator allowed a 10 nm bandpass at the 366 nm wavelength selection. In order to remove higher order wavelengths the light was again filtered just before collimation. The emitted light was then split by a quartz plate positioned 45° relative to the beam. Approximately 10% of the light from the source was directed to a UV enhanced silicon photodiode (EG & G Instruments, UV 040 BQ) detector mounted 90° to the main beam (comparison detector). The remainder of the light passed into the sample cell which was located immediately in front of another silicon photodiode detector (main detector). Upon light impingement the diode signals were converted to digital output by a two channel digital current integrator. The entire optical system was mounted onto an aluminium rail inside a light-tight box.

(ii) Optical Bench (Kratos)

The light source consisted of an Osram HBO 200W super pressure mercury lamp contained in a Kratos Lamp housing, and connected to a Kratos LPS 25T power supply. The grating monochromator (Kratos GM 100), attached to the lamp housing, was set at 366 nm and the entrance and

exit slits used allowed a 24 nm band pass. A Corning glass filter with a 322-383 nm window was placed immediately after the monochromator, and in front of a water IR filter. Inside a light-tight box the filtered light was then split by a quartz plate (75 mm x 75 mm x 1.5 mm) positioned 45° relative to the beam. Approximately 10% of the light from the source was directed to a UV enhanced silicone photodiode (EG & G Instruments, UV 040 BQ) detector mounted 90° to the main beam (comparison detector). The remainder of the light passed into the sample cell which was located immediately in front of another silicon photodiode detector (main detector). Upon light impingement the diode signals were converted to digital output by a two channel digital current integrator. The entire optical system was mounted onto an aluminium rail.

(iii) Actinometry

The light absorbed by the sample during quantum yield measurements was quantified by the comparison detector, and displayed as number of counts. Following every second quantum yield measurement the comparison detector in turn was calibrated against a potassium ferrioxalate solution [94,115].

A 0.06 M ferrioxalate solution was transferred into a 22 mm O.D. x 10 mm quartz actinometer cell, placed in front of the main detector, irradiated for a brief period, and comparison detector count recorded. The number of photons incident on the actinometric solution were determined according to the method of Parker [115], and used to calibrate the comparison detector as photons/count.

Experimental conditions during quantum yield and actinometric

measurements were such that the solutions did absorb all the light, and no traversed light was recorded by the main detector.

(iv) Isobestic Point Determination

A 4 ml solution of 1-benzoyl-5-bromo-7-nitroindoline (1.45×10^{-4} M) in acetonitrile or acetonitrile-water (mole fraction of water = .53) was transferred into a 1 cm x 1 cm UV-cuvette equipped with a pyrex sleave, degassed by three freeze-pump-thaw cycles, and subsequently sealed. The samples were irradiated with 15-RPR 3500 lamps. UV spectra of the solution were obtained at 0, 30, 60, 90, 150 and 450 seconds total irradiation times.

(v) In Acetonitrile-Water as Solvent (aerated)

Quantum yield values for disappearance of 10a in acetonitrile-water (aerated) were obtained on the PRA optical bench.

Irradiation solutions with various mole fractions of water were prepared by pipetting 5 ml of a 10a-acetonitrile stock solution into a 50 ml volumetric flask, and diluting the stock solution with acetonitrile and 0 ml, 2 ml, 5 ml, 10 ml, 20 ml, and 30 ml of water. 5.5 ml of the solution to be irradiated was introduced from calibrated pipettes into a 22 mm O.D. x 20 mm actinometer cell, placed in front of the main detector of the PRA optical bench, and irradiated for about 2 hours. After irradiation, a UV spectrum of the solution was obtained on the Hewlett-Packard 8451A spectrophotometer, and the absorption value of λ_{max} in the 350 nm region recorded. Similarly, a spectrum of the unirradiated solution was obtained and again the absorption value of λ_{max} in

Table 12

Raw Quantum Yield Data for Disappearance of 10a in Aerated Acetonitrile-Water

[10a] x 10^3 a	H_2O b	counts	Einsteins/ count x 10^{10}	Absorption (initial)	Absorption (final)	ε (reactant)	Φ x 10^2
2.814	0	7900	3.64	1.00297	.965255	3564	2.02
2.814	0	7900	3.64	1.00297	.963836	3564	2.10
2.769	0	7900	3.84	.987533	.935913	3567	2.64
2.769	0	7900	3.84	.987533	.939849	3567	2.44
2.814	.11	7907	3.64	.9919735	.956817	3525	1.91
2.814	.11	7901	3.64	.9919735	.956771	3525	1.91
2.769	.11	7901	3.84	.974853	.948013	3521	1.62
2.814	.24	7900	3.64	.9939645	.965255	3532	1.55
2.814	.24	7900	3.64	.9939645	.966995	3532	1.46
2.769	.24	7900	3.84	.974517	.942901	3509	1.49
2.769	.24	7900	3.84	.974517	.947158	3509	1.43
2.814	.42	7900	3.64	.988899	.966079	3514	1.24
2.814	.42	7900	3.64	.988899	.964172	3514	1.35
2.769	.42	7900	3.84	.965347	.936813	3487	1.50
2.769	.42	7900	3.84	.965347	.935073	3487	1.59
2.814	.66	7900	3.64	.991577	.966583	3523	1.36
2.814	.66	7901	3.64	.988540	.968856	3513	1.07
2.769	.66	7900	3.84	.965713	.939941	3476	1.19
2.769	.66	7900	3.84	.965713	.937805	3476	1.30
2.814	.81	7900	3.64	.984512	.966308	3498	.995
2.814	.81	7900	3.64	.989349	.963882	3516	1.39
2.769	.81	7900	3.84	.972167	.948608	3506	1.15
2.769	.81	7900	3.84	.972167	.953491	3506	.973

a 10a-acetonitrile stock solution concentration.
b Mole fraction of water.

the 350 nm region recorded. The raw quantum yield data are given in Table 12.

(vi) In Acetonitrile-Water as Solvent (degassed)

Quantum yield values for disappearance of 10a in acetonitrile-water (degassed) were obtained on the Kratos optical bench. The glassware used for the irradiation of the samples consisted of a 22 mm O.D. x 20 mm cylindrical quartz cell attached via a side arm to a heavy-walled pyrex glass tubing. On top of the glass tubing was an O-ring type stopcock with a B 10/19 external joint.

Irradiation solutions with various mole fractions of water were prepared by pipetting 6 ml of a 10a-acetonitrile stock solution into a 25 ml volumetric flask and diluting the stock solution with acetonitrile and 0 ml, 1 ml, 2.5 ml, 5 ml and 10 ml of water. 5.5 ml of the solution to be irradiated was introduced from calibrated pipettes through the stopcock port into the glass tubing. The stopcock was then assembled, and solution degassed with four freeze (77 K)-pump-thaw cycles. After degassing procedure the solution was transferred from the glass tubing section into the cylindrical quartz cell. The assembly was placed in front of the main detector of the Kratos optical bench, and irradiated for 2.5 hours. Immediately after irradiation 2 ml of the solution was pipetted into a 5 ml volumetric flask, and diluted with the appropriate solvent system. A UV absorption spectrum between 320-400 nm was obtained on the Perkin-Elmer Lambda 9 spectrophotometer and the absorption value of λ_{max} in 350 nm region recorded. Similarly, 2 ml of the unirradiated solution was pipetted into a 5 ml volumetric flask, again

diluted with the appropriate solvent system, and the absorption value of λ_{max} in 350 nm region recorded. The raw quantum yield data for 10a disappearance in degassed acetonitrile-water are given in Table 13.

(vii) In Tetrahydrofuran-Water as Solvent (aerated)

The experimental procedure for the disappearance quantum yield of 10a in tetrahydrofuran-water (aerated) was identical to "In Acetonitrile-Water as Solvent (aerated)" with the exception that the solutions were prepared with tetrahydrofuran instead of acetonitrile as the solvent.

The raw quantum yield data for 10a disappearance in aerated tetrahydrofuran-water are given in Table 14.

(viii) In Tetrahydrofuran-Water as Solvent (degassed)

The experimental procedure for the disappearance quantum yield of 10a in tetrahydrofuran-water (degassed) was identical to "In Acetonitrile-Water as Solvent (aerated)" with the exception that the solutions were prepared with tetrahydrofuran instead of acetonitrile as the solvent. Also all solutions were degassed with three freeze (77 K)-pump-thaw cycles. The raw quantum yield data for disappearance of 10a in degassed tetrahydrofuran-water are given in Table 15.

(ix) Electron Transfer Quenching

All quantum yields for disappearance of 10a in the presence of the 1,4-dimethoxybenzene quencher were obtained using the Kratos optical bench.

The appropriate amount of 1,4-dimethoxybenzene was weighed into a

Table 13

Raw Quantum Yield Data for Disappearance of 10a in Degassed Acetonitrile-Water

[10a] x 10^3 [a]	H_2O [b]	counts	Einsteins/ count x 10^9	Absorption (initial)	Absorption (final)	ε (reactant)	Φ x 10^2
2.859	0	2020	4.03	.813	.759	3554	2.57
2.859	0	2021	4.03	.813	.768	3554	2.14
2.860	0	1800	4.25	.837	.787	3658	2.46
2.860	.11	1823	4.09	.842	.805	3680	1.85
2.856	.11	1767	4.23	.8495	.813	3718	1.81
2.856	.11	1745	4.23	.8495	.811	3718	1.93
2.860	.24	1738	4.38	.833	.801	3640	1.61
2.856	.24	1901	4.21	.817	.778	3576	1.87
2.856	.24	1907	4.21	.817	.777	3576	1.92
2.860	.42	1701	4.37	.838	.803	3662	1.77
2.856	.42	1442	4.73	.841	.811	3681	1.64
2.860	.66	1850	4.35	.845	.807	3693	1.60[c]
2.860	.66	1850	4.35	.845	.807	3693	1.76
2.860	.66	1663	4.89	.809	.781	3536	1.34

[a] 10a-acetonitrile stock solution concentration.

[b] Mole fraction of water.

[c] Volume irradiated was 5.0 ml.

Table 14

Raw Quantum Yield Data for Disappearance of 10a in Aerated Tetrahydrofuran-Water

[10a] x 10^3 a	H_2O b	counts	Einsteins/ count x 10^{10}	Absorption (initial)	Absorption (final)	ε (reactant)	Φ x 10^2
2.650	0	2100	8.48	1.04486	1.02822	3850	1.27
2.650	0	2100	8.48	1.04486	1.02426	3850	1.58
2.650	.08	2100	8.48	1.04486	1.02812	3850	1.28
2.650	.08	2100	8.48	1.04486	1.02806	3850	1.29
2.650	.08	3200	4.74	.993927	.981018	3751	1.11
2.650	.08	3201	4.74	.993927	.978744	3751	1.40
2.650	.33	3200	4.74	.984863	.975036	3716	.92
2.650	.33	3200	4.74	.984863	.973663	3716	1.04
2.640	.53	3202	4.74	.982986	.965393	3709	1.64
2.650	.53	3201	4.74	.982986	.966354	3709	1.55
2.921	.75	1186	53.0	.896	.844	3835	2.86c
2.650	.82	3200	4.74	.955245	.926803	3605	2.73
2.650	.82	3201	4.74	.959335	.929565	3627	2.98

a 10a-tetrahydrofuran stock solution.

b Mole fraction of water.

c Value obtained using the Kratos optical bench, and Perkin-Elmer Lambda 9 spectrophotometer.

Table 15

Raw Quantum Yield Data for Disappearance of 10a in Degassed Tetrahydrofuran-Water

[10a] x 10^3 [a]	H_2O [b]	counts	Einsteins/ count x 10^{10}	Absorption (initial)	Absorption (final)	ε (reactant)	Φ x 10^2
2.782	0	4501	3.50	1.05674	1.03962	3798	1.57
2.782	0	4501	3.50	1.05674	1.03958	3798	1.52
2.782	.16	4500	3.50	1.04159	1.03186	3743	.908
2.782	.16	4500	3.50	1.04159	1.03286	3743	.785
2.782	.33	4500	3.50	1.04225	1.03286	3746	.844
2.782	.33	4500	3.50	1.04225	1.03375	3746	.792
2.782	.53	4501	3.50	1.03605	1.02278	3723	1.24
2.782	.53	4500	3.50	1.03605	1.02281	3723	1.20
2.782	.75	4500	3.50	1.02050	.989501	3668	2.84
2.782	.75	4503	3.50	1.02511	1.00091	3684	2.29
2.782	.87	4500	3.50	1.0016	.968383	3600	3.22

[a] 10a-tetrahydrofuran stock solution concentration.

[b] Mole fraction of water.

25 ml volumetric flask, 5 ml of a 10a-acetonitrile stock solution pipetted into the same volumetric flask, and contents diluted with acetonitrile. For quantum yield measurements in aqueous acetonitrile solution the 1,4-dimethoxybenzene-stock solution was diluted with 10 ml of water and then acetonitrile. 5.3 ml of the solution to be irradiated was transferred into a 22 mm O.D. x 20 mm actinometer cell, placed in front of the main detector and irradiated for 2.5 hours. After irradiation 2 ml of the solution was pipetted into a 5 ml volumetric flask, and diluted with the appropriate solvent system. A UV absorption spectrum between 320-400 nm was obtained on the Perkin-Elmer Lambda 9 spectrophotometer and the absorption value of λ_{max} in 350 nm region recorded. Similarly, 2 ml of the unirradiated solution was pipetted into a 5 ml volumetric flask, again diluted with the appropriate solvent system, and the absorption value of λ_{max} in 350 nm region recorded.

The raw quantum yield data for disappearance of 10a in acetonitrile and 1,4-dimethoxybenzene are given in Table 16. Table 17 lists the data for 10a disappearance in acetonitrile-water and 1,4-dimethoxybenzene.

(x) Triplet State Quenching

Quantum yield values for disappearance of 10a in the presence of 1,3-cyclohexadiene quencher were obtained using the Kratos optical bench. The glassware, irradiation procedure, and subsequent quantitative analysis were similar to experimental procedure outlined in "In Acetonitrile-Water as Solvent (degassed)".

Solutions with 0 M, .0208 M, .0305 M, .0460 M, .0842 M, and

Table 16

Raw Quantum Yield Data for Disappearance of 10a in Aerated Acetonitrile-1,4-Dimethoxybenzene

[10a] x 10^3 [a]	[1,4-dimethoxybenzene] x 10^2	counts	Einsteins/count x 10^9	Absorption (initial)	Absorption (final)	ε (reactant)	Φ x 10^2	Φ^0/Φ
2.880	0	4112	2.59	.834	.759	3619	2.58	1.00
2.880	0	4132	2.59	.834	.755	3619	2.70	
2.880	.92	4128	2.59	.834	.760	3619	2.53	1.00
2.880	.92	4071	2.59	.834	.755	3619	2.74	
2.880	1.6	3866	2.53	.834	.766	3619	2.55	1.04
2.880	1.6	3851	2.53	.834	.767	3619	2.52	
2.880	2.58	4047	2.53	.836	.763	3619	2.61	1.01

[a] 10a-acetonitrile stock solution concentration.

Table 17

Raw Quantum Yield Data for Disappearance of 10a in Aerated Acetonitrile-Water[a] and 1,4-Dimethoxybenzene

[10a] x 10^3 [b]	[1,4-dimethoxybenzene] x 10^2	counts	Einsteins/count x 10^9	Absorption (initial)	Absorption (final)	ε (reactant)	Φ x 10^2	Φ^0/Φ
2.892	0	3684	2.76	.820	.775	3544	1.65	1.00
2.892	0	3518	2.76	.820	.777	3544	1.66	
2.892	0.49	3888	2.80	.820	.792	3544	.962	1.81
2.892	0.49	3861	2.80	.820	.795	3544	.865	
2.892	1.01	3818	2.80	.819	.793	3540	.910	1.82
2.892	1.01	3817	2.80	.819	.793	3540	.910	
2.892	1.55	3884	2.67	.820	.803	3544	.613	2.77
2.892	1.55	3861	2.67	.820	.812	3544	.580	
2.892	2.15	3972	2.67	.812	.800	3544	.427	4.03
2.892	2.15	3937	2.67	.812	.801	3544	.395	
2.892	2.48	4000	2.70	.820	.808	3544	.415	4.56
2.892	2.48	4011	2.70	.820	.811	3544	.311	

[a] Mole fraction of water = .66.

[b] 10a-acetonitrile stock solution concentration.

.1549 M 1,3-cyclohexadiene were prepared by first weighing the appropriate amount of 1,3-cyclohexadiene into a 25 ml volumetric flask, then pipetting 5 ml of a 10a-acetonitrile stock solution and 10 ml of water into the same flask. Finally, the mixture was diluted to the mark with acetonitrile. 5.0 ml of the solution to be irradiated was transferred into the sealable irradiation cell, degassed, and irradiated on the optical bench.

The raw quantum yield data for disappearance of 10a in acetonitrile-water and 1,3-cyclohexadiene are given in Table 18.

(xi) As a Function of 4'-Substituent (Hammett-LFER)

Quantum yield values for disappearance of 4'-substituted 10a in tetrahydrofuran-water were obtained for X = H, Cl, Me and OMe on the PRA optical bench and for X = CN on the Kratos optical bench. The quantum yields were determined for aerated tetrahydrofuran-water solutions where the mole fraction of water was .33.

The experimental procedure for irradiation on the PRA optical bench, and subsequent quantitative analysis, was similar to "In Acetonitrile-Water as Solvent (aerated)" page 141 . The experimental procedure for irradiation on the Kratos optical bench was similar to procedure outlined in "Electron transfer quenching" page 144 , except 1,4-dimethoxybenzene quencher was deleted.

Raw quantum yield data for disappearance of 4'-substituted 10a in tetrahydrofuran-water are given in Table 19.

Table 18

Raw Quantum Yield Data for Disappearance of 10a in Degassed Acetonitrile-Water-1,3-Cyclohexadiene[a]

[10a] x 10^3 [b]	[1,3-cyclohexadiene]	counts	Einsteins/count x 10^9	Absorption (initial)	Absorption (final)	ϵ (reactant)	Φ x 10^2	Φ^0/Φ
3.061	0	2277	4.23	.871	.832	3556	1.42	1.00
2.978	0	2239	4.27	.841	.799	3530	1.56	
2.978	0	2108	4.07	.836	.794	3509	1.60	
2.978	0.0208	2265	4.27	.838	.802	3517	1.32	1.16
2.978	0.0305	2095	4.07	.832	.800	3492	1.34	1.14
2.978	0.0460	2243	4.23	.870	.846	3552	.89	1.72
2.978	0.0842	2242	4.27	.836	.809	3509	1.00	1.53
2.978	0.1549	2152	4.07	.837	.813	3513	.98	1.56

[a] Mole fraction of water = .66.

[b] 10a-acetonitrile stock solution concentration.

Table 19

Raw Quantum Yield Data for Disappearance of 4'-Substituted 10a in Aerated Tetrahydrofuran-Water

X	conc.[a] moles/liter x 10^3	counts	Einsteins/ count x 10^{10}	Absorption (initial)	Absorption (final)	ε (reactant)	Φ x 10^2
H	2.705	2558	9.14	1.00411	.98146	3712	1.31
H	2.705	2589	9.14	1.00411	.983886	3712	1.15
Cl	2.416	1649	8.09	1.03594	1.00515	4288	2.69
Cl	2.416	2995	8.09	1.03594	.983016	4288	2.55
Me	2.290	1212	9.14	1.07125	1.03843	3905	4.00
Me	2.290	2515	9.14	1.07125	1.00479	3905	3.80
OMe	2.418	2736	9.33	1.00727	.963119	4166	2.08
OMe	2.418	4167	9.33	1.00727	.931335	4166	2.34
CN	2.673	3031	34.9	.994	.815	4648	4.82
CN	2.673	1509	34.9	.994	.902	4648	4.98

[a] 4'-substituted 10a-tetrahydrofuran stock solution concentration.

I. CYCLIC VOLTAMETRY

(i) Equipment

Cyclic voltametric reduction measurements of 10a were performed on a CV-27 cyclic voltamograph. For graphing of current-voltage measurements an Omnigraph 2000 X-Y recorder was attached to the voltamograph. A Micro-V magnetic stirrer functioned both as a stand and as a stirring mechanism for the solution inside a 20 ml glass sample cell. Inside the sample cell was also a working electrode with a platinum bead (0.03 cm^2) embedded on a cobalt glass seal, a platinum wire (0.42 mm dia.) auxiliary electrode, and a saturated calomel reference electrode (SCE, Metrohm AG, Switzerland). In order to prevent contamination, the SCE was isolated from the substrate solution by a glass frit.

(ii) Measurements

A solution of tetraammonium perchlorate (0.1 M) in 3 ml of acetonitrile, or acetonitrile-water, was introduced into the sample cell. Prior to placing the electrodes into the sample cell they were rinsed with acetone, acetonitrile, and then wiped dry. The electrodes were placed close together in the solution in order to minimize the ohmic resistance. After deoxygenation of the solution with dry argon a background scan was run over the scan range 0 to -1.8 V to ensure no reducible substances were present. 10a was then dissolved in the same solution to make a 1-2 mM substrate concentration. Again the solution was completely deoxygenated with dry argon, and scanned such that scan

reversal occurred just after the first maximum cathode peak with scan rates of .1, .5 and 1.0 Vs^{-1}.

CHAPTER IV

APPENDIX

A. CALCULATION OF QUANTUM YIELD (Φ)

The quantum yield for the disappearance of a photolyte is defined by:

$$\Phi_x = \frac{\text{number of reacted molecules of X}}{\text{number of quanta of light absorbed by X}} \qquad (59)$$

Equation (44) can be rewritten [115] as:

$$\Phi_x = \frac{(C_i - C_f)}{\int_o^t Q dt} * \frac{V}{1000} \qquad (60)$$

where C_i is the concentration (moles/liter) at t=0, C_f is the instantaneous concentration (moles/liter) at time t, Q are the Einsteins of light absorbed at time t, and V is the volume (ml) of solution irradiated.

The photochemical reaction of 10a was monitored by recording

electronic absorption spectra of each solution prior to and after each irradiation. By solving the Beer-Lambert equation $A = \varepsilon\ c\ l$ for c and substituting into equation (60) also accounting for the difference in irradiation and monitoring concentrations then

$$\Phi_x = \frac{(A_i - A_f)}{\varepsilon\ l \int_o^t Q dt} * \frac{V}{1000} * \frac{C_{irr}}{C_A} \qquad (61)$$

Substituting the average value $\bar{Q}_{ot}$ for the integral $\int_o^t Q dt$ yields:

$$\Phi_x = \frac{(A_i - A_f)}{\varepsilon\ l\ \bar{Q}_{ot}} * \frac{V}{1000} * \frac{C_{irr}}{C_A} \qquad (62)$$

Furthermore, the average value $\bar{Q}_{ot}$ was measured by using silicone diode counters which were calibrated against potassium ferrioxalate. After substituting counts * I for $\bar{Q}_{ot}$ the quantum yield, Φ , for the disappearance of 10a was calculated from the following equation:

$$\Phi = \frac{(A_i - A_f) * V * C_{irr}}{\varepsilon * l * 1000 * counts * I * C_A} \qquad (63)$$

where A_i = absorbance at t=0

A_f = absorbance after irradiation

V = Volume of irradiated solution in ml

C_{irr} = concentration of irradiated solution

ε = extinction coefficient of compound irradiated

l = path length of UV-cuvette in cm

counts = counts by silicon diode

I = Einsteins/count

C_A = concentration of solution from which UV-absorbance data was obtained.

REFERENCES

1) S.K. Chadda, C.V. Rogerson, I.O. Tse-Sheepy, B.E. McCarry, J.M. Dickson, and R.F. Childs, J. Appl. Polymer Sci., 34, 2713 (1987).

2) K. Sollner, Biochem. Z. 244, 370 (1932).

3) A. Schindler, M. Gratzl, and K.L. Platt, J. Polymer Sci., Polymer Chem. 15, 1541 (1977).

4) A. Akimo, Chem. Econ. and Eng. Rev. 17, 185 (1985).

5) E. Havinga, R. De Jongh, and W. Dorst, Rec. Trav. Chim., 75, 378 (1956).

6) T. Wieland, C. Lamperstorfer, and C. Birr, Makromol. Chem., 92, 279 (1966).

7) D.H.R. Barton, T. Nakano, and P.G. Sammes, J. Chem. Soc. (c), 332 (1968).

8) J.A. Barltrop, and P. Schofield, J. Chem. Soc., 4758 (1965).

9) J.A. Barltrop, P.J. Plant, and P. Schofield, Chem. Commun., 822 (1966).

10) A. Patchornik, B. Amit, and R.B. Woodward, J. Am. Chem. Soc., 92, 6333 (1970).

11) B. Amit, U. Zehavi, and A. Patchornik, J. Org. Chem., 39, 192 (1974).

12) B. Amit, U. Zehavi, and A. Patchornik, J. Org. Chem., 37, 2281 (1972); ibid, 37, 2285 (1972).

13) B. Amit, U. Zehavi, and A. Patchornik, J. Am. Chem. Soc., 95, 5673 (1973).

14) M. Rubinstein, B. Amit, and A. Patchornik, Tetrahedron Letters, 1445 (1975).

15) J. Engels, and R. Reidys, Experimenta, 34, 1? (1978).

16) D.H. Rich, and S.K. Gurwara, J. Am. Chem. Soc., 97, 1575 (1975).

17) D.H. Rich, and S.K. Gurwara, Tetrahedron Letters, 301 (1975).

18) F.S. Tjoeng, W. Staines, S. St. Pierre, and R.S. Hodges, Biochem. Biophys. Acta, 490, 489 (1977).

19) J. Hebert, and D. Gravel, Can. J. Chem., 52, 187 (1974).

20) B. Amit, and A. Patchornik, Tetrahedron Letters, 2205 (1973).

21) B. Amit, D.A. Ben-Efraim, and A. Patchornik, J. Chem. Soc. Perkin I, 57 (1976).

22) B. Amit, D.A. Ben-Efraim, and A. Patchornik, J. Am. Chem. Soc., 98, 843 (1976).

23) G. Ciamician, and P. Silber, Ber., 34, 2040 (1901).

24) Y.L. Chow in "The Chemistry of Amino, Nitroso, and Nitro Compounds, and their Derivatives", Part I, ed. S. Patai, John Wiley and Sons, Toronto, 1982 pg. 183.

25) D. Doepp in "Triplet States II", Springer-Verlag, Berlin, 1975, pg. 49 - 85.

26) A.N. Frolov, N.A. Kutznetsova, and A.V. El'tsov, Rüss. Chem. Rev., 45, 1024 (1976).

27) G. Buechi, and D.E. Ayer, J. Am. Chem. Soc., 78, 689 (1956).

28) J.L. Charlton, C.C. Liao, and P. deMayo, J. Am. Chem. Soc., 93, 2463 (1971).

29) J. Cornelisse, and E. Havinga, Chem. Rev., 75, 353 (1975).

30) C.A.G.O. Varma, F.L. Plantenga, A.H. Huizer, J.P. Zwart, Ph. Bergwerf, and J.P.M. van der Ploeg, J. Photochem., 24, 133 (1984).

31) O.L. Chapman, A.A. Griswold, E. Hoganson, G. Lenz, and J. Reasoner, Pure Appl. Chem., 9, 585 (1964).

32) R. Hurley, and A.C. Testa, J. Am. Chem. Soc., 88, 4330, (1966).

33) S. Hashimoto, and K. Kano, Bull. Chem. Soc. Jpn., 45, 549 (1972).

34) C. Capellos, and K. Suryanarayana, Int. J. Chem. Kinet., 8, 529 (1976).

35) J.A. Barltrop, and N.J. Bunce, J. Chem. Soc. (c), 1467 (1968).

36) J. Brown, and W. Williams, Chem. Comm. 495 (1966).

37) R. Hurley, and A.C. Testa, J. Am. Chem. Soc., 90, 1949 (1968).

38) R. Ruakowicz, and A.C. Testa, Spectrochim. Acta, 27A, 787 (1971).

39) A.N. Frolov, A.V. El'tsov, I.M. Sosonkin, and N.A. Kuznetsova, J. Org. Chem. USSR, 9, 999 (1973).

40) C. Capellos, and F. Lang, Int. J. Chem. Kinet., 9, 409 (1977).

41) H. Goerner, and D. Schulte-Frohlinde, J. Phys. Chem. 82, 2653 (1978).

42) C. Reichardt, and K. Dimroth, Fortschrt. Chem. Forschung, 11, 1 (1966).

43) D.J. Cowley, Helvetia Chim. A., 61, 184 (1978).

44) J. Wolleben, and A.C. Testa, J. Phys. Chem., 81, 429 (1977).

45) W. Trotter, and A.C. Testa, J. Am. Chem. Soc., 90, 7044 (1968).

46) C. Capellos, and F. Lang, Int. J. Chem. Kinet., 9, 943 (1977).

47) D.J. Cowley, and L.H. Sutcliffe, J. Chem. Soc. (B), 569 (1970).

48) R.B. Sleight, and L.H. Sutcliffe, Trans. Faraday Soc., 67, 2195 (1971).

49) L. Lunazzi, G. Placucci, and N. Ronchi, J. Chem. Soc. Perkin II, 1132 (1977).

50) M.V. George, and J.C. Scaiano, J. Phys. Chem., 84, 492 (1980).

51) F. Sachs, and R. Kempf, Ber. Deut. Chem. Ges., 35, 2704 (1902).

52) E. Hadjeliadis, and E. Hayon, J. Phys. Chem., 74, 3184 (1970).

53) B.C. Gunn, and M.F.G. Stevens, J. Chem. Soc. Perkin I, 1682 (1973).

54) Y. Maki, M. Suzuki, T. Hosokami, and T. Furuta, J. Chem. Soc. Perkin I, 1354 (1974).

55) P.W. Binkley, and T.W. Flechtner in "Synthetic Organic Photochemistry", Edited by W.M. Horspool, Plenum Press, New York, 1984, pg. 402.

56) C. Capellos, and G. Porter, J. Chem. Soc. Faraday Trans·II, 70, 1159 (1974).

57) J.G. Pacifici, G. Irick Jr., and C.G. Anderson, J. Am. Chem. Soc., 91, 565 (1969).

58) A.N. Frovlov, N.A. Kuznetsova, A.V. El'tsov, and N.I. Rtishchev, J. Org. Chem. USSR, 9, 988 (1973).

59) O. Santos, and A.C. Testa, J. Photochem., 28, 131 (1985).

60) G.G. Wubbels, J.W. Jordan, and N.S. Mills, J. Am. Chem. Soc., 95, 1281 (1973).

61) A. Cu, and A.C. Testa, J. Photochem., 6, 277 (1977).

62) J.C. Anderson, and C.B. Reese, Proc. Chem. Soc., 217 (1960).

63) D. Elad, D.V. Rao, and V.I. Stenberg, J. Org. Chem., 30, 3252 (1965).

64) D.J. Carlsson, L.H. Gan, and D.M. Wiles, Can. J. Chem., 53, 2337 (1975).

65) S. Ishida, Y. Hashida, H. Shizuka, and K. Matsui, Bull. Chem. Soc. Jpn., 52, 1135 (1979).

66) H. Shizuka, and I. Tanaka, Bull. Chem. Soc. Jpn., 41, 2343 (1968).

67) H. Shizuka, Bull. Chem. Soc. Jpn., 42, 52 (1969); ibid, 42, 57 (1969).

68) C.E. Kalmus, and D.M. Hercules, J. Am. Chem. Soc., 96, 449 (1973).

69) R. Nakagaki, M. Hiramatsu, T. Watanabe, Y. Tanimoto, and S. Nagakura, J. Phys. Chem., 89, 3222 (1985).

70) N.J. Turro in "Modern Molecular Photochemistry", pg. 542 The Benjamin/Cummings Publishing Company, Inc., 1978, Don Mills, Ont.

71) T. Hasegawa, S. Kosaku, J. Ueno, and S.Oguchi, Bull. Chem. Soc. Jpn., 55, 3659 (1982).

72) H. Garcia, R. Martinez-Utrilla, and M.A. Miranda, Tetrahedron, 41, 3131 (1985).

73) J. Hill, Chem. Comm., 260 (1966).

74) O. Hoshino, S. Sawaki, N. Miyazaki, and B. Umezawa, Chem. Comm., 1572 (1971).

75) E. Lippert, W. Lueder, and H. Boos, in "Advances in Molecular Spectroscopy", ed. A. Mangini, Pergamon Press, Oxford, 1962.

76) Z.R. Grabowski, and J. Dobkowski, Pure and Appl. Chem., 55, 245 (1983).

77) Y. Wang, and K.B. Eisenthal, J. Chem. Phys., 77, 6076 (1982).

78) A.J. Kallir, G.W. Suter, and U.P. Wild, J. Phys. Chem., 91, 60 (1987).

79) L.H. Catalani, and T. Wilson, J. Am. Chem. Soc., 109, 7458 (1987).

80) C.J. Pouchert, J.R. Campbell, The Aldrich Library of NMR Spectra, Volume 6, Spectrum 141D.

81) E. Pretch, J. Seibl, W. Simon, and T. Clera, Spectral Data for Structure Determination of Organic Compounds, Springer-Verlag, New York, 1983.

82) M.D. Cohen, and E. Fischer, J. Chem. Soc., 3044 (1962).

83) Ref. 24, pg. 184.

84) H.G. Aurich in "The Chemistry of Amino, Nitroso and Nitro Compounds and their Derivatives, Supplement F, ed. S. Patai, Interscience 1982, pt. 1, pg. 580.

85) D.R. Burfield, K.H. Lee, and R.H. Smithers, J. Org. Chem., 42, 3060 (1977).

86) Y.A. Arbuzov, T.A. Piska, Doklady Akad. Nauk. SSSR, 116, 71 (1957) Chem. Abstr., 52, 6257 (1958).

87) H. Langhals, Angew. Chem. Int. Ed., 21, 724 (1982).

88) V. Gutmann, Electrochim. Acta, 21, 661 (1976).

89) E.M. Kosower, J. Am. Chem. Soc., 80, 3253 (1958).

90) K. Dimroth, C. Reichardt, T. Siepmann, and F. Bohlmann, Liebigs Ann. Chem., 661, 1 (1963).

91) H. Langhals, Nouv. J. Chim., 5, 97 (1981).

92) C. Reichardt, Angew. Chem. Int. Ed., 18, 98 (1979).

93) S. Dincturk, R.A. Jackson, M. Townson, H. Agirbas, N.C. Billingham, and G. March, J. Chem. Soc., Perkin II, 1121 (1981).

94) J.G. Calvert, and J.N. Pitts Jr., Photochemistry, Wiley, New York, 1967 pg. 783 - 786.

95) U. Schmidt, K. Kabitzke, and K. Markau, Monatsh. Chem. 97, 1000 (1966).

96) W.C. Danen, and F.A. Neugebauer, Angew. Chem. Int. Ed., 14, 783 (1975).

97) D. Bellus, P. Hrdlovic, and P. Slama, Collect, Czech. Chem. Commun., 33, 2646 (1968).

98) R.O. Kan, and R.L. Furey, Tetrahedron Lett., 2573 (1966).

99) F.D. Lewis, R.T. Lauterbach, H.G. Heine, W. Hartmann, and H. Rudolph, J. Am. Chem. Soc., 97, 1519 (1975).

100) J.M. Dust, and D.R. Arnold, J. Am. Chem. Soc., 105, 1221 (1983).

101) X. Creary, M.E. Mehrsheikh-Mohammadi, and S. McDonald, J. Org. Chem., 52, 3254 (1987).

102) D. Rehm, and A. Weller, Ber. Bunsenges. Phys. Chem., 73, 834 (1969).

103) J. Libman, J. Chem. Soc. Chem. Comm., 868 (1977).

104) D.D.M. Wayner, and D.R. Arnold, Can. J. Chem., 63 (1985).

106) J.C. Dalton, and N.J. Turro, Mol. Photochem., 2, 133 (1970).

107) J.T. Thurston, and R.L. Shriner, J. Org. Chem., 2, 183 (1937).

108) S. Pass, B. Amit, and A. Patchornik, J. Am. Chem. Soc., 103, 7674 (1981).

109) M.B. Zimmt, C. Doubleday Jr., and N.J. Turro, J. Am. Chem. Soc., 108, 3618 (1986) and references therein.

110) R.D. Small Jr., and J.C. Scaiano, Chem. Phys. Lett., 59, 246 (1978).

111) A.S. Kabankin, G.M. Zhidomirov, and A.L. Buchachenko, J. Magn. Resonance, 9, 199 (1973).

112) H.A. Morrisor in "The Chemistry of the Nitro and Nitroso Groups", ed. H. Feuer, Interscience, 1969, pt. 1, pg. 165.

113) W.G. Gall, B.D. Astill and V. Boekelheide, J. Org. Chem., 20, 1538 (1955).

114) C.G. Hatcher, and C.A. Parker, Proc. Roy. Soc., A 235, 518 (1956).

115) O. Kling, E. Nikolaiski, H.L. Schlaefer, Ber. Bunsenges. Phys. Chem., 67, 883 (1963).